Report No. CCEER 15-07

DESIGN AND CONSTRUCTION OF BRIDGE COLUMNS INCORPORATING MECHANICAL BAR SPLICES IN PLASTIC HINGE ZONES

Mostafa Tazarv
M. Saiid Saiidi

A report submitted to the
Accelerated Bridge Construction - University Transportation Center
(ABC-UTC)
Contract Number DTRT13-G-UTC41

Center for Civil Engineering Earthquake Research

University of Nevada, Reno
Department of Civil and Environmental Engineering, MS 258
1664 N. Virginia St.
Reno, NV 89557

August 2015

Abstract

Accelerated bridge construction (ABC) relies heavily on prefabricated reinforced concrete members. One method to connect prefabricated columns to footings or cap beams is through the use of mechanical bar splices commonly referred to as couplers. Even though current seismic codes prohibit the application of couplers in the plastic hinge area of columns located in moderate and high seismic zones, recent studies have revealed the feasibility of precast columns utilizing couplers in the plastic hinge zones helping expand ABC in these zones.

Several types of mechanical bar splices each with a unique performance and anchoring mechanism are available in the U.S. market. Five of these were included in this study: shear screw, headed bar, grouted, threaded, and swaged couplers. A state-of-the-art literature search was conducted to compile and interpret data on the seismic performance of these coupler types as well as columns incorporating these couplers in the plastic hinge zones. Findings were summarized and tabulated. Subsequently, coupler acceptance criteria for seismic applications and acceptance criteria for ductile columns incorporating couplers in plastic hinges were developed. Then the seismic performance of the couplers and the columns was evaluated. It was found that the coupler performance varies for different loading rates and even for the same type of coupler produced by different manufactures. Furthermore, the location of couplers in columns was critical for large size couplers. Special detailing was studied by different researchers to achieve large displacement capacities. Satisfactory performance was usually observed for small size couplers in which their location had insignificant effect on the column seismic behavior. Findings from the literature study as well as the coupler evaluation indicated that a rigorous testing schedule is needed to completely understand the seismic performance of each coupler type and series. Constructability and speed of construction for each coupler type were also studied. It was found that the application of mechanical bar couplers at both ends of precast columns will shorten the construction time by approximately 60% for a three-column bent regardless of the type of the coupler. Since conclusive trends could not be established with limited test data, an extensive parametric study was carried out to investigate coupler effects on the column seismic behavior. A generic stress-strain model was also developed to represent behavior of all types of couplers. It was found that the coupler length, the coupler location, and the rigidity of the coupler significantly affect the displacement ductility capacity of mechanically spliced columns. Furthermore, a simple design equation was developed in which the spliced column displacement ductility capacity can be estimated based on the basic characteristic and geometry of the coupler and the column. Finally, a design guideline as well as examples were developed to facilitate the field deployment of precast columns incorporating mechanical bar splices.

Acknowledgements

The present study was funded by the United States Department of Transportation (USDOT) through the University Transportation Center - Accelerated Bridge Construction (ABC-UTC) Grant No. DTRT13-G-UTC41. However, the material and opinions presented herein are those of the authors and do not necessarily represent the views of USDOT. Special thanks are due Ms. Lydia Mercado, the USDOT Research Program Manager, for her support and advice. The project Steering Committee members, Mr. Ahmad Abu-Hawash of the Iowa Department of Transportation, Dr. Bijan Khaleghi of the Washington Department of Transportation, Mr. Elmer Marx of the Alaska Department of Transportation, and Mr. Tom Ostrom of the California Department of Transportation, are thanked for their comment and advice. The authors would like to thank Dr. Kshitij Shrestha, a visiting scholar at the University of Nevada Reno, as well as Mr. Colton Schaefer, an undergraduate researcher, for their assistance in the project. The input from Ms. Carmen Swanwick of the Utah Department of Transportation and Mr. Mohammad Javad Ameli of the University of Utah is appreciated.

Executive Summary

ES.1 Introduction

Prefabricated bridge elements and systems are the key components of accelerated bridge construction (ABC). The application of prefabricated superstructure elements dates back to more than half a century ago. However, precast bridge columns are rarely used in moderate and high seismic regions due to uncertainty in their connections to footings and bent caps. Bridge columns in moderate and high seismic zones are designed to be very ductile regardless of casting method, thus their connections must accommodate very large inelastic rotations. One method to connect prefabricated columns to footings or cap beams is through the use of mechanical bar splices, also known as couplers. Current bridge seismic codes prohibit the application of couplers in the plastic hinge area of bridge columns located in moderate and high seismic regions. However, promising detailing was developed in recent years revealing the feasibility of precast columns utilizing couplers in plastic hinge zones.

ES.2 Objectives

The main objectives of the present study were to compile and interpret data on the constructability and seismic behavior of different types of mechanical bar splices and to investigate coupler effects on the seismic performance of mechanically spliced bridge columns. Five tasks were included in this project to meet the objectives: (1) conducting literature search, (2) determining characteristic seismic performance of different couplers, (3) evaluating the constructability of different coupler types and columns with these couplers, (4) developing methods to estimate mechanically spliced column displacement ductility capacities, and (5) developing design guidelines for prefabricated bridge columns utilizing coupler connections. Highlights of different aspects of the study and important findings are presented herein.

ES.3 Literature Review

A state-of-the-art literature search was conducted to collect experimental data regarding five common types of mechanical bar splices (Fig. ES-1): (1) shear screw couplers, (2) headed bar couplers, (3) grouted sleeve couplers, (4) threaded couples, and (5) swaged couplers. Test data included in this report was the performance of coupler itself under axial loading and the seismic performance of columns incorporating these coupler types in plastic hinge regions. The literature search findings were summarized in various tables and figures. Tables ES-1 and ES-2 present two samples of the table

summaries. Furthermore, the current U.S. code limitations for mechanical bar splices were presented (Table ES-3).

(a) Shear Screw Coupler
[ancon.co.uk]

(b) Headed Bar Coupler
[hrc-usa.com]

(c) Grouted Sleeve Couplers
[splicesleeve.com]

[erico.com]
(d) Threaded Coupler

[armaturis.com]

(e) Swaged Coupler
[ancon.com.au]

Figure ES-1. Mechanical Reinforcing Bar Couplers

Table ES-1. Summary of Studies on Shear Screw Couplers (Sample)

Study	Coupler	Bar Size	Bar Type	Mode of Failure	Remarks
Lloyd (2001)	Three-screw, "Bar-Lock L-Series"	No. 6 (Ø19 *mm*) & No. 8 (Ø25 *mm*)	ASTM A615 Grade 60	Bar pullout, bar fracture	90% of the ultimate strength of the bar can be achieved
Hillis and Saiidi (2009)	Three-screw "Zap Screwlok Type 2"	No. 4 SMA bars to Steel Bars	NiTi SMA & Grade 60 Steel bars	SMA bar fractured inside the grip	No coupler failure and no SMA bar fracture inside the coupler was observed
Rowell et al. (2009)	Seven-screw "Zap Screwlok Type 2"	No. 10 (Ø32 mm)	ASTM A615 Grade 60	Mainly bar fracture inside couplers	Lower strength and significantly lower strain capacities were observed due to premature failure of bars
Huaco and Jirsa (2012)	Three-screw (S-series) and four-screw (B Series)	No. 8 (Ø25 *mm*)	ASTM A706 Grade 60	Bar fractured inside or away from coupler	Bar fractured on the edge of three-screw couplers and bar fractured outside four-screw couplers, three times higher strain capacity for longer couplers was observed
Alam et al. (2010)	Three-screw "Bar-Lock S"	No. 4 to 6 (Ø13 to 19 *mm*)	Grades 40 and 60	Bar fracture	Low slippage was observed before yielding, sufficient strength was reported

Table ES-2. Summary of Seismic Performance of Column Test Models with Grouted Sleeve Couplers (Sample)

Reference	Column Geometry	Coupler Length	Remarks
Haber et al. (2014)	No. of Columns: Two, Scale Factor: 50% Variable: Pedestal, Section: Circular, Dim.: 24 *in*. (610 *mm*), Long. Bars: 11 No. 8 (Ø25 *mm*), Trans. Bars: No. 3 (Ø10 *mm*) Spirals at 2 *in*. (51 *mm*)	14.6d_b: used at one level	Both columns showed 40% lower displacement capacity compared to the cast-in-place column performance (couplers were installed immediately above either footing surface or pedestal)
Tazarv and Saiidi (2014)	No. of Columns: One, Scale Factor: 50% Section: Circular, Dim.: 24 *in*. (610 *mm*), Long. Bars: 11 No. 8 (Ø25 *mm*), Trans. Bars: No. 3 (Ø10 *mm*) Spirals at 2 *in*. (51 *mm*)	14.6d_b: used in one level	Column showed the same seismic performance compared to the cast-in-place column performance; (couplers were installed immediately above a pedestal)
Pantelides et al. (2014)	No. of Columns: Three, Scale Factor: 50% Variable: Coupler Location, Section: Octagonal, Dim.: 21 *in*. (533 *mm*), Long. Bars: 6 No. 8 (Ø25 *mm*), Trans. Bars: No. 4 (Ø13 *mm*) Spirals at 2.5 *in*. (63 *mm*)	14.6d_b: standard couplers were used at one level in column-to-footing connections	Columns showed 25 to 40% lower displacement ductility capacity compared to a reference column, the best performance was observed for the column with couplers immediately above the footing surface and debonded bars below the couplers
Pantelides et al. (2014)	No. of Columns: Three, Scale Factor: 50% Variable: Coupler Location, Section: Octagonal, Dim.: 21 *in*. (533 *mm*), Long. Bars: 6 No. 8 (Ø25 *mm*), Trans. Bars: No. 4 (Ø13 *mm*) Spirals at 2.5 *in*. (63 *mm*)	8.6d_b: modified couplers were used in column-to-cap beam connections	Columns showed 41 to 51% lower displacement ductility capacity compared to a reference column, the best performance was observed for the column with couplers embedded in the cap beam

Note: d_b is the longitudinal bar diameter; D is either the column diameter or the column largest side dimension

Table ES-3. Current US Code Restrictions on Mechanical Bar Couplers

Code	Splice Type	Stress Limit	Strain Limit	Max Slip	Location Restriction
ACI318 (2014)	Type 1	$\geq 1.25f_y$	None	None	Shall not be used in the plastic hinge of ductile members of special moment frames neither in longitudinal nor in transvers bars (Article 18.2.7)
	Type 2	$\geq 1.0f_u$	None	None	Shall not be used within one-half of the beam depth in special moment frames but are allowed in any other members at any location (Articles 18.2.7 & 25.5.7)
Caltrans SDC (2013)	Service	None	> 2%	None	No splicing is allowed in "No-Splice Zone" of ductile members, which is the plastic hinge region. Ultimate splices are permitted outside of the "No-Splice Zone" for ductile members. Service splices are allowed in capacity protected members (Ch. 8)
	Ultimate	None	> 9% for No. 10 (32 *mm*) and smaller[(a)] > 6% for No. 11 (36 *mm*) and larger[(a)]	None	
AASHTO (2013 & 2014)	Full Mechanical Connection[(b)]	$\geq 1.25f_y$	None	No. 3-14: 0.01 *in*. No. 18: 0.03 *in*.	Shall not be used in plastic hinge of columns in SDC C and D (AASHTO Guide Spec 2014, Article 8.8.3)

[(a)] For ASTM A706 Reinforcing Steel Bars. There is also a maximum strain demand limit (e.g. 2% for ultimate splices and 0.2% (the bar yield strain) for service splices) [Caltrans Memo to Designers 20-9].
[(b)] AASHTO LRFD (2013) Article 5.11.5.2.2.

ES.4 Characteristic Seismic Performance of Different Couplers

As presented in Table ES-3, the current U.S. codes prohibit the application of mechanical bar splices in the plastic hinge zone but allow the application of couplers in non-ductile, capacity-protected structural members, and outside plastic hinge zones of columns. Some of these codes categorize couplers (e.g. service, ultimate, type 2) for different usage. Acceptance criteria are spelled out in these codes, but it is important to note that these criteria may not be suitable for seismic applications since the criteria implicitly assume that the couplers are only used in non-critical sections where no significant plastic deformations and strains are expected under seismic actions. Minimum acceptance criteria for utilization of couplers in plastic hinges were proposed as:

1. Total length of a mechanical bar splice (L_{sp}) shall not exceed $15d_b$ (d_b is the diameter of the smaller of the two spliced bars). This is to minimize adverse effects of coupler length on rotational capacity of a ductile member.
2. A spliced bar shall fracture outside coupler region regardless of loading type (e.g. monolithic, cyclic, or dynamic). The coupler region is defined as the length of a coupler plus $1.0d_b$ from each face of the coupler (Fig. ES-2). Only ASTM A706 reinforcing steel bars shall be used for seismic applications.

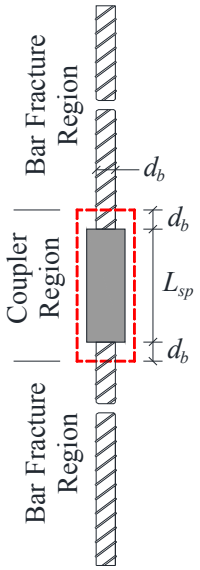

Figure ES-2. Coupler and Fracture Regions

The available coupler test data was evaluated using the criteria described in the previous section to accept or reject a coupler for application in plastic hinges of bridge columns. Table ES-4 presents the results of evaluation for shear screw coupler types as a sample. Note that acceptance of a coupler for seismic applications does not guarantee satisfactory performance of columns incorporating these couplers in plastic hinges of columns in high seismic regions.

Table ES-4. Evaluation of Shear Screw Couplers (Sample)

Study	Coupler	Mode of Failure	Strain Capacity	Remark
Lloyd (2001)	Three-screw, "Bar-Lock L-Series" Length: $12.3d_b$	Bar pullout (30% of the samples), bar fracture in coupler region (37% of data)	Less than 4%	Not recommended
Hillis and Saiidi (2009)	Three-screw "Zap Screwlok Type 2" Length: $14d_b$	SMA bar fractured inside the grip	SMA strain was 6.9%	Recommended
Rowell et al. (2009)	Seven-screw "Zap Screwlok Type 2" Length: $15d_b$	Mainly bar fracture inside couplers	Less than 2.7%	Not recommended
Huaco and Jirsa (2012)	Three-screw (S-series) and four-screw (B Series) Length < $10d_b$	Bar fractured inside three-screw couplers, bar fractured away from four-screw couplers	N/A	Four-screw is recommended
Alam et al. (2010)	Three-screw "Bar-Lock S" Length: $8.4d_b$	Bar fracture	N/A	Recommended

It was found that each coupler performance varies for different loading rates and even for the same type of coupler produced by different manufactures. It was concluded that an extensive experimental program is needed to evaluate each coupler type made by different manufacturer for seismic applications. The test program should include static, cyclic, and dynamic loading to sufficiently evaluate each coupler type.

For seismic response of columns with couplers (CWC) to be acceptable, certain displacement ductility capacity and lateral load strength requirements should be met. It is reasonable to base these requirements relative to ductility and strength of a similar reference column with no couplers (CIP). The proposed acceptance criteria for columns incorporating couplers in plastic hinges are:

1. When the displacement ductility capacity of CIP is five or less, the displacement ductility capacity of CWC should be at least equal to the ductility capacity of CIP. For other cases, the displacement ductility capacity of CWC should be the greatest of (a) 90% of CIP ductility capacity, and (b) five. Either displacement or drift capacity may be used in the evaluation of columns with advanced materials.
2. The lateral load strength of CWC should not be less than 95% of the CIP strength when the displacement ductility capacity of CIP is five or less. For other cases, the lateral strength of CWC should not be less than 90% of CIP strength.

Mechanically spliced columns were seismically evaluated based on these criteria and the results were summarized in various tables and figures (e.g. Table ES-5 and Fig. ES-3). It was found that the location of couplers in the plastic hinge area is critical for large size couplers, and special detailing is needed to achieve large displacement capacities. Satisfactory performance was usually observed for small size couplers in which their location had minor effect on the column seismic behavior.

Table ES-5. Evaluation of Seismic Performance of Column Test Models with Threaded Couplers (Sample)

Reference	Coupler Length	Coupler Location	Evaluation Result
Lehman et al. (2001)	Not available, (approximately $3.6d_b$ based on detailing shown for spiral), couplers were used at two levels	Bottom couplers were installed in the footings, top couplers were installed $1.5D$ above the bottom couplers	Passed (the repaired column showed 30% higher lateral strength and 40% higher displacement capacity compared to the original column)
Saiidi and Wang (2006)	$4.0d_b$: used at two levels	Bottom couplers were installed 4 *in*. (102 *mm*) below the footing surface, top couplers were installed $1.17D$ above the bottom couplers	N/A (there is no reference column but both original and repaired columns exhibited large displacement capacity (5.8% drift ratio) with no bar fracture)
Saiidi et al. (2009)	$4.0d_b$: used at two levels	Bottom couplers were installed 4 *in*. (102 *mm*) below the footing surface, top couplers were installed $1.4D$ above the bottom couplers	Passed (both columns exhibited equal or better drift capacity (10 or 14% drift ratio) compared to the reference column with no bar fracture up to 14% drift ratio, note that lower 22% lateral strength of coupler columns was because of SMA bars not the coupler effect)
Varela and Saiidi (2014)	$3.4d_b$: used at two levels	Bottom couplers were installed 2 *in*. (51 *mm*) below the footing surface on center, top couplers were installed $0.85D$ above the bottom couplers on center	N/A (there is no reference column to compare but the column exhibited 11.8% drift ratio, which is beyond practical range for conventional columns)

Note: d_b is the longitudinal bar diameter; D is either the column diameter or the column largest side dimension

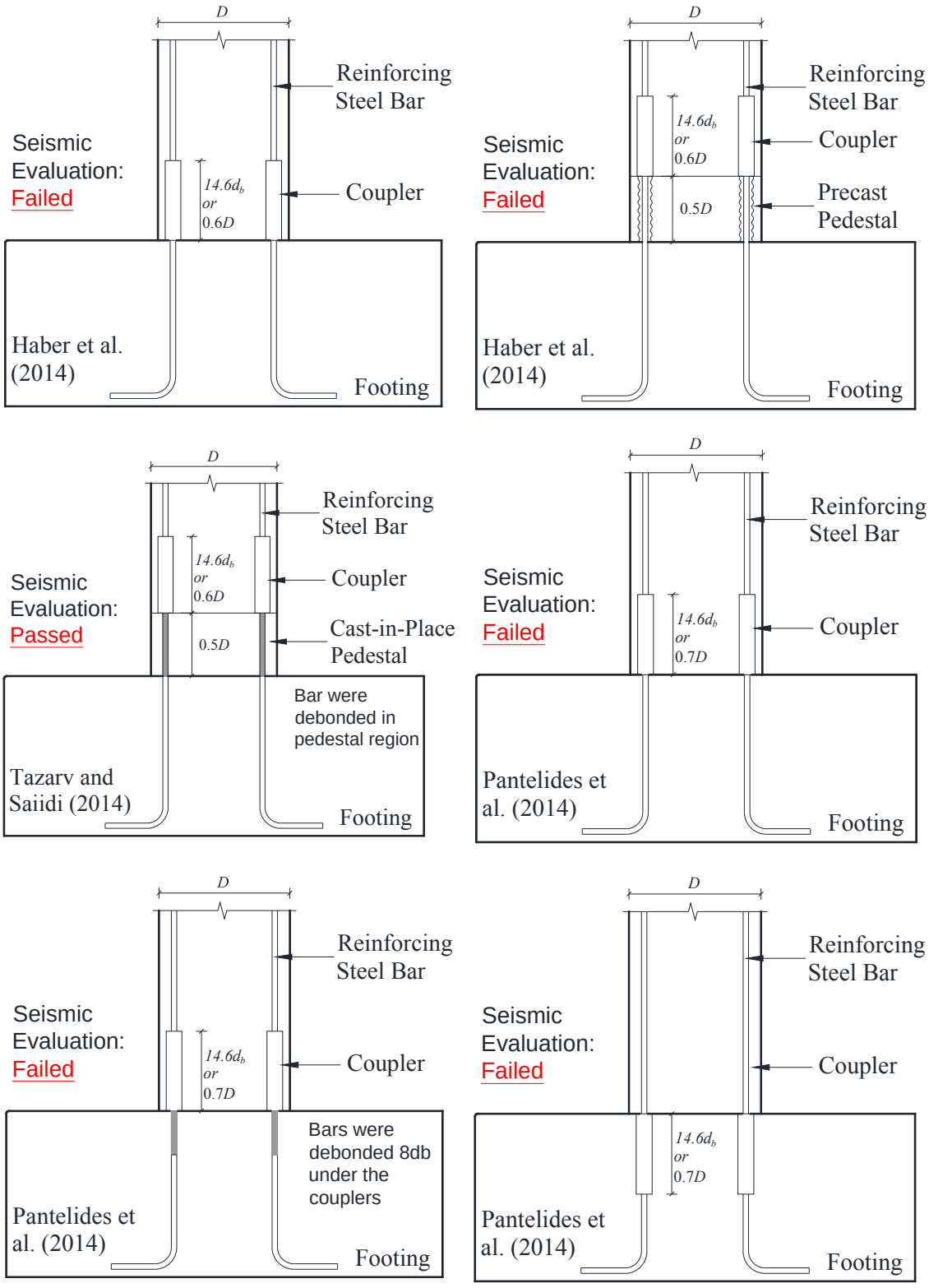

Figure ES-3. Evaluation of Columns Incorporating Grouted Couplers (Sample)

ES. 5 Constructability of Different Coupler Types

The constructability of different coupler types was evaluated to further assist designers in the selection of different coupler types. Important considerations that are needed before field deployment were highlighted (Table ES-6), and the speed of construction for each coupler type and the speed of construction for precast columns incorporating couplers were evaluated. It was found that the application of mechanical bar couplers at both ends of precast columns will shorten the construction time by approximately 60% for a three-column bent regardless of the type of the coupler.

Table ES-6. Constructability of Mechanical Bar Couplers

Item/Coupler	Shear Screw	Headed Bar	Grouted Sleeve	Threaded	Swaged
Bar End Preparation	Not Needed	Heading	Not Needed	Threading	Not Needed
Special Equipment	Wrench or Nut Runner	Wrench, Heading Machine	Grout Pump	Die and Tap	Press Machine
Additional Material/Piece	Screw	No Need	Grout/Sealing	No Need	No Need
Tolerance and Alignment	Loose	Tight	Loose	Tight	Loose
Field Erection Speed for precasting	Very Fast	Fast	Very Fast	Fast	Fast
Time to Complete one Splice	1 *min*	5 *min*	24 *hours*	5 *min*	5 *min*

ES.6 Coupler Effects on Seismic Performance of Columns

The available test data showed that the seismic performance of columns incorporating mechanical bar splices in the plastic hinge area is not the same as conventional column performance. Since the test data was scarce, an extensive parametric study was carried out to investigate coupler effects on the column overall behavior. The study included stress-strain model development for couplers, validation of the coupler model by test data, conducting analyses and interpreting the results, and development and validation of simple design equation accounting for coupler effects on the column displacement ductility capacity.

A generic stress-strain model was developed to represent behavior of all types of couplers (Fig. ES-4). When a mechanical bar splice is under tension, it can be assumed that only a portion of the coupler length contributes to the overall elongation of the connection and the remaining portion of the coupler (βL_{sp}) is rigid due to the relatively large diameter of the coupler or its anchoring mechanism. β is defined as the coupler rigid length factor. Therefore, for the same tensile force, the coupler region axial deformation will be lower resulting in a lower strain in the coupler region (ε_{sp}) compared to the strain of the connecting reinforcing bar (ε_s):

$$\varepsilon_{sp}/\varepsilon_s = (L_{cr} - \beta L_{sp})/L_{cr} \quad \text{(ES-1)}$$

where L_{cr} is the length of the coupler region and L_{sp} is the coupler length. Overall, the stress-strain relationship of any type of mechanical bar splice can be determined by

knowing only the coupler rigid length factor (β). The condition in which $\beta = 0$ is similar to a non-spliced connection in which the stress-strain of the coupler region is the same as the reinforcing bar stress-strain.

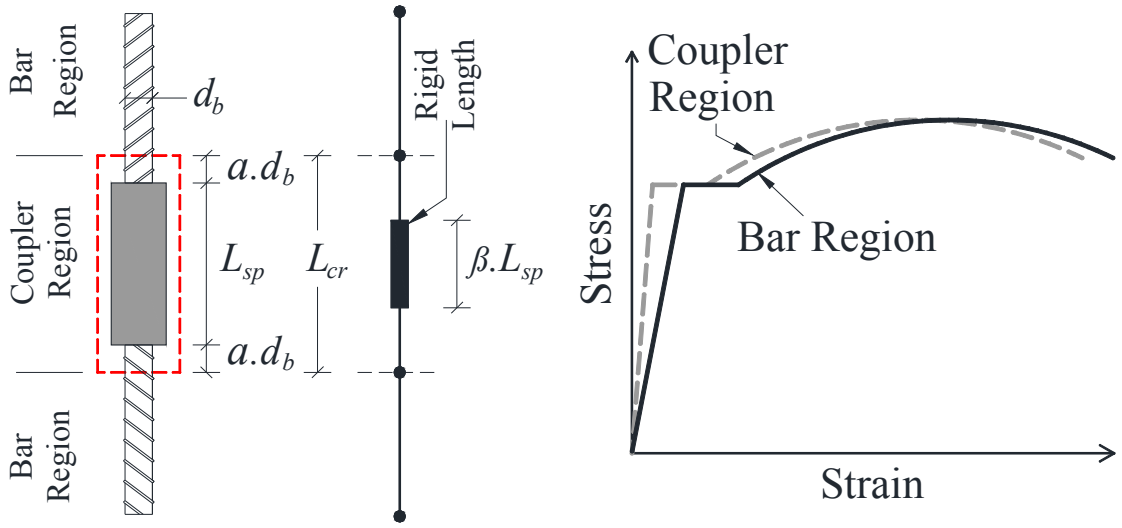

(a) Coupler Region (b) Stress-Strain Model for Couplers

Figure ES-4. Stress-Strain Model for Mechanical Bar Splices

Table ES-7 presents the measured coupler rigid length factors for headed bar and grouted couplers. Currently, there is no test data to obtain this factor for shear screw, threaded, and swaged couplers but factors were suggested in Table ES-7 for these couplers based on engineering judgement and data for other coupler types. More testing is required to determine the coupler rigid length factor for different coupler types and series before field deployment.

Table ES-7. Coupler Rigid Length Factor

Coupler type	$\frac{\varepsilon_{sp}}{\varepsilon_s}$ from Test	Measured β	Suggested[(a)]
Shear Screw	N/A	N/A	0.5
Headed Bar	0.7	0.77	0.75
Grouted Sleeve	0.42	0.64	0.65
Threaded	N/A	N/A	0.25
Swaged	N/A	N/A	0.5

Note: "Suggested" values need to be verified for different coupler types and coupler series.

Subsequently, 12 conventional cast-in-place columns were designed according to the AASHTO Guide Specifications (2014) to serve as reference non-spliced columns. Then, more than 550 analyses were conducted to investigate the effects of different coupler parameters on the displacement ductility capacity of the 12 aforementioned columns. One sample result is shown in Fig. ES-5. It was found that the coupler length, the

coupler location, and the rigidity of the coupler significantly affect the displacement ductility capacity of mechanically spliced columns. Furthermore, the results showed that mechanical bar splices can reduce the displacement ductility capacity of the spliced column by up to 40% when very rigid, very long couplers are installed immediately above the column-to-footing interface. Shifting the couplers from the column-to-footing interface by one-half the column diameter ($0.5D_c$) significantly improved the displacement ductility capacity of the spliced columns and made them comparable to CIP columns. Another finding was that the coupler effect was more profound on columns with higher ductilities. For example, the displacement ductility of a spliced column is expected to be 95% of the CIP column displacement ductility when the CIP displacement ductility is 3. However, this ratio is 85% when the CIP displacement ductility is 7.

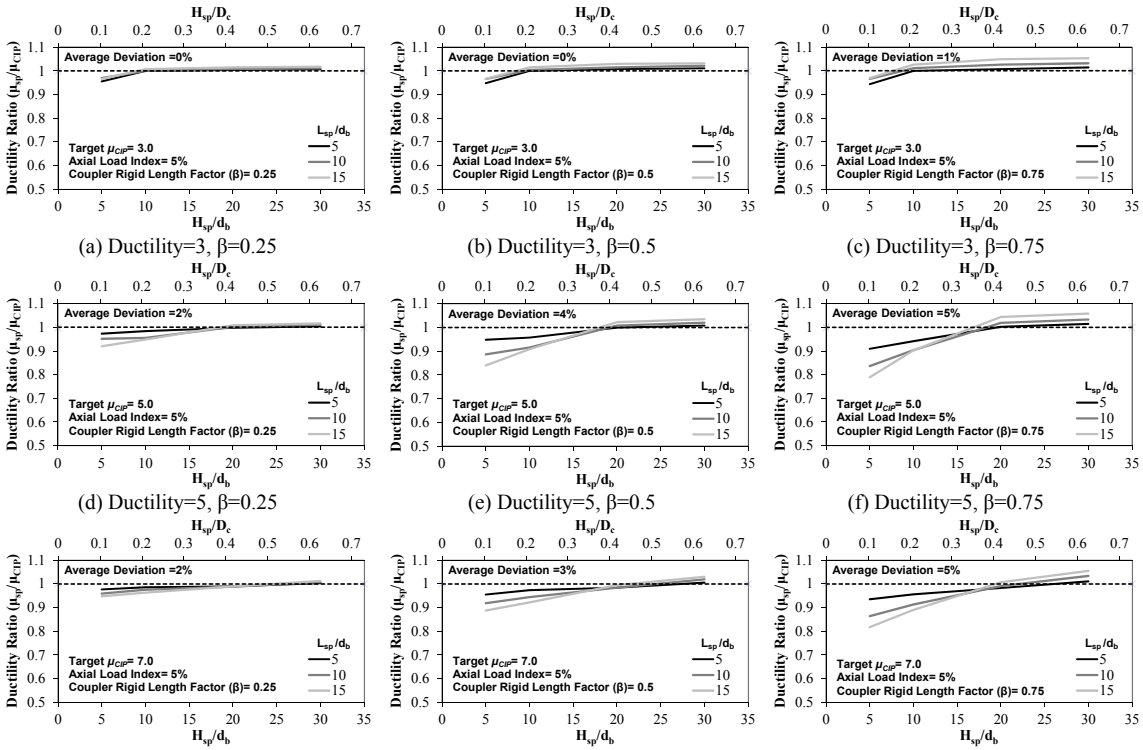

(a) Ductility=3, β=0.25 (b) Ductility=3, β=0.5 (c) Ductility=3, β=0.75

(d) Ductility=5, β=0.25 (e) Ductility=5, β=0.5 (f) Ductility=5, β=0.75

(g) Ductility=7, β=0.25 (h) Ductility=7, β=0.5 (i) Ductility=7, β=0.75

Figure ES-5. Effect of Coupler Lengh on Ductility of Columns with Aspect Ratio=4 and Axial Load Index=5%

Finally, a simple design equation was developed (Eq. ES-2) to estimate the spliced column displacement ductility as:

$$\mu_{sp}/\mu_{CIP} = (1 - 0.18\beta)(\frac{H_{sp}}{L_{sp}})^{0.1\beta} \quad \text{(ES-2)}$$

where μ_{sp} is the spliced column displacement ductility, μ_{CIP} is the non-spliced cast-in-place column displacement ductility, H_{sp} is the pedestal height, L_{sp} is the coupler length, and β is the coupler rigid length factor.

The proposed design equation is relatively simple and offers several advantages. The most important of which is that the designer can design columns using current codes (e.g. AASHTO Guide Specifications) then the reduced displacement ductility capacity can be estimated for the spliced column using the proposed equation.

Table ES-8 presents three examples in which the calculated displacement ductility of spliced columns was compared with the measured displacement ductility of the reference columns. The selected test models had no bar debonding and no grouted ducts. It can be seen that the calculated displacement ductility of the spliced columns was very close to the measured ductilities for all three examples.

Table ES-8. Validation of Design Equation Accounting for Coupler Effects

Reference/ Column	Calculated	Measured
Haber et al. (2014)/ GCNP Column with grouted couplers immediately above the footing surface	$\beta = 0.65$ $H_{sp} = 0.$ use $H_{sp} = 0.1\ in.\ (2.5\ mm)$ $L_{sp} = 14.57\ in.\ (370\ mm)$ thus $\frac{\mu_{sp}}{\mu_{CIP}} = (1 - 0.18\beta)\left(\frac{H_{sp}}{L_{sp}}\right)^{0.1\beta} = \boxed{0.64}$	$\frac{\mu_{sp}}{\mu_{CIP}} = \frac{4.52}{7.36} = \boxed{0.61}$
Haber et al. (2014)/ HCNP Column with headed bar couplers 4 *in*. (102 *mm*) above the column-to-footing interface	$\beta = 0.75$ $H_{sp} = 4\ in.\ (102\ mm)$ $L_{sp} = 3.13\ in.\ (79\ mm)$ thus $\frac{\mu_{sp}}{\mu_{CIP}} = (1 - 0.18\beta)\left(\frac{H_{sp}}{L_{sp}}\right)^{0.1\beta} = \boxed{0.88}$	$\frac{\mu_{sp}}{\mu_{CIP}} = \frac{6.49}{7.36} = \boxed{0.88}$
Pantelides et al. (2014)/ GGSS-1 Column with grouted couplers immediately above the footing surface	$\beta = 0.65$ $H_{sp} = 0.$ use $H_{sp} = 0.1\ in.\ (2.5\ mm)$ $L_{sp} = 14.57\ in.\ (370\ mm)$ thus $\frac{\mu_{sp}}{\mu_{CIP}} = (1 - 0.18\beta)\left(\frac{H_{sp}}{L_{sp}}\right)^{0.1\beta} = \boxed{0.64}$	$\frac{\mu_{sp}}{\mu_{CIP}} = \frac{5.4}{8.9} = \boxed{0.61}$

ES.7 Design Guideline and Examples

A design guideline (Chapter 5) as well as examples (Chapter 6) were developed to facilitate the field deployment of precast columns incorporating mechanical bar splices. The proposed guidelines include both recommendation and commentary to further aid designers. The examples demonstrate the proposed analysis and design steps for full-scale two-column bents incorporating grouted couplers in the column plastic hinge zones.

ES.8 Concluding Remarks

Findings from the literature search, evaluations, and analytical studies on mechanically spliced bridge columns led to the following conclusions:

1. Coupler performance varies for different loading rates and even for the same type of coupler produced by different manufactures. A rigorous testing program is needed to completely understand the performance of each coupler type and series.
2. Test data showed that the location of couplers in columns was critical for large couplers, and improved detailing should be devised to achieve large displacement capacities.
3. Satisfactory seismic performance was usually observed for small size couplers.
4. The application of mechanical bar splices at both ends of precast columns can shorten the construction time by approximately 60% for a three-column bent regardless of the type of coupler.
5. Coupler length should be less than $15d_b$ for seismic applications where d_b is the column longitudinal reinforcing bar diameter.
6. Couplers may be accepted for seismic application when the connecting bar/s fracture outside the coupler region, which includes the coupler length plus $1.0d_b$ from each end of the coupler. Couplers with dominant mode of bar fracture inside the coupler region or bar pullout should not be used in the plastic hinge of columns.
7. The stress-strain model developed for couplers is a simple and viable modeling method to account for the coupler effect in analysis and design of mechanically spliced elements. A coupler material model can be determined by only the coupler rigid length factor.
8. The parametric study showed that the coupler length, the coupler location, and the rigidity of the coupler significantly affect the displacement ductility capacity of mechanically spliced columns. Longer couplers, couplers closer to the column to adjoining member interface, and stiffer couplers may reduce a spliced column displacement ductility capacity by 40%.
9. The proposed simple design equation accounts for the coupler effect on the mechanically spliced column displacement ductility capacity and may be used for design of these columns.

Table of Content

List of Tables

List of Figures

Chapter 1. Literature Search

1.1 Introduction

Mechanical bar splices, commonly referred to as bar couplers, were originally developed to reduce splice length, to reduce bar congestion in splice zone, and to potentially reduce costs since a lower amount of steel is used. Several types of bar splices have been developed as shown in Fig. 1-1 and new splices are emerging. Among these and other splice devices, mechanical bars splices, which transfer both tensile and compressive forces, are the focus of the present study. The tension-compression couplers can be generally categorized as (1) shear screw couplers (SSC), (2) headed bar couplers (HC), (3) grouted sleeve couplers (GC), (4) threaded couplers (TC), and (5) swaged couplers (SC). An example for each coupler type is illustrated in Fig. 1-2 and 1-4.

Mechanical bar couplers have been extensively utilized in capacity protected or non-critical areas of structural members but their application in plastic hinge of ductile members is scarce or totally banned. In the last few years, there has been an increasing interest to utilize bar couplers in precast bridge column connections. Noting that columns are allowed to undergo substantial nonlinearity while bridge collapse is prevented, such application for bar couplers needs sufficient test data and special detailing. To be able to incorporate these couplers in bridges and especially bridge columns, seismic performance of couplers, seismic performance of columns with these couplers, and new guidelines and specifications are necessary.

In this section, limitations on the application of bar couplers in current US codes are presented. A comprehensive literature study was performed on available test data regarding the performance of coupler specimens and columns with couplers, and findings are presented herein.

1.2 Couplers in US Codes

Characteristics and installation methods vary among different coupler types. The mechanism of force transfer through the coupler also varies depending on the coupler type. Even though bar couplers have been extensively used in reinforced concrete construction, they are either prohibited or allowed with limitations in plastic hinges of ductile members of bridges and buildings. Table 1-1 presents restrictions in the current AASHTO, Caltrans, and ACI codes. Figure 1-3 illustrates the Caltrans strain limitations for an ASTM A706 bar. Furthermore, Caltrans provides a list of proprietary couplers with acceptable performance (App. A). ACI 439.37 (2007) presents a list of mechanical bar splices available in the US market, identifies their limitations, and provides

information regarding bar end preparation and coupler configurations, but no specification or acceptance criterion is presented.

1.3 Performance of Couplers

Tensile tests are usually performed to evaluate the performance of bar couplers. The coupler types shown in Fig. 1-2 and 1-4 are the focus of this study. A summary of previous studies on these couplers is presented in this section.

1.3.1 Shear Screw Couplers (SSC)

Strength performance of shear screw couplers under monotonic and cyclic loading was investigated by Lloyd (2001). Couplers used in this study were Bar-Lock L-Series. Two sizes of ASTM A615 Grade 60 bars, No. 6 (Ø19 *mm*) and No. 8 (Ø25 *mm*), were tested. Monotonic and cyclic tensile tests were performed on 160 coupler specimens. The monotonic test results showed that SSC can guarantee development of 90% of the ultimate tensile strength of reinforcing bars. In 24 of 80 connection tests the spliced bars pulled out from the couplers. None of the bars or couplers failed in 80 cyclic tests in which 100 cycles of loading between 5 to 90% of the specified yield strength was completed. Some of these specimens were subsequently tested under an additional 100 cycles of loading. No signs of deterioration and no failure was observed. Furthermore, eight of the specimens that experienced 100 cycles of loading were monotonically pulled to failure. Similar strength compared to the corresponding specimens receiving no cyclic loading was achieved. Slip tests showed that there is no tendency for the rebar to move within the coupler prior to developing the full splice strength. It was concluded that Bar-Lock L-Series couplers are acceptable alternative mechanical splices for nuclear safety-related applications. This specific coupler is categorized by Caltrans as "service" splices, but there are other SSC couplers that are categorized as "ultimate" splices by Caltrans (App. A).

Four SMA-steel bar connections were tested by Hillis and Saiidi (2009) under slow-strain rate using shear screw couplers (Fig. 1-5). This SSC type had three screws to link the coupler to each bar. No. 4 (Ø13 *mm*) SMA bars were connected to the same size Grade 60 reinforcing steel bars. The SCC splice could develop the full tensile capacity and ductility of the spliced SMA bars. No failure of the couplers and no slippage at the coupler region were observed. All the specimens failed due to rupture of SMA bars at the thread fixed in the tensile test machine grip, away from the coupler region.

Rowell et al. (2009) tested nine shear screw coupler specimens connecting No. 10 (Ø32 *mm*) ASTM A615 Grade 60 steel bars under three strain rates: slow-rate (3500 micro-strains/*sec*), intermediate-rate (65000 micro-strains/*sec*) and rapid-rate (3200000 micro-strains/*sec*). Three specimens were tested under each strain rate. The couplers had seven screws to link each bar to the coupler. At slow-strain rate, bars fractured inside the coupler at the screw closest to the edge of the coupler in all three specimens, and the average ultimate load for the splice was 27% lower than that of the reference bars (Fig. 1-6a). The ductility was also significantly lower than that of the control bars. At

intermediate-strain rate, bars fractured inside the coupler in all three specimens and the average ultimate load for the splice was 16% lower than that of the reference bars (Fig. 1-6b). The average maximum elongation was reduced to 3% in comparison to 10% for the control bars. At high-strain rate, bars either ruptured inside the coupler or pulled out from the coupler (Fig. 1-6c). The average ultimate load for SSC splice was 24% lower than that of the reference bars and the average maximum strain was significantly lower (3%) than that of the control bars (14%). In summary, the dominant mode of failure was the bar rupture under the first or the second screw for these shear seven-screw couplers. This premature failure was due to stress concentration under the shear screws resulting in a lower ultimate stress and significantly lower ductility compared to the control bars.

Huaco and Jirsa (2012) (and later Huaco, 2013) tested two types of shear screw couplers, three-screw (ERICO S-series) and four-screw (ERICO B-series) for each bar, under half- and full-cycle loading tests. Ten specimens in which No 8 (Ø25 *mm*) ASTM A706 Grade 60 steel bars were connected to the couplers were tested, four with half-cycle loading protocol and six with full-cycle loading regime. The bar fractured on the edge of SSC with three screws (Fig. 1-7a) while the bar fractured outside of the coupler region with four screws (Fig. 1-7b). It was observed in the full cyclic tests that the longer SSC can sustain three times higher strains before the bars fracture compared to the shorter SSC.

Alam et al. (2010) tested nine specimens in which No. 4 to 6 (Ø13 to 19 *mm*) deformed and plain steel bars were connected using three-screw Dayton shear screw couplers. The test results showed that the full ultimate strength of both deformed and smooth bars can be achieved. The bars ruptured outside the splice in all specimens. Slippage of bars inside the couplers was minimal before yielding but significant slippage was reported after yielding. In an attempt to utilize this type of couplers for SMA bars, a modified version of the coupler was developed (Fig. 1-8) in which the number of screws for SMA bar was increased from three to nine and the screw ends were flat to avoid stress concentration. The SMA bars fractured at a strain of 6.4% inside the coupler due to stress or strain concentration.

Table 1-2 presents a summary of experimental studies performed on shear-screw couplers. It can be concluded that the tensile strength of these type of couplers may be sufficient for seismic applications depending on the product and manufacturer. However, these couplers generally limit the strain capacity of the bars due to stress or strain concentration under screws. This limitation is critical for seismic applications especially in the plastic hinge region where large deformations are expected.

1.3.2 Headed Bar Couplers (HC)

Experimental investigation on headed bar couplers was presented in a few studies. Sritharan et al. (1999) reported testing of several headed bar coupler specimens before the utilization of these couplers in a cap beam test model. Consistent mode of failure was observed in the tests but no additional information could be found in literature about the tests.

Rowell et al. (2009) tested nine specimens with headed bar couplers. The loading rates and the bar size were the same as those presented for shear screw couplers in the previous section. Full ultimate strength and significant strain capacity were observed at slow-strain rate tests. The average maximum strain was 11% in comparison to 10% for the control bars. The bars fractured outside the heat affected zone in these tests (Fig. 1-9a). Prior to connecting the bars, each bar is heated and the bar end is flattened to act as a head. At intermediate-strain rate, the average ultimate load for HC splice was comparable to the reference bars. The average maximum strain was reduced to 6% in comparison to 10% that was measured for the control bars. Bars fractured either inside or outside of the couplers (Fig. 1-9b). At high-strain rates, the average ultimate load for HC splice was 10% lower than that of the reference bars. The average maximum elongation was reduced to 7% in comparison to 14% achieved in the control bar tests. Similar to the intermediate strain rate tests, the bar rupture was either in the heat affected zones or outside the heat affected zone (Fig. 1-9c).

Haber et al. (2013) performed monotonic, cyclic, and dynamic tests on No. 8 (Ø25 *mm*) ASTM A706 Grade 60 steel bars in which bars were connected using headed bar couplers. Four, four, and two specimens were respectively tested under static, dynamic, and cyclic loading protocols. The mode of failure was bar fracture outside the couplers in all specimens (Fig. 1-10). Figure 1-11 shows the measured stress-strain relationship of specimens under static and dynamic testing. It can be seen that headed bar couplers allowed steel bars to sufficiently deform and the ultimate strain capacities of bars were achieved in both tests. Furthermore, large strains were measured in the coupler region, which can be a beneficial factor when these couplers are used in plastic hinges. Similar behavior was observed in cyclic tests.

A summary of the available test data on the performance of headed bar couplers is presented in Table 1-3. It can be inferred that the ultimate stress and strain capacities of bars can be achieved utilizing this coupler type.

1.3.3 Grouted sleeve couplers (GC)

Noureddine (1996) performed four tests on No. 18 (Ø57 *mm*) ASTM A615 and A705 Grade 60 steel bars in which grouted couplers were used to link the bars. Two specimens per each bar type were tested (Fig. 1-12). The specimens were tested under monotonic tensile loading to fracture. The average ultimate load for GC was comparable to the control bars. The average ultimate strains were approximately 7 and 12% for A615 and A705 bars, respectively. Three specimens failed due to bar rupture away from the coupler region and one sleeve failed at 3% strain.

Michigan Department of Transportation, MDOT, (Jansson, 2008) tested epoxy coated bars in open air connected with GC in which cyclic loading on three No. 6 (Ø19 *mm*) bars and three No. 11 (Ø36 *mm*) bars were tested in accordance with ASTM A1034. The tests were conducted on both thread-grout couplers (TGC) and splice sleeve grouted couplers (SSGC). For TGCs, the average slip was respectively 0.004 *in*. (0.1 *mm*) and 0.005 *in*. (0.13 *mm*) for the No. 6 (Ø19 *mm*) bars and No. 11 (Ø36 *mm*) bars, respectively. Fatigue testing demonstrated that the splices were able to withstand at least 1,000,000 cycles with

a stress range of 18 *ksi* (124 *MPa*), as specified by AASHTO LRFD. In ultimate load testing all specimens except for one (11AI) exceeded the AASHTO LRFD and MDOT requirement of 125 percent the yield strength, and specimen 11AI failed at a lower load. For SSGCs, the average slip was 0.007 *in*. (0.18 *mm*) and 0.009 *in*. (0.23 *mm*) for the No. 6 (Ø19 *mm*) bars and No. 11 (Ø36 *mm*) bars, respectively. Fatigue testing demonstrated that the splices were able to withstand at least 1,000,000 cycles with a stress range of 18 *ksi* (124 *MPa*). The average ultimate strength was 166 and 175% of the yield strength for the No. 6 (Ø19 *mm*) and No. 11 (Ø36 *mm*) bars, respectively. For TGCs, the threaded section of the coupler were found to be the common failure location for all splices tests, which are depicted in Figure 1-13, either due to fracture of the bar at the reduced threaded section or by shear failure of the threads themselves (Fig. 1-14). For SSGCs, different failure modes were observed but there was no discernable effect of the type of failure mode on the ultimate load of the splices (Fig. 1-15 and 1-16). Since both the thread-grout couplers and the splice sleeve grouted couplers performed well under testing for slip, fatigue, ultimate strength, and creep, they were recommended for MDOT use. It should be noted that there was no data on the strain capacity, which can be critical for seismic applications.

Rowell et al. (2009) tested nine No. 10 (Ø32 *mm*) ASTM A615 Grade 60 steel bars with grouted sleeve couplers. The specimens were subjected to the following three strain rates: slow-rate (3000-4000 $\mu\varepsilon/sec$), intermediate-rate (62000-65000 $\mu\varepsilon/sec$) and rapid-rate tests (3.2-3.8x10^6 $\mu\varepsilon/sec$). For each strain rate, three specimens were tested. The average yield and ultimate load for GC was comparable to those measured in the reference bars at slow-stain rate (Fig. 1-17). The average maximum strain was 6% in comparison to 10% for the control bars. At intermediate-strain rates, the average yield and the ultimate loads for GC were comparable to those of the control bars (Fig. 1-18). The average maximum elongation was reduced to 9% in comparison to 11% measured in the control bars. At rapid-strain rates, the average yield and ultimate loads for GC matched those of the control bars (Fig. 1-19). However, the average maximum strain was lower, 8% compared to 14% for the control bars. Three different failure modes were observed in the tests: rupture of the bar away from the grouted sleeve, pull out of the bar from the grouted sleeve, and failure of the sleeve.

Haber et al. (2013) performed tensile tests on No. 8 (Ø25 *mm*) ASTM A615 Grade 60 steel bars connected using grouted couplers. The specimens with GC connections were subjected to two strain rates, slow-rate (1000-8000 $\mu\varepsilon/sec$) and intermediate-rate (70000 $\mu\varepsilon/sec$). Three specimens for each strain rate were tested. Furthermore, cyclic tests were performed to investigate the effect of strain reversals. The average ultimate load for GC splice was comparable to the reference bar ultimate strengths. The average maximum strain was the same as that for the control bars (16%) at slow loading rate and also for the intermediate-rate. The strain in the sleeve region was very low, with maximum strain of 0.7%. Figure 1-20 shows the measured stress-strain relationship of specimens under static and dynamic testing. The loading rate had negligible effects on the coupler performance, and ultimate capacities of the bars were developed. All the GC specimens failed due to bar fracture away from the coupler region (Fig. 1-21).

Ameli et al. (2015) tested six thread-grout couplers (TGC) connecting No. 8 (Ø25 *mm*) Grade 60 reinforcing steel bars. Bars pulled out from the grouted end of the couplers in all samples (Fig. 1-22). The splice withstood 1.2 times the bar yield strength prior to the bar pullout. This failure mode is attributed to the relatively low strength of the grout that was used in the test splice. The grout strength was 9.4 *ksi* (64.8 *MPa*) but the grout strength in MDOT tests (Jansson, 2008) with the same coupler type was 14.7 *ksi* (101.3 *MPa*). The manufacturer 28-day specified grout strength is 8500 *psi* (58.6 *MPa*).

A summary of available test data on the performance of grouted sleeve couplers is presented in Table 1-4, which is used in the following sections for the evaluation of this coupler type.

1.3.4 Threaded couplers (Straight thread and taper thread) (TC)

Noureddine (1996) performed tensile tests on No. 18 (Ø57 *mm*) ASTM A615 and A705 Grade 60 reinforcing steel bars. Four taper threaded coupler splice specimens were tested under monotonic tensile loading to failure. The average ultimate load for TC was 15% smaller than those observed for the control bars. The average ultimate strain was 2% for both A615 and A705 bar specimens, which was extremely low. All the TC specimens failed due to stripping of the threads (Fig. 1-23).

Rowell et al. (2009) tested 18 No. 10 (Ø32 *mm*) ASTM A615 Grade 60 mechanical splices in which nine taper threaded couplers and nine straight threaded couplers were incorporated to connect the bars (Fig. 1-24). Both type of coupler connections were subjected to three strain rates, slow-rate (3000-4000 $\mu\varepsilon/sec$), intermediate-rate (62000-65000 $\mu\varepsilon/sec$), and rapid-rate tests (3.2-3.8x10^6 $\mu\varepsilon/sec$). The average yield and ultimate loads for both coupler types were comparable to those of the reference bars at slow strain rate. For taper threaded couplers, the average maximum strain was 11% in comparison to 10% measured for the control bars. For straight threaded couplers, the average maximum strain was 7%, which was lower than that of the control bar. For taper threaded couplers at the intermediate-strain rate, the average yield load was comparable to the control bars, but the average ultimate load for the taper TC was 8% lower than the control bars. The average maximum elongation was 50% lower than that of the control bars. For straight threaded couplers, both yield and ultimate loads were close to the control bar. The ultimate elongation was 10% in comparison to 11% for control bar. At rapid-strain rate, the average yield load for taper threaded couplers was the same as the control bar yield load but the ultimate load was 24% lower than that of the control bar. The average maximum strain was 2% in comparison to 14% for control bars. For straight threaded couplers, both yield and ultimate loads were comparable to those measured in the control bars. The maximum strain measured was 11% compared to 12% measured in the control specimen. In summary, taper threaded couplers showed inferior performance with premature failure of the bars at the thread. However, the ultimate stress and strain capacities of the bars were developed when the straight threaded couplers were utilized.

A summary of the available test data on the performance of threaded couplers is presented in Table 1-5.

1.3.5 Swaged Couplers (SC)

Noureddine (1996) tested four No. 18 (Ø57 *mm*) ASTM A615 and A705 Grade 60 reinforcing steel bars, which were connected by swaged couplers. The specimens were tested under monotonic tensile loading to failure. The average ultimate load for the splice was comparable to that of the control bars. The average ultimate strain was respectively 8 and 9% for A615 and A705 bar specimens. The failure mode was either bar fracture away from splice or bar pull-out from the sleeve (Fig. 1-25). The study pointed that this splice is effective with energy dissipation mechanism through friction without serious degradation in load but its effectiveness cannot be relied for seismic cyclic forces that induces reversible loading.

Yang et al. (2014) tested three tensile specimens consisting of No. 8 (Ø25 *mm*) ASTM A615 Grade 60 steel bars connected using swaged couplers. The average yield and ultimate loads for these specimens were respectively 65 *ksi* (448 *MPa*) and 98 *ksi* (675 *MPa*), which were comparable to those measured for the reference bars. The average maximum strain exceeded 8%. All specimens failed due to bar rupture away from the coupler region (Fig. 1-26).

A summary of the available test data on the performance of swaged couplers is presented in Table 1-6.

1.4 Performance of Columns with Couplers

The seismic performance of columns incorporating different types of mechanical bar couplers has been investigated in a few studies. This section summarizes the findings from the literature search on this topic.

1.4.1 Columns with Shear Screw Couplers (SSC)

A quarter-scale, four-span bridge was tested by Cruz and Saiidi (2012) in which shear screw couplers were used in one of the three, two-column bents to connect SMA bars to steel bars anchored in the footing and steel bars above the plastic hinge at the column base (Fig. 1-27). The bridge was tested on shake tables under seven simulated earthquake runs. The measured force-displacement envelopes for the bent is shown in Fig. 1-28. It can be seen that the drift capacity of the bent exceeded 5% with no bar fracture or coupler failure. The testing of the bridge model was terminated due to failure in a different bent.

Huaco and Jirsa (2012) and Huaco (2013) incorporated short and long shear screw couplers in the repair of two severely damaged concrete columns, which were tested under a double-curvature configuration under cyclic loading (Fig. 1-29). The repair of the first column consisted the utilization of short SSCs at the column base after removing concrete and the original reinforcement (Fig. 1-30) as well as the incorporation of glass fiber reinforced polymer (GFRP) at the top of the column. Since the damage in the second column was severe, the column concrete and reinforcement were completely

replaced with new materials but the original column was cut into two halves and each repaired segment was tested as a cantilever (Fig. 1-31). Short SSCs were incorporated in the base of one of the columns to connect the repaired segment to the existing footing and long SSCs were used in the second piece at the base. The difference between the short and long couplers is the length of the coupler to accommodate a higher number of screws. Three screws were used in the short couplers for each bar and four screws were utilized in the long coupler for each bar. Figure 1-32 shows the measured original and repaired column force-displacement hysteretic curves. It can be seen than the columns with short SSCs exhibited lower drift capacity compared to the reference test model but with similar lateral strength, and the column with longer SSC couplers showed higher drift capacity and higher strength compared to the reference test model. The limited drift capacity of the columns with short SCCs was attributed to the insufficient strain capacity of the short shear screw couplers. Six bars fractured under low displacements due to stress concentration under the end screw of the short SSCs close to the column base. Flat-end screws reduced stress concentration, thus shifting the bar fracture point to outside the long SCCs and resulting in large displacement capacity for the column.

Yang et al. (2014) used shear screw couplers (similar to the long couplers in the previous study) in the plastic hinge of a severely damaged bridge column to replace buckled bars with new reinforcement (Fig. 1-33). The couplers were the only SSC that are rated as "ultimate" splices by Caltrans. FRP was utilized on the entire column height to increase confinement as well as shear capacity of the column. The repaired column (R-Calt-1) was tested under reversed cyclic loading to failure. Figure 1-34 shows the measured repaired and original columns force-displacement behavior. The repaired column exhibited a displacement ductility capacity of 4.9, which was 4% higher than that of the original column. The lateral strength of the repaired column was 20% higher than that of the original column on average.

In summary, it can be inferred that columns with the long shear screw couplers will exhibit better seismic performance over columns with short shear screw couplers since bars connected with short shear screw couplers will experience premature failure. Table 1-7 presents the summary of findings regarding columns with SSCs.

1.4.2 Columns with Headed Bar Couplers (HC)

Haber et al. (2014) tested two, half-scale precast bridge columns in which headed bar couplers were incorporated in the plastic hinge area to connect the columns to the footings (Fig. 1-35). Precast pedestal was utilized in one of the specimens (HCPP) to shift the couplers away from footing surface and to investigate effects of lower moment demand on the couplers. The columns were tested under slow cyclic loading to failure, and the response was compared with that of a reference cast-in-place column (CIP). The test results showed that both columns are viable precast columns for high seismic areas since similar mode of failure, plastic hinge damage, lateral strength, and displacement ductility capacities were observed compared to CIP. Figure 1-36 shows the measured force-drift envelope of the columns. It can be seen that all columns exhibited excellent displacement ductility capacity, which was 40% more than the AASHTO allowable

displacement ductility demand for single column bents (ductility of five, which is equivalent to 6.75% drift ratio for CIP). Therefore, it can be concluded that headed bar couplers allow columns to deform freely and to develop large displacement ductility suitable for high seismic regions of the country.

Tazarv and Saiidi (2014) incorporated headed bar couplers in a half-scale precast bridge column test model to link reinforcing NiTi shape memory alloy (SMA) bars to reinforcing SMA bars (Fig. 1-37). Other advanced materials such as ultra-high performance concrete (UHPC) and engineered cementitious composite (ECC) were utilized in the column-to-footing connection and the plastic hinge area, respectively. The column was tested similarly to the columns tested by Haber et al. (2013) and the response was compared to CIP. Column showed minimal damage, insignificant residual displacement, higher lateral strength, and slightly better displacement capacity (Fig. 1-38). The headed bar couplers allowed the column to undergo large deformations and no premature failure was observed.

Nakashoji and Saiidi (2014) tested two cast-in-place SMA-reinforced ECC bridge columns under cyclic loads. A reference RC column was also tested. Headed bar couplers were utilized to connect reinforcing SMA bars to reinforcing steel bars. The test variable was the length of SMA bars incorporated in plastic hinge area (Fig. 1-39) in which one column (entitled as SR99-LSE) was built with 1.0*D* long SMA bars (*D* is the column side dimension) and another column (entitled as SR99-SSE) was constructed with 0.75*D* long SMA bars. The drift capacity in both columns was substantially higher than that of the reference column (Fig. 1-40) confirming that headed bar couplers used in plastic hinge zone allowed the columns develop full plastic moment with high drift capacity.

Table 1-8 presents a summary of the findings on the seismic performance of columns with headed bar couplers.

1.4.3 Columns with Grouted sleeve couplers (GC)

Haber et al. (2014) built two half-scale precast bridge columns utilizing grouted couplers (Fig. 1-41). Similar to their previous test models, one column was built with precast pedestal (GCPP) and another column was constructed without pedestal (GCNP). Both columns were tested under cyclic loading to failure. The lateral strength of the columns was the same up to the first bar fracture compared to the reference column (CIP) but the displacement capacity and displacement ductility capacity of both columns were only 60% of those of CIP (Fig. 1-43). The relatively low displacement capacity was because of strain concentration under grouted sleeve couplers or precast pedestal in which bulky grouted couplers behaved similarly to large size reinforcement shifting the yielding below the coupler region, and also grouted ducts incorporated in the precast pedestal made the pedestal very stiff shifting damage below the pedestal. Tazarv and Saiidi (2014) proposed a new detailing for grouted coupler columns to enhance displacement ductility capacity in which the longitudinal bars were debonded in pedestal and the pedestal was cast-in-place (Fig. 1-42). A column was constructed using the new detailing (GCDP) and was tested under the same loading protocol used by Haber et al.

(2014). The force-drift envelope for GCDP is also shown in Figure 1-43. The displacement capacity was increased by 47% and the displacement ductility capacity was seven, which met the design target.

Pantelides et al. (2014) tested six half-scale precast bridge columns utilizing grouted couplers in which normal grouted couplers (such as shown in Fig. 1-12) were used in column-to-footing connections of three specimens and modified grouted couplers (such as shown in Fig. 1-13) were utilized in column-to-cap beam connections of the remaining three test models (Fig. 1-44). Couplers were grouted at both ends of the normal grouted couplers but in the modified grouted couplers one end of couplers was threaded to reduce the coupler length. The columns were tested under slow cyclic loading. The measured force-drift response of the columns with standard couplers at the column base is shown in Fig. 1-45. These columns exhibited 25 to 40% lower displacement ductility capacity compared to the reference cast-in-place column (CIP). The most ductile column was the column with grouted couplers installed immediately above the footing surface and with $8d_b$-debonded bars below the coupler level. The displacement ductility capacity of CIP was 8.9. Figure 1-46 shows force-drift relationship of column test models with modified couplers used in column-to-cap beam connections. It can be seen that the displacement ductility capacity of these columns was substantially lower (41 to 51%) than that of the reference column confirming that the modified grouted couplers are not suitable for high seismic regions.

A new detailing was proposed by Belleri and Riva (2012) (and later by Popa et al., 2014) for building columns. In this detail, corrugated steel ducts are placed in the plastic hinge of columns, footing starter bars are anchored in the ducts, then ducts are grouted after the column installation. Even though similar seismic behavior to reference specimens was reported in these studies, the application of this detailing would be difficult for bridge columns due to size of the ducts and large number of reinforcing bars that are needed in bridge columns.

A summary of the findings for grouted couplers is presented in Table 1-9.

1.4.4 Columns with Threaded couplers (TC)

Lehman et al. (2001) repaired a severely damaged column using threaded couplers then tested under cyclic loads. The column concrete in the plastic hinge area as well as a partial depth of footing concrete were removed and new reinforcement was connected to the column and footing existing bars using threaded couplers (Fig. 1-47). Force-displacement hysteretic curves for the original and the repaired column is shown in Fig. 1-48. It can be seen that the lateral strength in the repaired column was higher and the displacement capacity was improved compared to the original column. The higher displacement capacity of the repaired column was because of 2 *in*. (51 *mm*) extra clear cover which increased the column longitudinal bar resistance against buckling and fracture.

Saiidi and Wang (2006) utilized threaded couplers in a quarter-scale bridge column to connect reinforcing SMA bars to reinforcing steel bars in plastic hinge region (Fig. 1-49).

The column was tested on a shake table under 11 runs (Run 11 was 300% of the design level earthquake) during which the drift ratio was 4.8%. The test was stopped after Run 11 to prevent SMA bar failure. The column was then repaired by replacing the conventional concrete of the plastic hinge with ECC. The repaired column was tested under 15 runs (Run 15 was 400% of the design level earthquake) in which a drift capacity of 5.7% was reported. Figure 1-50 shows the force-displacement envelope of the two columns. Test was stopped because the selected motion was not able to impose more deformation to the column. Minor damage of ECC and no SMA bar fracture was observed in these tests. The threaded couplers performed well by allowing the column to deform freely and by transferring the stresses to adjoining bars.

Saiidi et al. (2009) tested two cast-in-place columns in which threaded couplers were incorporated in the plastic hinge region of these columns to link SMA bars to steel bars (Fig. 1-51). Conventional concrete was utilized in one of the SMA columns (RNC) and ECC was used in the plastic hinge of another SMA column (RNE). A reference column with conventional concrete and reinforcing steel bars was also tested (RSC). These columns were tested under cyclic loading to failure. Fig. 1-52 shows the measured force-drift envelope for the columns. The columns with threaded couplers showed equal or improved drift capacity compared to the reference column confirming the suitability of the application of threaded couplers in the plastic hinge of columns located in high seismic regions. No bar fracture was reported up to 10% drift ratio cycles. The test was continued for RNE to 14% drift ratio cycles in which one of the SMA bars fractured at the thread inside one of the bottom couplers.

A quarter-scale bridge column was tested by Varela and Saiidi (2014) in which threaded couplers were utilized to link reinforcing Copper-based SMA bars to reinforcing steel bars (Fig. 1-53). The column was tested on a shake table up to 350% of the design level earthquake. The column withstood a drift ratio of 11.8% in which two SMA bars fractured in a ductile manner. The ECC in the column plastic hinge was removed after testing to locate the bar fracture. It was found that both SMA bars fractured away from the threaded couplers as shown in Fig. 1-54. The authors also used threaded couplers in the plastic hinge of six deconstructible bridge columns and a three, two-column bent bridge model. The threaded couplers maintained the integrity of the connections in these tests and allowed the columns to deform freely (NSF-PFI Project, 2014).

Table 1-10 summarizes the findings on the seismic performance of columns with treaded couplers. It is worth mentioning that all of the abovementioned test models have utilized straight threaded couplers and column performance with taper threaded coupler yet to be studied.

1.4.5 Columns with Swaged Couplers (SC)

Yang et al. (2014) used swaged couplers in the plastic hinge of a severely damaged bridge column to replace buckled bars with new reinforcement (Fig. 1-55). FRP was utilized on the entire column height to increase confinement as well as the shear capacity of the column. The repaired column (R-Calt-2) was tested under reversed cyclic loading to failure. Figure 1-56 shows the measured repaired and original force-displacement

relationships. The repaired column exhibited a displacement ductility capacity of 2.4, which was 59% lower than that of the original column. The low displacement ductility of the repaired column was because of early termination of the test due to rupture of the FRP wrap under torsional loading. It was reported that the column ductility might have been higher since there was no bar fracture. The lateral strength of the repaired column was 30% higher than that of the original column.

Table 1-11 presents the summary of the findings. Due to a lack of extensive test data at the time of this writing, it would be difficult to conclusively evaluate the seismic performance of these couplers when used in columns.

1.5. Summary

A comprehensive literature search was conducted to collect experimental data regarding the most common types of mechanical bar splices. Test data included in this report was the performance of coupler itself under axial loading and the seismic performance of columns incorporating these coupler types in plastic hinge regions. The findings were summarized and tabulated in Table 1-1 to 1-11. These data will be used in the following sections to evaluate the performance of couplers and columns with these couplers.

Chapter 2. Seismic Performance of Couplers and Columns with Couplers

2.1 Introduction

A comprehensive literature review on the performance of five common types of mechanical bar splices was conducted in the previous section and the key findings were summarized. The findings are utilized in this section to evaluate the performance of different couplers.

Four steps need to be undertaken to evaluate the seismic performance of different mechanical bar splices for incorporation in column plastic hinge zones: (1) development of coupler acceptance criteria for seismic applications, (2) evaluation of seismic performance of couplers, (3) development of acceptance criteria for ductile columns incorporating couplers is plastic hinge region, and (4) evaluation of seismic performance of columns with couplers. These steps are presented herein.

2.2 Acceptable Seismic Performance for Couplers

As stated before, the current US codes prohibit the application of mechanical bar splices in the plastic hinge zone but allow the application of couplers in non-ductile, capacity-protected structural members, and outside plastic hinge zones of columns. Some of these codes categorize couplers (e.g. service, ultimate, type 2) for different usage. Acceptance criteria are spelled out in these codes, but it is important to note that these criteria (Table 1-1) may not be suitable for seismic applications since the criteria implicitly assume that the couplers are only used in non-critical sections where no significant plastic deformations and strains are expected under seismic actions.

The criteria required by the Caltrans Memo to Designers 20-9 (2014) are adopted as baseline in the present study, but major modifications are made to develop minimum acceptance criteria for the utilization of couplers in plastic hinges. The requirements are:

1. Total length of a mechanical bar splice (L_{sp}) shall not exceed $15d_b$ (d_b is the diameter of the smaller of the two spliced bars) (Fig. 2-1a). This is to minimize adverse effects of coupler length on rotational capacity of a ductile member.

2. A spliced bar shall fracture outside coupler region regardless of loading type (e.g. monolithic, cyclic, or dynamic). The coupler region is defined as the length of a coupler plus 1.0d_b from each face of the coupler (Fig. 2-1b). Only ASTM A706 reinforcing steel bars shall be used for seismic applications.

Tensile testing of spliced bars shall be according to California Test 670 (2004). This test procedure is only applicable to couplers with total length of 10d_b or less ($L_{sp} \leq 10d_b$). Nevertheless, this test procedure is slightly modified in the present study to allow larger couplers for testing in which the length of the middle zone used for strain measurement is changed from a fixed length of 8 *in*. (200 *mm*) to $L_{sp} + 2d_b$. Fig. 2-1c illustrates the proposed strain measurement zones. The maximum strain measured outside the coupler region is the strain capacity of the spliced bar. Bar slip is not considered as a critical parameter for mechanical bar couplers since small slippage may be a source of energy dissipation under cyclic loading and may be desirable. For the purpose of analytical modeling, the coupler slip (including elongation of the bars inside the coupler region) can be estimated by measuring the strain of the middle zone shown in Fig. 2-1c.

The AASHTO Guide Specifications (2014) presents the expected mechanical properties for ASTM 706 reinforcing steel bars. These requirements are adopted in the present study. For example, the strain capacity of a spliced bar (the largest strain measured over an 8-*in*. (200-*mm*) gage length of the spliced bar outside the coupler region as shown in Fig. 2-1c) should exceed 12% for No 10 (Ø32 *mm*) and smaller bars. For No 11 (Ø36 *mm*) and larger bars the strain capacity of the spliced bar shall exceed 9% (Fig. 2-1d). Other types of steel bars shall not be used as bridge columns longitudinal reinforcement in seismic zones.

2.3 Evaluation of Seismic Performance of Couplers

A summary of air test of couplers conducted by several researchers was presented in Tables 1-2 to 1-6. The criteria described in the previous section were utilized to accept or reject a coupler for application in plastic hinges of bridge columns. Note that acceptance of a coupler for seismic applications does not guarantee satisfactory performance of columns incorporating these couplers in plastic hinges of columns in high seismic regions.

Table 2-1 to 2-5 present the results of evaluation for different coupler types for potential seismic applications based on the criteria discussed in the previous section. It can be seen that shear screw couplers may or may not meet the criteria depending on the manufacturer and product series. Eight shear screw coupler types are available in the US market at the time of this writing. Due to a lack of test data, each shear screw coupler type needs to be tested according to the proposed method for a better evaluation. Headed bar couplers have shown satisfactory performance under slow loading. However, their performance is uncertain under dynamic loading because these couplers met the minimum requirements in one study but failed in another study. Threaded-grouted couplers are not recommended for seismic applications. Results of studies on regular grouted couplers have been mixed in that these couplers met the minimum requirements in one study but failed in three other studies. Taper threaded couplers are not

recommended, but straight threaded couplers meet the minimum requirements. Swaged couplers also meet the acceptance criteria and may be used in critical section of ductile members.

In general, an extensive experimental program is needed to evaluate each coupler type made by different manufacturer for seismic applications. The test program should include static, cyclic, and dynamic loading to sufficiently evaluate each coupler type.

2.4 Acceptable Seismic Performance for Columns with Couplers

For seismic response of columns with couplers (CWC) to be acceptable, certain displacement ductility capacity and lateral load strength requirements should be met. It is reasonable to base these requirements relative to ductility and strength of a similar reference column with no couplers (CIP). The proposed acceptance criteria for columns incorporating couplers in plastic hinges are:

1. When the displacement ductility capacity of CIP is five or less, the displacement ductility capacity of CWC should be at least equal to the ductility capacity of CIP. For other cases, the displacement ductility capacity of CWC should be the greatest of (a) 90% of CIP ductility capacity, and (b) five. Either displacement or drift capacity may be used in evaluation of columns with advanced materials.
2. The lateral load strength of CWC should not be less than 95% of the CIP strength when the displacement ductility capacity of CIP is five or less. For other cases, the lateral strength of CWC should not be less than 90% of CIP strength.

These requirements are to ensure that the application of couplers will not adversely affect the displacement ductility and the lateral load capacity of a column. The allowance of 10% for displacement ductility capacity is made only for very ductile columns. The 10% allowance in the lateral strength is within scatter in measured lateral load strength of similar columns. Premature failure of couplers (e.g. bar pullout from couplers or coupler fracture) could affect the ductility or the lateral strength, but the size and location of couplers generally only affect the ductility.

2.5 Evaluation of Seismic Performance of Columns with Couplers

Past application of mechanical bar splices in plastic hinge region of columns was reviewed in the previous sections and a summary of the findings was presented in Table 1-7 to 1-11. These columns are seismically evaluated based on the criteria specified in the previous section, and the results are presented in Table 2-6 to 2-10.

Table 2-6 presents the evaluation results for columns with shear screw couplers. It can be inferred that the seismic performance of columns incorporating shear screw couplers depends on the coupler performance, location of the couplers, and distance of the couplers when they are used at two levels as shown in Fig. 2-2. It can be seen that the seismic performance of columns utilizing shear screw couplers at two levels was

generally better than those with shear screw couplers at one level. The seismic performance of columns incorporating two-level couplers with a minimum coupler distance of 1.0D (or 36d_b) was satisfactory.

All column test models incorporating headed bar couplers passed the minimum requirements and exhibited satisfactory seismic performance (Table 2-7). Headed bar couplers were used at two levels (Fig. 2-3). Neither location of these couplers nor distance between the couplers had significant effect on the overall performance of the columns. All of these columns were tested under slow cyclic loading. Since headed bar couplers showed poor performance under dynamic loading in one study (Table 2-2), shake table testing of columns with this coupler type should be conducted for complete evaluation.

Test data regarding the seismic performance of columns utilizing grouted coupler is more extensive than data for other coupler types (Table 2-8). None of the column test models with this coupler type met the requirements except for one column in which grouted couplers were shifted half a column diameter (0.5D) above the footing surface and the column longitudinal bars were debonded in a cast-in-place pedestal. As shown in Fig. 2-4, the length of these couplers is relatively large, which limits the column rotational deformation in the coupler region. Furthermore, these couplers are bulky and behave similarly to large size reinforcement resulting in shifting the nonlinearity away from the coupler region. It can be inferred from the test data (Fig. 2-4) that debonding of column longitudinal bars in the vicinity of the grouted couplers significantly enhanced the seismic performance due to spread of bar yielding.

Test data is available only for columns with straight threaded couplers (Table 2-9). Seismic evaluation of these columns showed that three out of four columns with this coupler type met the minimum requirements and the location of the coupler had insignificant effect on the overall behavior (Fig. 2-5). One column model could not be evaluated due to a lack of test data for a reference column, but this column showed 14% drift ratio capacity, which is beyond the practical range. The minimum distance between two vertical couplers was 26d_b (or 0.85D).

The only available test data on the seismic performance of column utilizing swaged couplers (Table 2-10 and Fig. 2-6) is inconclusive because the column was subjected to high torsion, which was not present in other column tests.

2.6. Summary

Minimum requirements were established to evaluate performance of mechanical bar splices for seismic applications and to evaluate seismic performance of columns incorporating couplers in the plastic hinge region. It was found that coupler performance varies for different loading rates and even for the same type of coupler produced by different manufactures. Furthermore, the location of the coupler is critical for large size couplers, and special detailing is needed to achieve large displacement capacities. Satisfactory performance was usually observed for small size couplers in which their location had insignificant effect on the column seismic behavior.

Chapter 3. Evaluate Constructability of Different Coupler Types

3.1 Introduction

A state-of-the-art literature review on the performance of five common types of mechanical bar splices was performed in previous sections, the key findings were tabulated, and methods were developed to evaluate the performance of couplers for seismic applications and to evaluate the seismic performance of columns incorporating couplers in plastic hinge zones. The constructability of different coupler types is discussed in this chapter and evaluated to further assist designers in the selection of different coupler types. The approach to address the constructability of couplers is based on ACI 439.3R-07 (2007), which provides information regarding many mechanical bar coupler types, their installation procedure, and tolerance.

3.2 Constructability of Different Coupler Types

Five common coupler types are shown in Fig. 1-2. Each coupler type is unique with respect to physical features and installation procedure. For example, bars are inserted into a sleeve in a shear screw coupler, then the screws are torqued to a specified level. The size of the sleeve, number of the screws, and torque vary depending on the manufacturer. In a grouted sleeve coupler, the bars are anchored by filling the sleeve with non-shrink, high-early strength grout. Other couplers have their own installation procedure and manufacturer guidelines have to be followed to ensure the quality of splices.

Clear cover for sections with couplers shall be based on design codes (e.g. AASHTO LRFD or AASHTO Guide Spec) thus the clear cover for mechanically spliced bar members is generally thicker than that in typical cast-in-place sections. The minimum and maximum clear distances between the mechanical splices are recommended to be the same as those specified for reinforcing steel bars. That is, large diameter couplers may be staggered to meet the bar distance requirements. Another case for staggering is when a special tool that is needed to complete the splice (e.g. press machine in swaged couplers) is bulky and would not fit between two couplers to complete the splice. Table 3-1 presents tools that are needed to complete different mechanical bar splices.

Table 3-1 also presents other construction considerations that must be reviewed by the engineer prior to the field application. The end of the spliced bars shall be prepared in headed bar couplers and threaded couplers. Heading can be done off- or on-site but in-situ threading of bars for repair is impractical. Type, size, and grade of screws in shear screw couplers must be verified and provided by the manufacturer. Grout in the grouted couplers shall be provided by the coupler manufacturer only and conventional grout or grout from other coupler manufacturers should not be used. Some of the coupler types such as headed bar couplers or threaded couplers impose very tight constructional tolerances.

3.3 Speed of Construction for Different Couplers

Table 3-1 presents two measures to evaluate the construction speed of each coupler type: (1) field erection speed for precasting in which the coupler installation method and its tolerance were considered, and (2) time that is needed to complete one splice. Since coupling mechanism in the headed bar couplers and the threaded couplers is essentially related to the threads requiring tight tolerances, these couplers may not be erected as fast as the others. All couplers require relatively short time to install and become functional but the grout in grouted couplers requires curing for at least 24 hours.

3.4 Speed of Construction for Columns with Different Couplers

It is expected that the application of mechanical bar couplers for precast columns will substantially reduce on-site construction time with potential cost saving. Marsh et al. (2011) estimated the time that is needed to complete a fully cast-in-place, three-column bent (Fig. 3-1) then compared the results with a similar bent but incorporating precast columns and precast cap beam. The bent was sized as a typical freeway overpass in Washington State and grouted coupler was assumed in the precast bent. The work of Marsh et al. was extended to other types of couplers in the present study (Table 3-2). It can be inferred that the application of mechanical bar splices as the main precast member connection will shorten the on-site activity by 60% or more compared to the cast-in-place bent. Regardless of the type of the coupler being used, the time saving was almost the same for these couplers.

3.5. Summary

This chapter was dedicated to the constructability of different coupler types. Important considerations that are needed before field deployment were highlighted, and speed of construction for each coupler type and speed of construction for precast columns incorporating couplers were evaluated. It was found that the application of mechanical bar couplers at both ends of precast columns will shorten the construction time by approximately 60% for a three-column bent regardless of the type of the coupler.

Chapter 4. Effect of Mechanical Bar Splices on Seismic Performance of Bridge Columns

4.1 Introduction

Findings of the literature search demonstrated that size, location, and type of mechanical bar splices can significantly affect the seismic performance of columns incorporating splices in the plastic hinge region. There is a variety of coupler types available in the U.S. market, each with a unique mechanism and performance. The volume of seismic performance data for columns incorporating these couplers is limited. Hence, conclusive trends cannot be established based on merely the available test data that were discussed in previous chapters. Therefore, an extensive parametric analytical study was conducted and described in this chapter to understand the trend of the coupler effect on the bridge column seismic behavior.

4.2 Generic Model for Mechanical Bar Splices

The coupler region and bar regions can be determined for each mechanical bar splice as shown in Fig. 4-1a. The coupler region length (L_{cr}) includes the coupler length (L_{sp}) plus α times the bar diameter ($\alpha . d_b$) from each end of the coupler in which α was previously specified to be 1.0 (chapter 2). When a mechanical bar splice is under tension, it can be assumed that only a portion of the coupler length contributes to the overall elongation of the connection and the remaining portion of the coupler (βL_{sp}) is rigid due to the relatively large diameter of the coupler or its anchoring mechanism. β is defined as the coupler rigid length factor. Therefore, for the same tensile force, the coupler region axial deformation will be lower resulting in a lower strain in the coupler region (ε_{sp}) compared to the strain of the connecting reinforcing bar (ε_s):

$$\frac{\varepsilon_{sp}}{\varepsilon_s} = \frac{L_{cr} - \beta L_{sp}}{L_{cr}} \tag{4-1}$$

or:

$$\frac{\varepsilon_{sp}}{\varepsilon_s} = \frac{(1-\beta)L_{sp} + 2\alpha d_b}{L_{sp} + 2\alpha d_b} \tag{4-2}$$

It can be assumed that the bar stress is independent of the presence of the coupler or its size, stiffness, and anchoring mechanism as long as the couplers are stronger than the connecting bars. It is well understood that couplers that are not at least as strong as the connecting bars are unacceptable.

Overall, the stress-strain relationship of any type of mechanical bar splices (Fig. 4-1b) can be determined by knowing only the coupler rigid length factor (β). The condition in which $\beta = 0$ is similar to a non-spliced connection in which the stress-strain of the coupler region is the same as the reinforcement stress-strain. Strain modification accounting for the coupler effect was first proposed by Haber et al. (2015) in which they introduced elastic and plastic scaling factors to modify the coupler strains.

4.3 Coupler Rigid Length Factor

Haber et al. (2015) analytically investigated the seismic performance of bridge columns incorporating grouted couplers. Air test results of the grouted couplers and the headed bar couplers were also presented in this study. They reported that there is approximately a linear relationship between the coupler region strains and the connecting steel bar strains as shown in Fig. 4-2. The linear relationship is more apparent for strains greater than 2%. The coupler rigid length factor (β) can be calculated based on the slope of the curves. Table 4-1 presents the measured coupler rigid length factors for headed bar and grouted couplers. Currently, there is no test data to obtain this factor for shear screw, threaded, and swaged couplers but factors are suggested in Table 4-1 for these couplers based on an engineering judgement and data for other coupler types. More testing is required to determine the coupler rigid length factor for different coupler types and series before field deployment.

To validate the proposed coupler modeling method, the measured and the calculated stress-strain relationships of a grouted coupler are shown in Fig. 4-3. It can be seen that the model captures the measured behavior well. Figure 4-4 shows the stress-strain relationship of the coupler region for two extreme rigid length factors. It is clear that the larger β significantly increases the overall stiffness.

4.4 Mechanically Spliced Column Model Verification

Haber et al. (2014) tested four half-scale precast columns incorporating mechanical bar splices as discussed in previous chapters. The grouted coupler column test model with pedestal (GCPP) was selected for the validation of the proposed coupler modeling method. Haber et al. (2013) developed an analytical model for this column to simulate the measured response. The bond-slip at the column-to-footing interface, bar slip at both ends of the couplers, coupler force-displacement relationship, and precast pedestal with grouted ducts were included in the model. To validate the coupler modeling method in bridge column analysis, the analytical model developed by Haber et al. (2013) was utilized in this section but the elements representing the coupler bond-slip effects and the coupler force-displacement relationship were replaced by steel fibers mimicking the proposed coupler stress-strain behavior. Figure 4-5 shows the measured and calculated

pushover curves. It can be seen that there is a good correlation between the calculated and the measured data.

4.5 Parametric Study

An extensive parametric study was carried out to investigate coupler effects on the seismic performance of bridge columns. Twelve reference cast-in-place (CIP) reinforced concrete columns with no couplers were designed according to the AASHTO Guide Specifications (2014) to achieve displacement ductility capacity of 3, 5, and 7. Two axial load indexes of 5 and 10%, and three column aspect ratios of 4, 6, and 8 were included in the analysis. The axial load index is defined as the ratio of the column axial load to the product of the specified column concrete compressive strength and the column gross section area. The aspect ratio is the ratio of the column height to the column diameter. Table 4-2 presents basic properties assumed in the design and analyses and Fig. 4-6 shows pushover relationship for a few sample of the CIP columns.

4.5.1 Spliced Column Model

Figure 4-7 shows the detail of the spliced column model incorporating single-level couplers. It is assumed that the column has a pedestal to help alleviate plastic hinge rotation demand on the couplers by shifting the coupler location. Three force-based elements, each with five integration points were used to model the pedestal, coupler region, and the remaining portion of the column. The properties of the steel fibers in sections within the coupler region were based on the proposed coupler stress-strain relationship while the original reinforcing steel fibers were used in other fiber-sections. Pushover analysis was performed to investigate the coupler effect on the force-displacement behavior of the spliced columns. The ultimate displacement of each column was determined when either core concrete failed (when core concrete strain was 1.5 times the ultimate strain capacity of the calculated core concrete), reinforcing steel bars at the column-to-footing level fractured (when the steel strain reached the ultimate strain capacity specified by the AASHTO Guide Specifications), or the lateral load dropped by 15% . The displacement ductility was calculated as the ratio of the ultimate displacement capacity to the effective yield displacement as defined in the AASHTO Guide Specifications (2014). The $P-\Delta$ effect was included in all columns.

The effect of double-level couplers spaced vertically at S_{sp} on center was also studied. The modeling method for these columns was the same as that demonstrated for the spliced columns with single-level couplers but two more elements were added in which one element was to model the column sections between the two levels of the couplers and the second element was to include the second coupler region.

4.5.2 Parameters

Effects of variation in important parameters related to couplers was studied for the columns described in the previous section. These parameters were coupler length (L_{sp}), pedestal height (H_{sp}), coupler rigid length factor (β), and the vertical distance of couplers

(S_{sp}) in the case of columns with a pair of couplers on each bar. The focus of the study was on the displacement ductility capacity of columns.

Three coupler lengths (L_{sp} = 5d_b, 10d_b, and 15d_b), four pedestal heights (H_{sp} = 5d_b, 10d_b, 20d_b, and 30d_b), three rigid length factors (β = 0.25, 0.50, 0.75), and two vertical coupler spaces (S_{sp} = 2L_{sp} and 4L_{sp}) were included in the analysis addressing all practical combinations of these parameters.

4.6 Parametric Study Results

Figures 4-8 to 4-16 show the results. Overall 560 analyses were carried out in the parametric study. The spliced column ductility (μ_{sp}) was normalized to its counterpart CIP column ductility (μ_{CIP}). Therefore, a normalized ductility ratio of one or greater indicates that the coupler had no adverse effect on the displacement ductility capacity. These figures clearly show that larger couplers, couplers closer to the column-to-footing interface, and more rigid couplers (e.g. grouted couplers) significantly reduce the spliced column displacement ductility capacity. In other words, coupler length (L_{sp}), pedestal height (H_{sp}), and coupler rigid length factor (β) are the most critical parameters that affect the displacement ductility capacity of mechanically spliced columns, but the effect of other parameters such as axial load index or the aspect ratio is minimal.

Furthermore, the results show that mechanical bar splices can reduce the displacement ductility capacity of the spliced column by up to 40% when very rigid, very long couplers are installed immediately above the column-to-footing interface. Shifting the couplers from the column-to-footing interface by one-half the column diameter (0.5D_c) significantly improved the displacement ductility capacity of the spliced columns and made them comparable to CIP columns. Another finding was that the coupler effect was more profound on columns with higher ductilities. For example, the displacement ductility of a spliced column is expected to be 95% of the CIP column displacement ductility when the CIP displacement ductility is 3. However, this ratio is 85% when the CIP displacement ductility is 7.

The effect of double-level couplers on the displacement ductility capacity is shown in Fig. 4-16. It was found that the ductility of columns with two couplers on a reinforcing bar is approximately the same as the ductility of single-level coupler columns when couplers are vertically spaced at least 2L_{sp} on center (or 1.0L_{sp} face-to-face).

4.7 Proposed Design Equation

To develop a design equation, the pedestal height (H_{sp}) was normalized to the coupler length (L_{sp}) then the ductility ratio was plotted against H_{sp} / L_{sp} for all analyses (Fig. 4-17). The results followed a hyperbolic relationship for a given coupler rigid length factor (β). Based on this observation, a hyperbolic equation accounting for the coupler effect based on the lower bound of the parametric study results was developed as:

$$\mu_{sp}/\mu_{CIP} = (1 - 0.18\beta)\left(\frac{H_{sp}}{L_{sp}}\right)^{0.1\beta} \quad (4\text{-}3)$$

where μ_{sp} is the spliced column displacement ductility and μ_{CIP} is the non-spliced cast-in-place column displacement ductility. H_{sp} can be taken as 0.1 $in.$ (2.5 mm) for columns in which the couplers are installed immediately above or below the column to adjoining member interface. The proposed equation is included in Fig. 4-17 for different coupler rigid length factors with solid lines. The equation is conservative in a way that the spliced column ductility was based on the lower bound of normalized ductility ratios, overestimating the ductility reduction for spliced columns. Furthermore, the proposed equation is independent of the displacement ductility itself, even though the parametric study showed that the non-spliced columns with lower target displacement ductility are less sensitive to the incorporation of couplers (Fig. 4-17a).

The proposed design equation is relatively simple and offers several advantages. The most important of which is that the designer can design columns using current codes (e.g. AASHTO Seismic Guide Specifications) then the reduced displacement ductility capacity can be estimated for the spliced column using the proposed equation.

4.8 Design Equation Validation

Table 4-3 presents three examples in which the calculated displacement ductility of spliced columns was compared with the measured displacement ductility of the reference columns. The selected test models had no bar debonding and no grouted ducts. It can be seen that the calculated displacement ductility of the spliced columns was very close to the measured ductilities for all three examples.

4.9 Summary

Findings of previous chapters showed that the seismic performance of columns incorporating mechanical bar splices in the plastic hinge area is not the same as conventional column performance. Since the test data was scarce, an extensive parametric study was carried out in this chapter to investigate coupler effects on the column overall behavior. First, a generic stress-strain model was developed to represent behavior of all types of couplers. Then, 12 conventional cast-in-place columns were designed according to the AASHTO Guide Specifications (2014) to serve as reference non-spliced columns. Subsequently, more than 550 analyses were conducted to investigate the effects of different coupler parameters on the displacement ductility capacity of the 12 aforementioned columns. It was found that the coupler length, the coupler location, and the rigidity of the coupler significantly affect the displacement ductility capacity of mechanically spliced columns. Finally, a simple design equation was developed to estimate the spliced column displacement ductility capacity relative to an equivalent non-spliced column based on the target displacement ductility and the coupler properties.

Chapter 5. Design Guidelines for Bridge Columns Incorporating Mechanical Bar Splices

5.1 Introduction

This chapter is dedicated to development of design guidelines for precast bridge column connections with mechanical bar splices reflecting findings reported in this project as well as recent studies. The proposed guidelines include recommendations (indicated by "R") and commentary (indicated by "C").

5.2 Proposed Guidelines

R1- Analysis and design of precast columns incorporating mechanical bar splices in the plastic hinge zones shall be in accordance to the AASHTO Guide Specifications (2014) except those requirements specified herein.

C1- Mechanically spliced precast bridge columns are analyzed and designed according to the AASHTO Guide Specifications (2014) but some of the modeling methods and design limitations need revision to take into account the mechanical bar splice (commonly referred to as "coupler") effects. Although the bulk of data that was utilized to develop these guidelines was obtained from precast column studies, these recommendations are also applicable to cast-in-place columns with couplers in plastic hinges.

R2- The coupler length (L_{sp}) shall not exceed 15 times the column longitudinal reinforcing bar diameter (d_b). When bars with two different sizes are linked by the coupler, L_{sp} shall be calculated based on the smaller bar diameter.

C2- Since couplers generally reduce column rotational capacity in the spliced zone, the length of couplers should be limited as specified.

R3- Only couplers in which failure occurs due to bar fracture outside the coupler region shall be permitted in the plastic hinge zone.

C3- The coupler region consists of the coupler length plus $1.0d_b$ away from each end of the coupler.

R4- The displacement ductility capacity of a mechanically spliced column shall be obtained from a pushover analysis.

C4- Moment-curvature analyses are unable to capture the coupler length and location effects on the displacement ductility capacity.

R5- The constitutive stress-strain relationship for a mechanical bar splice shall be as shown in Fig. R-1. In lieu of specific data for a particular coupler type, the properties provided in Table R-1 should be used.

C5- The length and the location of a coupler may be included in a pushover analysis using an additional fiber-section element (Element 2 in Fig. C-1) in which the constitutive relationship of the longitudinal reinforcement follows the coupler stress-strain behavior. The constitutive relationship for the remainder of the bar (Elements 1 and 3) is what is normally used for steel reinforcement.

R6- The displacement ductility capacity of a mechanically spliced column (μ_{sp}) shall be allowed to be calculated based to the conventional cast-in-place column displacement ductility capacity (μ_{CIP}) as:

$$\mu_{sp}/\mu_{CIP} = (1 - 0.18\beta)(\frac{H_{sp}}{L_{sp}})^{0.1\beta} \quad \text{(R-1)}$$

where β is the coupler rigid length factor obtained from the splice tensile tests or the coupler manufacturer and H_{sp} is the height of coupler from the column adjoining member interface (Fig. C-1). H_{sp} shall be taken 0.1 $in.$ (2.5 mm) when couplers are installed at the column to adjoining member interface.

C6- A mechanically spliced column displacement ductility capacity may be estimated using Eq. R-1 in lieu of a pushover analysis. A conventional column can be designed according to a displacement-based code (e.g. AASHTO Guide Specifications) then the displacement ductility capacity should be modified accounting for the coupler. Both moment-curvature and pushover analyses can be used to estimate the displacement ductility capacity of conventional columns. The coupler rigid length factor can be obtained from the coupler manufacturer for each product or from the splice tensile testing. In the absence of reliable test data or for preliminary design, the coupler rigid length factor may be conservatively taken as 1.0 assuming that the full length of the coupler is rigid.

R7- The spacing of two mechanical bar splices in the longitudinal direction of the member shall not be less than $2L_{sp}$ on center.

C7- Some of the proof-tested details to connect precat columns to their adjoining membes utilized two couplers per bar. The minimum distance specified for two couplers

installed on a bar ensures that the coupler adverse effect on the displacement ductility of the member is the same as that for members spliced with only one coupler on a bar.

5.3 Notation

d_b: Nominal diameter of column longitudinal reinforcing bar (*in., mm*)
f_y^{sp}: Expected yield stress in the coupler region (*ksi, MPa*)
f_u^{sp}: Expected tensile strength in the coupler region (*ksi, MPa*)
L_{sp}: Coupler length (*in., mm*)
L_{cr}: Coupler region length, $[L_{cr} = L_{sp} + 2d_b]$, (*in., mm*)
H_{sp}: Height of pedestal or distance between the bottom end of a coupler and the column adjoining member interface (*in., mm*)
S_{sp}: Spacing of couplers in the longitudinal direction of the member (*in., mm*)
β: Coupler rigid length factor obtained from mechanical splice test data or the coupler manufacture
ε_y^{sp}: Expected yield strain in coupler region
ε_{sh}^{sp}: Strain at onset of strain hardening in the coupler region
ε_u^{sp}: Ultimate tensile strain in the coupler region
μ_{CIP}: Displacement ductility capacity of conventional cast-in-place column
μ_{sp}: Displacement ductility capacity of spliced column

Chapter 6. Design Examples for Precast Bridge Columns Incorporating Mechanical Bar Splices

6.1 Introduction

A design guideline was presented in the previous chapter to facilitate the application of mechanical bar splices as a viable ABC connection. This chapter demonstrates the guideline application through two design examples of precast two-column bents utilizing grouted coupler connections. The grouted couplers were used at the base of the columns in the first example then were utilized at both ends of the columns in the second example. The examples include the application of the design equation to estimate the precast bent displacement ductility capacity.

6.2 Two-Column Bent Design

6.2.1 Cast-in-Place (CIP) Reference Bent

A CIP two-column bridge bent was designed based on the AASHTO Guide Specifications (2014) for a target displacement ductility of 6.0. Note that the initial design had to be based on the AASHTO LRFD Bridge Design Specifications (2013), which accounts for the frame action in calculating design forces. Fig. 6-1 shows the dimensions of the bent and Table 6-1 lists information about the bent and design considerations. Pushover analyses were performed using OpenSees (2014). The OpenSees modeling method of the CIP bent is summarized in Table 6-2 and pushover analysis results are shown in Fig. 6-2. The drift capacity of the bent was 4.7%, limited by compressive failure of the right column core concrete. The displacement ductility capacity of the bent was 6.57.

6.2.2 Coupler Properties

Grouted couplers were selected for the design of the precast bents. Table 6-3 presents the basic properties of the coupler as well as the material properties that were used in the coupler region of the bent model as steel fibers. Figure 6-3 shows the stress-strain relationships of the reinforcing steel bars and the grouted couplers. It can be seen that the

grouted coupler stress-strain relationship is significantly stiffer than that of the reinforcing steel bars in the initial and strain hardening parts.

6.3 Precast Bent with Couplers at Column Base Only

The grouted couplers were first incorporated at the base of the columns in which these couplers are installed immediately above the footing surface as shown in Fig. 6-4. The longitudinal bars were assumed to be fully bonded with concrete below and above the couplers. Figure 6-5 shows the precast bent pushover curves. It can be seen that the bent displacement ductility capacity was reduced from 6.57 to 5.14, a 22% reduction, due to the incorporation of the couplers.

6.4 Precast Bent with Couplers at Both Ends of Columns

To further investigate the coupler effects, grouted couplers were utilized at both ends of the columns (Fig. 6-6) immediately above or below the column to adjoining member interface. The pushover analysis (Fig. 6-7) showed that the bend displacement ductility capacity was reduced by 24% compared to that of the CIP bent because of the grouted couplers at both ends of the columns. Another finding was that the application of these couplers in the plastic hinges increased the lateral load capacity of the bent by 4%, which is insignificant.

6.5 Precast Bent Ductility Using Design Equation

The precast bent ductility may be estimated using the design equation presented in the guideline as:

$$\frac{\mu_{sp}}{\mu_{CIP}} = (1 - 0.18\beta)\left(\frac{H_{sp}}{L_{sp}}\right)^{0.1\beta} = (1 - 0.18 \times 0.65)\left(\frac{0.1}{16.4}\right)^{0.1\times 0.65} = 0.63$$

The proposed equation (H_{sp} is 0.1 in. when couplers are at the interface) suggests that the grouted couplers installed at either one end or both ends of columns will reduce the bent ductility by 37%, which is a conservative estimation of the bent ductility compared to what was found from the direct pushover analyses. Note that the design equation, which was originally developed for single-column bents, is independent of whether couplers are used at one or both ends of the columns.

The relatively large difference between the results from the pushover analyses and the design equation is because the equation is conservative particularly for cases with couplers installed at the interface. The difference and the degree of conservatism are smaller when the couplers are shifted. For example, when the grouted couplers in the second example were shifted by one-half column diameter ($0.5D$ = 24 in.) as shown in Fig. 6-8, the spliced bent displacement ductility capacity was 6.01 and 5.95 using the direct pushover analysis (Fig. 6-9) and the design equation, respectively, a difference of 1%.

In summary, the proposed equation is conservative and can be used as a viable tool for design of precast or cast-in-place columns with mechanical bar splices in lieu of conducting detailed pushover analysis.

Chapter 7. Summary and Conclusions

7.1 Summary

One of the key features of accelerated bridge construction (ABC) is prefabricated bridge columns. One method to connect prefabricated columns to footings or cap beams is through the use of mechanical bar splices or couplers. Current bridge seismic codes prohibit the application of couplers in the plastic hinge area of columns located in moderate and high seismic regions. Promising details have been developed in recent years demonstrating the feasibility of precast columns utilizing couplers in the plastic hinge zones. Recent research results provide an opportunity to revisit and perhaps remove the ban on couplers in current codes.

Several types of mechanical bar splices, each with different performance and anchoring mechanism are available in the U.S. market. Five of these were included in this study: shear screw, headed bar, grouted, threaded, and swaged couplers. A state-of-the-art literature search was conducted to compile and interpret data on the seismic performance of these coupler types as well as columns incorporating these couplers in column plastic hinge zones. Current U.S. codes were also reviewed to identify coupler limitations and applications. Findings were summarized and tabulated. Subsequently, coupler acceptance criteria for seismic applications and acceptance criteria for ductile columns incorporating couplers in plastic hinge region were developed. Then the seismic performance of the couplers and the columns was evaluated. Constructability and time saving of each coupler type were investigated. An extensive parametric study was conducted to investigate coupler effects on the column seismic behavior. A generic stress-strain model was also developed to simulate the behavior of all types of couplers. Furthermore, a simple design equation was developed to estimate the spliced column displacement ductility capacity based on the characteristic and geometry of the coupler and the column. The proposed equation was validated against columns test data. Finally, a design guideline as well as examples were developed to facilitate the field deployment of precast columns incorporating mechanical bar splices.

7.2 Conclusions

Findings from the literature search, evaluations, and analytical studies on mechanically spliced bridge columns led to the following conclusions:

1. Coupler performance varies for different loading rates and even for the same type of coupler produced by different manufactures. A rigorous testing program is needed to completely understand the performance of each coupler type and series.
2. Test data showed that the location of couplers in columns was critical for large couplers, and improved detailing should be devised to achieve large displacement capacities.
3. Satisfactory seismic performance was usually observed for small size couplers.
4. The application of mechanical bar splices at both ends of precast columns can shorten the construction time by approximately 60% for a three-column bent regardless of the type of coupler.
5. Coupler length should be less than $15d_b$ for seismic applications where d_b is the column longitudinal reinforcing bar diameter.
6. Couplers may be accepted for seismic application when the connecting bar/s fracture outside the coupler region, which includes the coupler length plus $1.0d_b$ from each end of the coupler. Couplers with dominant mode of bar fracture inside the coupler region or bar pullout should not be used in the plastic hinge of columns.
7. The stress-strain model developed for couplers is a simple and viable modeling method to account for the coupler effect in analysis and design of mechanically spliced elements. A coupler material model can be determined by only the coupler rigid length factor.
8. The parametric study showed that the coupler length, the coupler location, and the rigidity of the coupler significantly affect the displacement ductility capacity of mechanically spliced columns. Longer couplers, couplers closer to the column to adjoining member interface, and stiffer couplers may reduce a spliced column displacement ductility capacity by 40%.
9. The proposed simple design equation accounts for the coupler effect on the mechanically spliced column displacement ductility capacity and may be used for design of these columns.

References

1. AASHTO. (2013). "AASHTO LRFD Bridge Design Specification," Washington, DC, American Association of State Highway and Transportation Officials.
2. AASHTO. (2014). "AASHTO Guide Specifications for LRFD Seismic Bridge Design," Washington, DC: American Association of State Highway and Transportation Officials.
3. ACI 318. (2014). "Building Code Requirements for Reinforced Concrete," Detroit, Michigan: American Concrete Institute.
4. ACI 439.3R-07. (2007). "Types of Mechanical Splices for Reinforcing Bars," Reported by American Concrete Institute Committee 439, 24 pp.
5. Alam, M.S., Youssef, M.A., and Nehdi, M.L. (2010). "Exploratory Investigation on Mechanical Anchors for Connecting SMA Bars to Steel or FRP bars," Materials and Structures, Vol. 43, pp. 91-107.
6. Ameli, M.J., Parks, J.E., Brown, D.N., and Pantelides, C.P. (2015) "Seismic Evaluation of Grouted Splice Sleeve Connections for Reinforced Precast Concrete Column-to-Cap Beam Joints in Accelerated Bridge Construction," PCI Journal, March-April, pp. 80-103.
7. Belleri, A. and Riva, P. (2012). "Seismic Performance and Retrofit of Precast Concrete Grouted Sleeve Connections," *PCI Journal*, pp. 97-109.
8. California Test 670. (2004). "Method of Tests for Mechanical and Welded Reinforcing Steel Splices," Sacramento, CA, California Department of Transportation.
9. Caltrans. (2014). "Memo to Designers 20-9," Sacramento, CA, California Department of Transportation.
10. Caltrans. (2013). "Seismic Design Criteria (SDC)," version 1.7. Sacramento, CA, California Department of Transportation.
11. Cruz-Noguez, C.A., and Saiidi, M.S. (2010). "Experimental and Analytical Seismic Studies of a Four-Span Bridge System with Innovative Materials," Center for Civil Engineering Earthquake Research, Department of Civil and Environmental Engineering, University of Nevada, Reno, Nevada, Report No. CCEER-10-04, 685 pp.
12. Cruz-Noguez, C.A., and Saiidi, M.S. (2012). "Shake Table Studies of a 4-Span Bridge Model with Advanced Materials," *Journal of Structural Engineering, ASCE*, Vol. 138, No. 2, pp. 183-192.
13. Haber, Z.B., Saiidi, M.S., Sanders, D.H. (2015). "Behavior and Simplified Modeling of Mechanical Reinforcing Bar Splices," ACI Structural Journal, Vol. 112, No. 2, pp. 179-188.

14. Haber, Z.B., Saiidi, M.S. and Sanders, D.H. (2013). “Precast Column-Footing Connections for Accelerated Bridge Construction in Seismic Zones,” Center for Civil Engineering Earthquake Research, Department of Civil and Environmental Engineering, University of Nevada, Reno, Nevada, Report No. CCEER-13-08, 502 pp.
15. Haber, Z.B., Saiidi, M.S., and Sanders, D.H. (2014) Seismic Performance of Precast Columns with Mechanically Spliced Column-footing Connections. *ACI Structural Journal* 2014; Vol. 111, No. 3, pp. 339-650.
16. Hillis, D., and Saiidi, M.S. (2009). “Design, Construction, and Nonlinear Dynamic Analysis of Three Bridge Bents Used in a Bridge System Test,” Center for Civil Engineering Earthquake Research, Department of Civil and Environmental Engineering, University of Nevada, Reno, Nevada, Report No. CCEER-09-03, 82 pp.
17. Huaco, G. and Jirsa, J. (2012). "Performance of Damaged Column Retrofitted with Innovative Materials and Devices," 15th World Conference on Earthquake Engineering, 15WCEE, 10 pp.
18. Huaco, G. (2013). "Procedures to Rehabilitate Extremely Damaged Concrete Members Using Innovative Materials and Devices," PhD Dissertation, The University of Texas at Austin, 649 pp.
19. Jansson, P.O. (2008). “Evaluation of Grout-Filled Mechanical Splices for Precast Concrete Construction,” Michigan Department of Transportation, *MDOT Reort No. R-1512*, 74 pp.
20. Kanoh, Y., Imai, H., Matsuzaki, Y., and Sugano, S. (1988). “Performance Evaluation of Mechanical Joints of Reinforcing Bars,” *Proceedings of Ninth World Conference on Earthquake Engineering*, Tokoyo-Kyoto, Vol. IV, pp. 481-486.
21. Lehman, D.E., Gookin, S.E., Nacamuli, A.M. and Moehle, J.P. (2001). “Repair of Earthquake-Damaged Bridge Columns,” *ACI Structural Journal*, Vol. 98, No. 2, pp. 233-242.
22. Lloyd, W.R. (2001). "Qualification of the Bar-Lock Rebar Coupler for Use in Nuclear Safety-Related Applications Mechanical Testing Program and Performance Analysis," Idaho National Engineering and Environmental Laboratory Materials Department, Report No. INEEL/EXT-02-01387, 22 pp.
23. Marsh, M.L., Wernli, M., Garrett, B.E., Stanton, J.F., Eberhard, M.O. and Weinert, M.D. (2011). “Application of Accelerated Bridge Construction Connections in Moderate-to-High Seismic Regions,” Washington, D.C.: National Cooperative Highway Research Program (NCHRP) Report No. 698, 324 pp.
24. Nakashoji, B. and Saiidi, M.S. (2014). “Seismic Performance of Square Nickel-Titanium Reinforced ECC Columns with Headed Couplers,” Center For Civil Engineering Earthquake Research, Department Of Civil and Environmental Engineering, University of Nevada, Reno, Nevada, Report No. CCEER-14-05, 252 pp.
25. Nelson, R., Saiidi, M.S., and Sadrossadat-Zadeh, M. (2007) “Experimental Evaluation of Performance of Conventional Bridge Systems,” Center for Civil Engineering Earthquake Research, Department of Civil Engineering, University of Nevada, Reno, Nevada, Report No. CCEER-07-04, 464 pp.

26. Noureddine, I. (1996). “Plastic Energy Absorption Capacity of #18 Reinforcing Bar Splices under Monotonic Loading,” MSc Thesis, California State University, Sacramento, 108 pp.
27. NSF-PFI Project. (2014). Retrieved July 09, 2014, from http://wolfweb.unr.edu/homepage/saiidi/NSF-PFI/index.html.
28. O’Brien, M., Saiidi, M.S., and Sadrossadat-Zadeh, M. (2006). “A Study of Concrete Bridge Columns Using Innovative Materials Subjected to Cyclic Loading,” Center for Civil Engineering Earthquake Research, Department of Civil Engineering, University of Nevada, Reno, Nevada, Report No. CCEER-06-04, 246 pp.
29. Pantelides, C.P., Ameli, M.J., Parks, J.E., and Brown, D.N. (2014). “Seismic Evaluation of Grouted Splice Sleeve Connections for Precast RC Bridge Piers in ABC,” Utah Department of Transportation, Report No. UT-14.09, 168 pp.
30. Popa, V., Papurcu, A., Cotofana, D., and Pascu, R. (2014). “Experimental Testing on Emulative Connections for Precast Columns using Grouted Corrugated Steel Sleeves,” *Bulletin of Earthquake Engineering*, 10.1007/s10518-014-9715-9, 19 pp.
31. Rowell, S.P., Grey, C.E., Woodson, S.C., and Hager, K.P. (2009). “High Strain-Rate Testing of Mechanical Couplers,” US Army Corps of Engineers, Engineer Research and Development Center, Report No. ERDC TR-09-8, 74 pp.
32. Saiidi, M.S. and Wang H. (2006). “Exploratory Study of Seismic Response of Concrete Columns with Shape Memory Alloys Reinforcement,” *ACI Structural Journal*, Vol. 103, No. 3, pp. 436-443.
33. Saiidi, M.S., O'Brien, M. and Sadrossadat-Zadeh, M. (2009). “Cyclic Response of Concrete Bridge Columns Using Superelastic Nitinol and Bendable Concrete,” *ACI Structural Journal*, Vol. 106, No. 1, pp. 69-77.
34. Sritharan, S., Ingham, J., Priestley, M., and Seible, F. (1999). “Design and Persormance of Bridge Cap Beam/Column Using Headed Reinforcement and Mechanical Couplers,” Developments of Seismic Steel Reinforcement Products & Systems, SP-184, ACI Special Publication, Vol. 184, pp. 7-22.
35. Tazarv, M. and Saiidi, M.S. (2014). “Next Generation of Bridge Columns for Accelerated Bridge Construction in High Seismic Zones.” Center for Civil Engineering Earthquake Research, Department of Civil and Environmental Engineering, University of Nevada, Reno, Nevada, Report No. CCEER-14-06, 400 pp.
36. Varela, S. and Saiidi, M.S. (2014). “Dynamic Performance of Novel Bridge Columns with Shape Memory Alloy and ECC,” *International Journal of Bridge Engineering, IJBE*, Vol. 2, No. 3, pp. 29-58.
37. Wang, H. and Saiidi, M.S. (2005). “A Study of RC Columns with Shape Memory Alloy and Engineered Cementitious Composites,” Center for Civil Engineering Earthquake Research, Department of Civil Engineering, University of Nevada, Reno, Nevada, Report No. CCEER-05-1, 290 pp.
38. Yang, Y., Sneed, L.H., Morgan, A., Saiidi, M.S., Belarbi, A. (2014). “Repair of Earthquake-Damaged Bridge Columns with Interlocking Spirals and Fractured Bars,” California Department of Transportation Report No. CA 14-2179, 211 pp.

Tables

Table 1-1. Current US Code Restrictions on Mechanical Bar Couplers

Code	Splice Type	Stress Limit	Strain Limit	Max Slip	Location Restriction
ACI318 (2014)	Type 1	$\geq 1.25f_y$	None	None	Shall not be used in the plastic hinge of ductile members of special moment frames neither in longitudinal nor in transvers bars (Article 18.2.7)
	Type 2	$\geq 1.0f_u$	None	None	Shall not be used within one-half of the beam depth in special moment frames but are allowed in any other members at any location (Articles 18.2.7 & 25.5.7)
Caltrans SDC (2013)	Service	None	> 2%	None	No splicing is allowed in "No-Splice Zone" of ductile members, which is the plastic hinge region. Ultimate splices are permitted outside of the "No-Splice Zone" for ductile members. Service splices are allowed in capacity protected members (Ch. 8)
	Ultimate	None	> 9% for No. 10 (32 *mm*) and smaller[(a)] > 6% for No. 11 (36 *mm*) and larger[(a)]	None	
AASHTO (2013 & 2014)	Full Mechanical Connection[(b)]	$\geq 1.25f_y$	None	No. 3-14: 0.01 *in*. No. 18: 0.03 *in*.	Shall not be used in plastic hinge of columns in SDC C and D (AASHTO Guide Spec 2014, Article 8.8.3)

[(a)] For ASTM A706 Reinforcing Steel Bars. There is also a maximum strain demand limit (e.g. 2% for ultimate splices and 0.2% (the bar yield strain) for service splices) [Caltrans Memo to Designers 20-9].
[(b)]AASHTO LRFD (2013) Article 5.11.5.2.2.

Table 1-2. Summary of Studies on Shear Screw Couplers

Study	Coupler	Bar Size	Bar Type	Mode of Failure	Remarks
Lloyd (2001)	Three-screw, "Bar-Lock L-Series"	No. 6 (Ø19 *mm*) & No. 8 (Ø25 *mm*)	ASTM A615 Grade 60	Bar pullout, bar fracture	90% of the ultimate strength of the bar can be achieved
Hillis & Saiidi (2009)	Three-screw "Zap Screwlok Type 2"	No. 4 SMA bars to Steel Bars	NiTi SMA & Grade 60 Steel bars	SMA bar fractured inside the grip	No coupler failure and no SMA bar fracture inside the coupler was observed
Rowell et al. (2009)	Seven-screw "Zap Screwlok Type 2"	No. 10 (Ø32 mm)	ASTM A615 Grade 60	Mainly bar fracture inside couplers	Lower strength and significantly lower strain capacities were observed due to premature failure of bars
Huaco & Jirsa (2012)	Three-screw (S-series) and four-screw (B Series)	No. 8 (Ø25 *mm*)	ASTM A706 Grade 60	Bar fractured inside or away from coupler	Bar fractured on the edge of three-screw couplers and bar fractured outside of four-screw couplers, three times higher strain capacity for longer couplers was observed
Alam et al. (2010)	Three-screw "Bar-Lock S"	No. 4 to 6 (Ø13 to 19 *mm*)	Grades 40 and 60	Bar fracture	Low slippage was observed before yielding, sufficient strength was reported

Table 1-3. Summary of Studies on Headed Bar Couplers

Study	Bar Size	Bar Type	Mode of Failure	Remarks
Sritharan et al. (1999)	N/A	N/A	N/A	Consistent mode of failure
Rowell et al. (2009)	No. 10 (Ø32 mm)	ASTM A615 Grade 60	Bar fractured inside or outside of couplers	Approximately full ultimate strength was achieved in all tests, but the strain capacity of the system was adversely affected by increasing strain rate
Haber et al. (2013)	No. 8 (Ø25 mm)	ASTM A706 Grade 60	Bar fractured outside of couplers	Full ultimate stress and strain capacities were achieved under static, cyclic, and dynamic tests, strain in the coupler region was more than 8%

Table 1-4. Summary of Studies on Grouted Sleeve Couplers

Study	Bar Size	Bar Type	Mode of Failure	Remarks
Noureddine (1996)	No. 18 (Ø57 *mm*)	ASTM A615 Grade 60, ASTM A705 Grade 60	Bar fractured in three tests, coupler failed in one test	Ultimate loads were comparable to the reference bar load, bar fractured in three tests and large strains (e.g, 7% and 12%) were measured
Jansson (2008)	No. 6 (Ø19 *mm*), No. 11 (Ø36 *mm*)	Grade 60	Bar fracture, GC fracture, shear failure of threads	Minor slippage occurred, but still met AASHTO LRFD requirements. Ultimate loads and fatigue testing exceeded the requirements, no data on strain capacity
Rowell et al. (2009)	No. 10 (Ø32 *mm*)	ASTM A615 Grade 60	Bar pullout, bar fracture, GC fracture	For slow-, intermediate-, and rapid-strain tests, all specimens resulted in maximum strain less than the control bars
Haber et al. (2013)	No. 8 (Ø25 *mm*)	ASTM A615 Grade 60	Bar fracture	Bar fractured away from the coupler region in static, cyclic, and dynamic tests, ultimate stress and strain capacities of the bars were developed
Ameli et al. (2015)	No. 8 (Ø25 *mm*)	Grade 60	Bar pullout	Bar pulled out in all six samples. The grout strength was 9.4 *ksi*, 36% weaker than the grout used in Jansson (2008)

Table 1-5. Summary of Studies on Threaded Couplers

Study	Bar Size	Bar Type	Mode of Failure	Remarks
Noureddine (1996)	No. 18 (Ø57 mm), taper threaded	ASTM A615 Grade 60, ASTM A705 Grade 60	Shear failure of threads	Ultimate loads were 15% below control bars, premature failure (2% strain capacity) was reported due to failure of the threads
Rowell et al. (2009)	No. 10 (Ø32 mm)	ASTM A615 Grade 60	Tapered bars: bar rupture, thread failure. Straight bars: bar rupture	Bars connected with taper threaded couplers showed significantly lower strain capacity due to failure of the threads but bars connected with straight threaded couplers exhibited large stress and strain capacities similarly to the reference bars

Table 1-6. Summary of Studies on Swaged Couplers

Study	Bar Size	Bar Type	Mode of Failure	Remarks
Noureddine (1996)	No. 18 (Ø57 mm)	ASTM A615 Grade 60, ASTM A705 Grade 60	Bar pullout, bar fracture	Ultimate loads comparable to control bars. Large strains (more than 8%) was observed in the tests
Yang et al. (2014)	No. 8 (Ø25 mm)	ASTM A615 Grade 60	Bar fracture	Average max strain greater than 8%

Table 1-7. Summary of Seismic Performance of Column Test Models with Shear Screw Couplers

Reference	Column Geometry	Coupler Length	Remarks
Cruz and Saiidi (2012)	No. of Columns: a Two-Column Bent, Scale Factor: 25% Section: Circular, Dim.: 12 *in*. (305 *mm*), Long. Bars: 9 No. 4 (Ø13 *mm*) SMA, Trans. Bars: 0.11 *in*. (Ø2.9 *mm*) Spirals at 1.25 *in*. (32 *mm*)	$14d_b$: used at two levels	The bent with shear screw couplers showed more than 5% drift ratio capacity with no bar or coupler failure (bottom couplers embedded $12d_b$ into the footing on center, top couplers were 22 *in*. (1.83*D*) away from the bottom couplers on center)
Huaco (2013)	No. of Columns: Three, Scale Factor: 100% Variable: Repair Method, Section: Square, Side Dim.: 16 *in*. (406 *mm*), Long. Bars: 8 No. 8 (Ø25 *mm*), Trans. Bars: No. 3 (Ø10 *mm*) Ties at 6 *in*. (152 *mm*)	Short ($6.8d_b$): used either at two levels or one level; Long ($10d_b$): used in one level	Two repaired columns with short shear screw couplers showed lower drift capacity compared to the original column but with comparable lateral strength. The repaired column with long couplers (couplers used only at the column base) exhibited similar performance to the original column
Yang et al. (2014)	No. of Columns: One, Scale Factor: 50% Section: Interlocking, Dim.: 24 *in*. (610 *mm*) by 36 *in*. (914 *mm*), Long. Bars: 20 No. 8 (Ø25 *mm*), Trans. Bars: No. 4 (Ø13 *mm*) Spirals at 2.75 *in*. (70 *mm*)	$10d_b$: used at two levels	Repaired column showed 4% higher displacement ductility and 20% higher base shear capacity compared to the original test model (bottom end of the bottom couplers was embedded $5d_b$ into the footing, top couplers were 36 *in*. (1.0*D*) away from the bottom couplers on center)

Note: d_b is the longitudinal bar diameter; *D* is either the column diameter or the column largest side dimension

Table 1-8. Summary of Seismic Performance of Column Test Models with Headed Bar Couplers

Reference	Column Geometry	Coupler Length	Remarks
Haber et al. (2014)	No. of Columns: Two, Scale Factor: 50% Variable: Pedestal, Section: Circular, Dim.: 24 *in*. (610 *mm*), Long. Bars: 11 No. 8 (Ø25 *mm*), Trans. Bars: No. 3 (Ø10 *mm*) Spirals at 2 *in*. (51 *mm*)	3.13d_b: used at two levels	Both columns showed similar seismic performance to the cast-in-place column performance (bottom couplers were installed 5d_b above either footing surface or pedestal, top couplers were installed 12 *in*. (0.5*D*) above the bottom couplers)
Tazarv and Saiidi (2014)	No. of Columns: One, Scale Factor: 50% Section: Circular, Dim.: 24 *in*. (610 *mm*), Long. Bars: 10 No. 10 (Ø32 *mm*) SMA, Trans. Bars: No. 3 (Ø10 *mm*) Spirals at 2 *in*. (51 *mm*)	3.3d_b: used at two levels (coupler length is smaller if same size bars are used)	Column showed improved seismic performance over the cast-in-place column; Coupler was used to connect SMA bars to the steel bars (bottom couplers were installed immediately above footing surface, top couplers were installed 20 *in*. (0.85*D*) above the bottom couplers)
Nakashoji and Saiidi (2014)	No. of Columns: Two, Scale Factor: 30% Variable: SMA Bar Length, Section: Square with Circular Arrangement for Bars, Side Dim.: 20 *in*. (508 *mm*), Long. Bars: 16 No. 4 (Ø13 *mm*) SMA, Trans. Bars: No. 3 (Ø10 *mm*) Spirals at 1.8 *in*. (48 *mm*)	4.26d_b: used at two levels (coupler length is smaller if same size bars are used)	Columns showed better seismic performance over the cast-in-place column; Coupler was used to connect SMA bars to the steel bars (bottom couplers were installed in the footings, top couplers were installed 0.75*D* and 1.0*D* above the bottom couplers)

Note: d_b is the longitudinal bar diameter; *D* is either the column diameter or the column largest side dimension

Table 1-9. Summary of Seismic Performance of Column Test Models with Grouted Sleeve Couplers

Reference	Column Geometry	Coupler Length	Remarks
Haber et al. (2014)	No. of Columns: Two, Scale Factor: 50% Variable: Pedestal, Section: Circular, Dim.: 24 *in*. (610 *mm*), Long. Bars: 11 No. 8 (Ø25 *mm*), Trans. Bars: No. 3 (Ø10 *mm*) Spirals at 2 *in*. (51 *mm*)	14.6d_b: used at one level	Both columns showed 40% lower displacement capacity compared to the cast-in-place column performance (couplers were installed immediately above either footing surface or pedestal)
Tazarv and Saiidi (2014)	No. of Columns: One, Scale Factor: 50% Section: Circular, Dim.: 24 *in*. (610 *mm*), Long. Bars: 11 No. 8 (Ø25 *mm*), Trans. Bars: No. 3 (Ø10 *mm*) Spirals at 2 *in*. (51 *mm*)	14.6d_b: used in one level	Column showed the same seismic performance compared to the cast-in-place column performance; (couplers were installed immediately above a pedestal)
Pantelides et al. (2014)	No. of Columns: Three, Scale Factor: 50% Variable: Coupler Location, Section: Octagonal, Dim.: 21 *in*. (533 *mm*), Long. Bars: 6 No. 8 (Ø25 *mm*), Trans. Bars: No. 4 (Ø13 *mm*) Spirals at 2.5 *in*. (63 *mm*)	14.6d_b: standard couplers were used at one level in column-to-footing connections	Columns showed 25 to 40% lower displacement ductility capacity compared to a reference column, the best performance was observed for the column with couplers immediately above the footing surface and debonded bars below the couplers
Pantelides et al. (2014)	No. of Columns: Three, Scale Factor: 50% Variable: Coupler Location, Section: Octagonal, Dim.: 21 *in*. (533 *mm*), Long. Bars: 6 No. 8 (Ø25 *mm*), Trans. Bars: No. 4 (Ø13 *mm*) Spirals at 2.5 *in*. (63 *mm*)	8.6d_b: modified couplers were used in column-to-cap beam connections	Columns showed 41 to 69% lower displacement ductility capacity compared to a reference column, the best performance was observed for the column with couplers embedded in the cap beam

Note: d_b is the longitudinal bar diameter; D is either the column diameter or the column largest side dimension

Table 1-10. Summary of Seismic Performance of Column Test Models with Threaded Couplers

Reference	Column Geometry	Coupler Length	Remarks
Lehman et al. (2001)	No. of Columns: One, Scale Factor: 33% Section: Circular, Dim.: 24 *in*. (610 *mm*) in Original Column, increased to 28 *in*. (711 *mm*) in Repaired Column, Long. Bars: 11 No. 5 (Ø16 *mm*), Trans. Bars: No. 2 (Ø6 *mm*) Spirals at 1.25 *in*. (32 *mm*) in Original Column, increased to No. 3 (Ø10 *mm*) Spirals at 2.25 *in*. (57 *mm*) in Repaired	Not available, but it should be relatively small	The repaired column showed higher lateral strength and improved displacement capacity over the original column. Higher strength was because of higher ultimate strength for longitudinal bars and higher displacement capacity was because of 2 *in*. (51 *mm*) larger cover concrete, which increased bar resistance against buckling
Saiidi and Wang (2006)	No. of Columns: One, Scale Factor: 25% Section: Circular, Dim.: 12 *in*. (305 *mm*), Long. Bars: 15 No. 4 (Ø13 *mm*) SMA, Trans. Bars: 0.19 *in*. (Ø4.9 *mm*) Spirals at 1.6 *in*. (41 *mm*)	$4.0d_b$: used at two levels,	Both original and repaired columns exhibited large displacement capacity (5.8% drift ratio) with no bar fracture, (bottom couplers were installed 4 *in*. (102 *mm*) below the footing surface, top couplers were installed 1.17*D* above the bottom couplers)
Saiidi et al. (2009)	No. of Columns: Two, Scale Factor: 20% Section: Circular, Dim.: 10 *in*. (254 *mm*), Long. Bars: 8 No. 4 (Ø13 *mm*) SMA, Trans. Bars: 0.17 *in*. (Ø4.4 *mm*) Spirals at 1.5 *in*. (38 *mm*)	$4.0d_b$: used at two levels,	Both columns exhibited equal to or better drift capacity (10 or 14% drift ratio) compared to the reference column with no bar fracture up to 14% drift ratio, (bottom couplers were installed 4 *in*. (102 *mm*) below the footing surface, top couplers were installed 1.4*D* above the bottom couplers)
Varela and Saiidi (2014)	No. of Columns: One, Scale Factor: 25% Section: Circular, Dim.: 14 *in*. (356 *mm*), Long. Bars: 12- Ø0.45 *in*. (Ø11 *mm*) SMA, Trans. Bars: 0.25 *in*. (Ø6.3 *mm*) Spirals at 1.5 *in*. (38 *mm*)	$3.4d_b$: used at two levels,	The column exhibited 11.8% drift ratio, (bottom couplers were installed 2 *in*. (51 *mm*) below the footing surface on center, top couplers were installed 0.85*D* above the bottom couplers on center)

Note: d_b is the longitudinal bar diameter; *D* is either the column diameter or the column largest side dimension

Table 1-11. Summary of Seismic Performance of Column Test Models with Swaged Couplers

Reference	Column Geometry	Coupler Length	Remarks
Yang et al. (2014)	No. of Columns: One, Scale Factor: 50% Section: Interlocking, Dim.: 24 *in*. (610 *mm*) by 36 *in*. (914 *mm*), Long. Bars: 20 No. 8 (Ø25 *mm*), Trans. Bars: No. 4 (Ø13 *mm*) Spirals at 2.75 *in*. (70 *mm*)	$7d_b$: used at two levels	Repaired column showed 59% lower displacement ductility and 30% higher base shear capacity compared to the original test model (bottom couplers were installed immediately above the footing, top couplers were 36 *in*. (1.0*D*) away from the bottom couplers on center)

Note: d_b is the longitudinal bar diameter; *D* is either the column diameter or the column largest side dimension

Table 2-1. Evaluation of Shear Screw Couplers

Study	Coupler	Mode of Failure	Strain Capacity	Remark
Lloyd (2001)	Three-screw, "Bar-Lock L-Series" Length: $12.3d_b$	Bar pullout (30% of the samples), bar fracture in coupler region (37% of data)	Less than 4%	Not recommended
Hillis & Saiidi (2009)	Three-screw "Zap Screwlok Type 2" Length: $14d_b$	SMA bar fractured inside the grip	SMA strain was 6.9%	Recommended
Rowell et al. (2009)	Seven-screw "Zap Screwlok Type 2" Length: $15d_b$	Mainly bar fracture inside couplers	Less than 2.7%	Not recommended
Huaco & Jirsa (2012)	Three-screw (S-series) and four-screw (B Series) Length < $10d_b$	Bar fractured inside three-screw couplers, bar fractured away from four-screw couplers	N/A	Four-screw is recommended
Alam et al. (2010)	Three-screw "Bar-Lock S" Length: $8.4d_b$	Bar fracture	N/A	Recommended

Table 2-2. Evaluation of Headed Bar Couplers

Study	Mode of Failure	Strain Capacity	Remark
Rowell et al. (2009)	Bar fracture outside of the coupler region in slow tests; bar fractured inside couplers in rapid tests Length: $3d_b$	More than 10% in slow tests, less than 7% in rapid tests	Study indicates this coupler performance is load-dependent, this finding is in contrast with Haber's test results
Haber et al. (2013)	Bar fractured outside of couplers Length: $3.1d_b$	more than 14%	Recommended

Table 2-3. Evaluation of Grouted Sleeve Couplers

Study	Mode of Failure	Strain Capacity	Remark
Noureddine (1996)	Bar fractured in three tests, coupler failed in one test Length: $16d_b$	More than 11%	Not recommended
Jansson (2008)	NMB: Bar fracture (1 sample), coupler fracture (2 samples), bar pullout (3 samples) [Length: $14d_b$] Lenton Interlok: Failure of threads in all tests [Length: $8.5d_b$]	N/A	Not recommended
Rowell et al. (2009)	Bar pullout (22% of samples), bar fracture (33% of samples), coupler fracture (33% of samples) [9 samples in total] Length: $14d_b$	More than 6%	Not recommended
Haber et al. (2013)	Bar fracture, Length: $14.6d_b$	More than 13%	Recommended

Table 2-4. Evaluation of Threaded Couplers

Study	Mode of Failure	Strain Capacity	Remark
Noureddine (1996)	Taper threaded: Shear failure of threads Length: N/A but very small	Less than 2%	Not recommended
Rowell et al. (2009)	Taper threaded: bar rupture, thread failure [Length: $4.6d_b$] Straight threaded: bar rupture [Length: $6.3d_b$]	Less than 5% for taper threaded couplers More than 10% for straight threaded couplers	Only straight threaded couplers are recommended

Table 2-5. Evaluation of Swaged Couplers

Study	Mode of Failure	Strain Capacity	Remark
Noureddine (1996)	Bar pullout (2 samples of A6015), bar fracture (2 samples of A706) Length: N/A	More than 8 and 9% for A706 and A615, respectively	Recommended for ASTM A706
Yang et al. (2014)	Bar fracture (ASTM A615) Length: $7d_b$	N/A	Recommended

Table 2-6. Evaluation of Seismic Performance of Column Test Models with Shear Screw Couplers

Reference	Coupler Length	Coupler Location	Evaluation Result
Cruz and Saiidi (2012)	$14d_b$: used at two levels	Bottom couplers embedded $12d_b$ into the footing on center, top couplers were 22 *in*. (1.83*D*) away from the bottom couplers on center	N/A (the transverse displacement demand of SMA bent was 30% lower than that of Bent 3 tested by Nelson et al. (2007) at Run 6. Test was stopped due to fracture of bars in other bents)
Huaco (2013)	Short ($6.8d_b$): used either at two levels or one level; Long ($10d_b$): used at one level	For one column, short couplers were installed at two levels, the bottom couplers were immediately above the footing, the top couplers were 1.33*D* away from the bottom couplers on center For two columns, couplers were used at one level at the column base immediately above the footing	Passed (short couplers at two levels) Failed (short couplers at one level) Passed (long couplers at one level)
Yang et al. (2014)	$10d_b$: used at two levels	Bottom end of the bottom couplers was embedded $5d_b$ into the footing, top couplers were 36 *in*. (1.0*D*) away from the bottom couplers on center	Passed (4% higher displacement ductility and 20% higher base shear capacity compared to the original test model)

Note: d_b is the longitudinal bar diameter; *D* is either the column diameter or the column largest side dimension

Table 2-7. Evaluation of Seismic Performance of Column Test Models with Headed Bar Couplers

Reference	Coupler Length	Coupler Location	Evaluation Result
Haber et al. (2014)	3.13d_b: used at two levels	Bottom couplers were installed 5d_b above either footing surface or pedestal, top couplers were installed 12 *in*. (0.5D) above the bottom couplers on center	Passed (column with pedestal showed 4% lower displacement ductility capacity and the same base shear compared to a reference column with ductility of 7.3, column with no pedestal exhibited 12% lower ductility and the same lateral strength compared to the reference column)
Tazarv and Saiidi (2014)	3.3d_b: used at two levels	Bottom couplers were installed immediately above footing surface, top couplers were installed 20 *in*. (0.85D) above the bottom couplers	Passed (column showed higher displacement capacity and higher lateral strength compared to a reference column)
Nakashoji and Saiidi (2014)	4.26d_b: used at two levels	Bottom couplers were installed in the footings, top couplers were installed 0.75D and 1.0D above the bottom couplers	Passed (both columns showed higher displacement capacity and higher lateral strength compared to a reference column)

Note: d_b is the longitudinal bar diameter; D is either the column diameter or the column largest side dimension

Table 2-8. Evaluation of Seismic Performance of Column Test Models with Grouted Sleeve Couplers

Reference	Coupler Length	Coupler Location	Evaluation Result
Haber et al. (2014)	14.6d_b: used at one level	Couplers were installed immediately above either footing surface or pedestal	Failed (both columns showed 40% lower displacement capacity compared to a reference column)
Tazarv and Saiidi (2014)	14.6d_b: used at one level	Couplers were installed immediately above a pedestal	Passed (column exhibited 4% lower ductility and 8% lower lateral strength compared to a reference column with ductility of 7.3)
Pantelides et al. (2014)	14.6d_b: standard couplers at one level	Couplers were used at one level in column-to-footing connections	Failed (columns showed 25 to 40% lower displacement ductility capacity compared to a reference column)
Pantelides et al. (2014)	8.6d_b: modified couplers at one level	Couplers were used in column-to-cap beam connections	Failed (columns showed 41 to 51% lower displacement ductility capacity compared to a reference column)

Note: d_b is the longitudinal bar diameter; D is either the column diameter or the column largest side dimension

Table 2-9. Evaluation of Seismic Performance of Column Test Models with Threaded Couplers

Reference	Coupler Length	Coupler Location	Evaluation Result
Lehman et al. (2001)	Not available, (approximately 3.6d_b based on detailing shown for spiral), couplers were used at two levels	Bottom couplers were installed in the footings, top couplers were installed 1.5*D* above the bottom couplers	Passed (the repaired column showed 30% higher lateral strength and 40% higher displacement capacity compared to the original column)
Saiidi and Wang (2006)	4.0d_b: used at two levels	Bottom couplers were installed 4 *in*. (102 *mm*) below the footing surface, top couplers were installed 1.17*D* above the bottom couplers	N/A (there is no reference column but both original and repaired columns exhibited large displacement capacity (5.8% drift ratio) with no bar fracture)
Saiidi et al. (2009)	4.0d_b: used at two levels	Bottom couplers were installed 4 *in*. (102 *mm*) below the footing surface, top couplers were installed 1.4*D* above the bottom couplers	Passed (both columns exhibited equal or better drift capacity (10 or 14% drift ratio) compared to the reference column with no bar fracture up to 14% drift ratio, note that lower 22% lateral strength of coupler columns was because of SMA bars not the coupler effect)
Varela and Saiidi (2014)	3.4d_b: used at two levels	Bottom couplers were installed 2 *in*. (51 *mm*) below the footing surface on center, top couplers were installed 0.85*D* above the bottom couplers on center	N/A (there is no reference column to compare but the column exhibited 11.8% drift ratio, which is beyond practical range for conventional columns)

Note: d_b is the longitudinal bar diameter; *D* is either the column diameter or the column largest side dimension

Table 2-10. Evaluation of Seismic Performance of Column Test Models with Swaged Couplers

Reference	Coupler Length	Coupler Location	Evaluation Result
Yang et al. (2014)	7d_b: used at two levels	Bottom couplers were installed immediately above the footing, top couplers were 36 *in*. (1.0*D*) away from the bottom couplers on center	Failed (repaired column showed 59% lower displacement ductility and 30% higher base shear capacity compared to the original test model)

Note: d_b is the longitudinal bar diameter; *D* is either the column diameter or the column largest side dimension

Table 3-1. Constructability of Mechanical Bar Couplers

Item/Coupler	Shear Screw	Headed Bar	Grouted Sleeve	Threaded	Swaged
Bar End Preparation	Not Needed	Heading	Not Needed	Threading	Not Needed
Special Equipment	Wrench or Nut Runner	Wrench, Heading Machine	Grout Pump	Die and Tap	Press Machine
Additional Material/Piece	Screw	No Need	Grout/Sealing	No Need	No Need
Tolerance and Alignment	Loose	Tight	Loose	Tight	Loose
Field Erection Speed for precasting	Very Fast	Fast	Very Fast	Fast	Fast
Time to Complete one Splice	1 *min*	5 *min*	24 *hours*	5 *min*	5 *min*

Table 3-2. Construction Time (Day) for Precast Columns with Couplers

Construction Step	CIP	Shear Screw	Headed Bar	Grouted Sleeve	Threaded	Swaged
Column-to-Footing Connections						
Excavate Footing	1	1	1	1	1	1
Build Footing Formwork	2	2	2	2	2	2
Set Footing Rebar	1	1	1	1	1	1
Set Column Steel	1	N/A	N/A	N/A	N/A	N/A
Pour Footing Concrete	1	1	1	1	1	1
Grout Bedding Layer	N/A	N/A	N/A	0.25	N/A	N/A
Set/Level Column	N/A	0.25	0.25	0.25	0.25	0.25
Fasten Screws/Couplers	N/A	0.25	0.5	N/A	0.5	1
Grout Couplers	N/A	N/A	N/A	0.5	N/A	N/A
Grout Curing Time	N/A	N/A	N/A	1	N/A	N/A
Additional Steps for Different Detailing*	N/A	1	1	N/A	1	1
Build Column Formwork	1.5	N/A	N/A	N/A	N/A	N/A
Pour Column Concrete	1	N/A	N/A	N/A	N/A	N/A
Cure Time to 80% (Min 5 Days)	5	N/A	N/A	N/A	N/A	N/A
Construction Time	13.5	6.5	6.75	7	6.75	7.25
Time Saving for Column-to-Footing	--	7	6.75	6.5	6.75	6.25
Column-to-Cap Beam Connections						
Build Shoring/Soffit	4	N/A	N/A	N/A	N/A	N/A
Set Cap Beam Rebar	2	N/A	N/A	N/A	N/A	N/A
Finish Formwork/Pour Concrete	1	N/A	N/A	N/A	N/A	N/A
Set Shims/Shoring, Sealing, and Surveying	N/A	0.25	0.25	1	0.25	0.25
Grout Bedding Layer	N/A	N/A	N/A	0.25	N/A	N/A
Set/Level Cap Beam	N/A	0.25	0.25	0.25	0.25	0.25
Grout Couplers	N/A	N/A	N/A	0.5	N/A	N/A
Fasten Screws/Couplers	N/A	0.25	0.5	N/A	0.5	1
Additional Steps for Different Detailing*	N/A	1	1	N/A	1	1
Grout Cure Time	N/A	N/A	N/A	1	N/A	N/A
Cure Time to 80% (Min 5 Days)	5	N/A	N/A	N/A	N/A	N/A
Construction Time	12	1.75	2	3	2	2.5
Time Saving for Column-to-Cap Beam	--	10.25	10	9	10	9.5
Total Construction Time for Bent						
Total Bent Construction Time	25.5	8.25	8.75	10	8.75	9.75
Total Time Saving for Precast Bent	--	17.25	16.75	15.5	16.75	15.75
Total Time Saving for Precast Bent (%)	--	68	66	61	66	62

Note: Construction time for the CIP and the grouted coupler bent are based on Marsh et al. (2011).
It is assumed that columns and the cap beam are precast.

* It is not possible to complete a precast connection without taking additional steps. For example, to be able to use headed bar couplers in the plastic hinge area, a space is needed to fit the couplers inside the precast column thus casting of this space imposes extra step.

Table 4-1. Coupler Rigid Length Factor

Coupler type	$\frac{\varepsilon_{sp}}{\varepsilon_s}$ from Test	Measured β	Suggested[a]
Shear Screw	N/A	N/A	0.5
Headed Bar	0.7	0.77	0.75
Grouted Sleeve	0.42	0.64	0.65
Threaded	N/A	N/A	0.25
Swaged	N/A	N/A	0.5

Note: "Suggested" values need to be verified for different coupler types and coupler series.

Table 4-2. Reference RC Column Design Parameters

Parameter	Value
Column Diameter	4 *ft*
Aspect Ratio or AR	4, 6, 8
Column Length	16 *ft*, 24 *ft*, 32 *ft*
Concrete Compressive Strength	5.0 *ksi*
Axial Load Index or ALI	5% (452 kips), 10% (905 kips)
Longitudinal Reinforcement	22-#9 (ρ_l = 1.21%)
Transverse Reinforcement	ALI 5%- ductility 3: #3 hoops @10 *in*. (ρ_s = 0.1%) ALI 5%- ductility 5: #4 hoops @4 *in*. (ρ_s = 0.45%) ALI 5%- ductility 7: #5 hoops @3.5 *in*. (ρ_s = 0.81%) ALI 10%- ductility 3: #3 hoops @6 *in*. (ρ_s = 0.17%) ALI 10%- ductility 5: #4 hoops @3.5 *in*. (ρ_s = 0.52%) ALI 10%- ductility 7: #5 hoops @3 *in*. (ρ_s = 0.94%)
Cover Concrete	2 *in*.
Steel Properties	AASHTO Guide Specifications (2014)

Table 4-3. Validation of Design Equation Accounting for Coupler Effects

Reference/ Column	Calculated	Measured
Haber et al. (2014)/ GCNP Column with grouted couplers immediately above the footing surface	$\beta = 0.65$ $H_{sp} = 0.$ use $H_{sp} = 0.1\ in.\ (2.5\ mm)$ $L_{sp} = 14.57\ in.\ (370\ mm)$ thus $\frac{\mu_{sp}}{\mu_{CIP}} = (1 - 0.18\beta)\left(\frac{H_{sp}}{L_{sp}}\right)^{0.1\beta} = \boxed{0.64}$	$\frac{\mu_{sp}}{\mu_{CIP}} = \frac{4.52}{7.36} = \boxed{0.61}$
Haber et al. (2014)/ HCNP Column with headed bar couplers 5 *in*. (127 *mm*) above the column-to-footing interface	$\beta = 0.75$ $H_{sp} = 4\ in.\ (122\ mm)$ $L_{sp} = 3.13\ in.\ (79\ mm)$ thus $\frac{\mu_{sp}}{\mu_{CIP}} = (1 - 0.18\beta)\left(\frac{H_{sp}}{L_{sp}}\right)^{0.1\beta} = \boxed{0.88}$	$\frac{\mu_{sp}}{\mu_{CIP}} = \frac{6.49}{7.36} = \boxed{0.88}$
Pantelides et al. (2014)/ GGSS-1 Column with grouted couplers immediately above the footing surface	$\beta = 0.65$ $H_{sp} = 0.$ use $H_{sp} = 0.1\ in.\ (2.5\ mm)$ $L_{sp} = 14.57\ in.\ (370\ mm)$ thus $\frac{\mu_{sp}}{\mu_{CIP}} = (1 - 0.18\beta)\left(\frac{H_{sp}}{L_{sp}}\right)^{0.1\beta} = \boxed{0.64}$	$\frac{\mu_{sp}}{\mu_{CIP}} = \frac{5.4}{8.9} = \boxed{0.61}$

Table R-1. Coupler Stress-Strain Properties

Property	Notation	Connecting Bar Size	Value
Expected yield stress (*ksi*)	f_y^{sp}	#3- #18	68
Expected tensile strength (*ksi*)	f_u^{sp}	#3- #18	95
Expected yield strain	ε_y^{sp}	#3- #18	$0.0023(L_{cr} - \beta L_{sp})/L_{cr}$
Modulus of elasticity (*ksi*)	E_s^{sp}	#3- #18	$f_y^{sp}/\varepsilon_y^{sp}$
Onset of strain hardening	ε_{sh}^{sp}	#3- #18	$0.005(L_{cr} - \beta L_{sp})/L_{cr}$
Ultimate tensile strain	ε_u^{sp}	#4- #10	$0.09(L_{cr} - \beta L_{sp})/L_{cr}$
		#11- #18	$0.06(L_{cr} - \beta L_{sp})/L_{cr}$

Table 6-1. Design Parameters for Reference Two-Column Bent

Parameter	Remarks
Scale	Full
Column Height	30 *ft* (9.14 *m*) clear
Column Diameter	4 *ft* (1.22 *m*)
Column Long. Reinforcement	22-#9 (22-Ø29 *mm*), ρ_l =1.21%
Column Trans. Reinforcement	#6 (Ø19 *mm*) hoops at 3 *in*. (75 *mm*), ρ_s =1.36%
Cap Beam Length	48 *ft* (14.63 *m*) overall
Cap Dimension	6 *ft* by 6 *ft* (1.82 *m* by 1.82 *m*)
Concrete Strength for all Elements	4000 *psi* (27.6 *MPa*)
Cover Concrete for all Elements	2 *in*. (51 *mm*)
Dead Load excluding cap and columns weights	30.16 *kips*/*ft* (440.1 *kN*/*m*) resulting in 10% axial load index[(a)]
AASHTO LRFD Considerations and Results[(b)]	
Bridge Site	Downtown of Los Angeles, USA
Soil Site Class	*D*
Code Version in USGS Design Tool	AASHTO 2009
Design Seismic Spectrum	A_s=0.64, S_{DS}=1.515, S_{DS}=0.772, T_0=0.102 sec, T_s=0.51 sec
Hand Calculated Period of the Bent	1.28 *sec* using cracked stiffness for the columns
Earthquake Load Calculation	Response Spectrum Analysis, mass from dead load and elements weight
Response Modification Factor, *R*	5
Base Shear from Response Spectrum Analysis	214.5 *kips* (954 *kN*)
Design Level Bent Displacement	2.04 *in*. (52 *mm*) equivalent to 0.52% drift ratio
Design Load Combinations	$1.25D \pm 1.0EQ$; $0.9D \pm 1.0EQ$
AASHTO Guide Specification Consideration and Results[(c)]	
Bent Target Displacement Ductility Capacity	6.0
Cap Beam Model	Elastic element for pushover analysis
Bent Failure	Core concrete failure, bar fracture, or 15% reduction in lateral load resisting, whichever occurs first
Bent First Yield Displacement	2.06 *in*. (52 *mm*) equivalent to 0.52% drift ratio
Bent First Yield Force	291 *kips* (1295 *kN*)
Bent Effective Yield Displacement	2.83 *in*. (72 *mm*) equivalent to 0.71% drift ratio
Bent Effective Yield Force	400.5 *kips* (1781 *kN*)
Bent Displacement Capacity	18.61 *in*. (473 *mm*) equivalent to 4.7% drift ratio resulting in displacement ductility capacity of 6.57

Note:

[(a)] Axial Load Index is the ratio of the axial load to the product of the compressive strength of concrete and the column cross section area

[(b)] Based on AASHTO LRFD Bridge Design Specifications (2013)

[(c)] Based on AASHTO Guide Specifications for LRFD Seismic Bridge Design (2014)

Table 6.2- Modeling Method for Design of Reference Two-Column Bent

General Remarks	
Column Model: Element: *forceBeamColumn* with 5 integration points for both coupler regions and the reminder of the columns Section: Fiber section Cover Concrete Discretization: 10 radial by 10 circumferential Core Concrete Discretization: 30 radial by 10 circumferential $P-\Delta$ effects was included No bond-slip effects	Cap Beam: Element: *Elastic* element with a rigidity based on cap beam actual size
Column Concrete Fibers	
Application: unconfined concrete Type: *Concrete01* f'_{cc}= -4000 *psi* (-27.58 *MPa*) ε_{cc}= -0.002 *in./in.* f'_{cu}= 0.0 *psi* (0.0 *MPa*) ε_{cu}= -0.005 *in./in.*	Application: confined concrete (based on Mander's model) Type: *Concrete01* f'_{cc}= -6150 *psi* (-42.4 *MPa*) ε_{cc}= -0.0082 *in./in.* f'_{cu}= -5870 *psi* (-40.5 *MPa*) ε_{cu}= -0.02192 *in./in.*
Column Steel/Coupler Fibers	
Application: Column integration points (based on AASHTO Guide Specification) Type: *ReinforcingSteel* f_y= 68.0 *ksi* (468.8 *MPa*) f_{su}= 95.0 *ksi* (665.0 *MPa*) E_s= 29000 *ksi* (63252 *MPa*) E_{sh}= 0.043E_s ε_{sh}= 0.0125 *in./in.* (may use smaller value to converge*) ε_{su}= 0.09 *in./in.*	Application: Coupler region integration points (based on proposed guideline, see next table) Type: *ReinforcingSteel* f_y= 68.0 *ksi* (468.8 *MPa*) f_{su}= 95.0 *ksi* (665.0 *MPa*) E_s= 69078 *ksi* (476276 *MPa*) E_{sh}= 0.043E_s ε_{sh}= 0.0021 *in./in.* ε_{su}= 0.038 *in./in.*

* It was found that the yield plateau of this steel model is source of convergence issue in many cases. Smaller yield plateau (smaller ε_{sh}) compared to that specified in the AASHTO Guide Specifications may be used.

Table 6-3. Grouted Coupler Stress-Strain Properties

Property	**Notation**	**Description/Value**
Coupler Type	--	NMB Grouted Couplers
Coupler Length (*in.*)	L_{sp}	16.4
Coupler Region Length (*in.*)	L_{cr}	16.4+2*1.128=18.66
Coupler Rigid Length Factor	β	0.65
Expected yield stress (*ksi*)	f_y^{sp}	68
Expected tensile strength (*ksi*)	f_u^{sp}	95
Expected yield strain	ε_y^{sp}	$\frac{0.0023\left(L_{cr}-\beta L_{sp}\right)}{L_{cr}}=0.00098$
Modulus of elasticity (*ksi*)	E_s^{sp}	$\frac{f_y^{sp}}{\varepsilon_y^{sp}}=69078$
Onset of strain hardening	ε_{sh}^{sp}	$\frac{0.005\left(L_{cr}-\beta L_{sp}\right)}{L_{cr}}=0.0021$
Ultimate tensile strain	ε_u^{sp}	$\frac{0.09\left(L_{cr}-\beta L_{sp}\right)}{L_{cr}}=0.038$

Figures

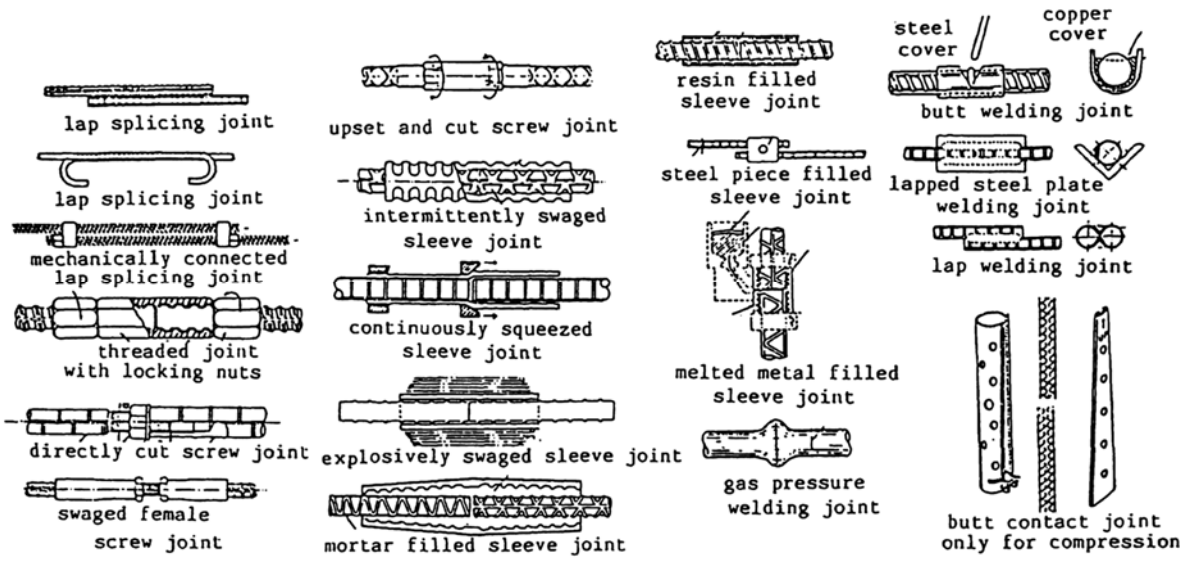

Figure 1-1. Reinforcing Bar Splices (Kanoh et al., 1988)

(a) Shear Screw Coupler
[ancon.co.uk]

(b) Headed Bar Coupler
[hrc-usa.com]

(c) Grouted Sleeve Couplers
[splicesleeve.com]

[erico.com]
(d) Threaded Coupler

[armaturis.com]

(e) Swaged Coupler
[ancon.com.au]

Figure 1-2. Mechanical Reinforcing Bar Couplers

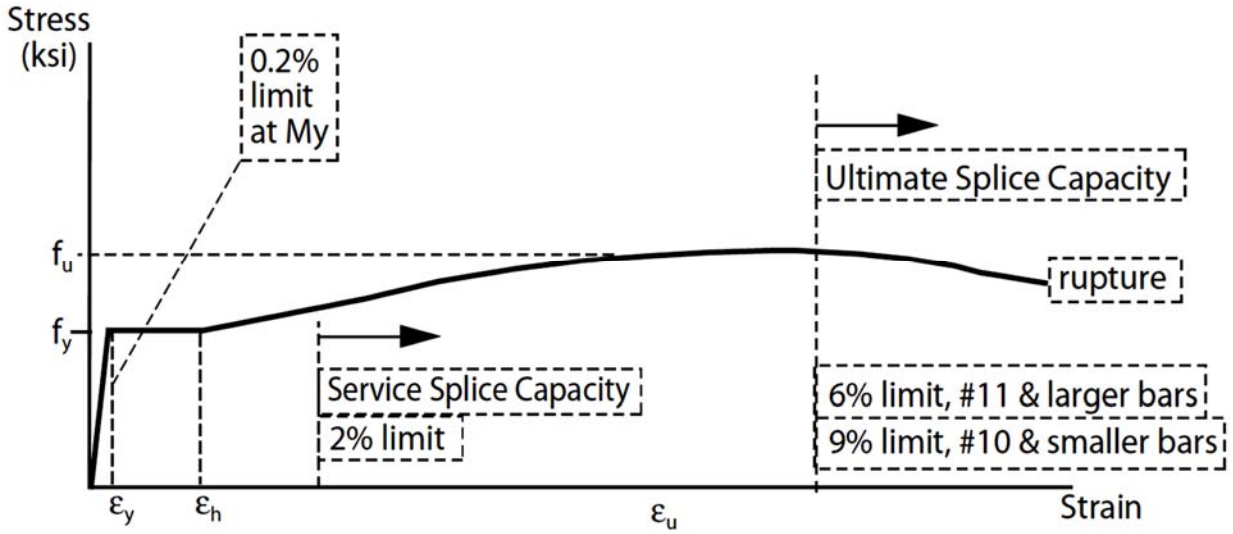

Figure 1-3. Caltrans Strain Limit for ASTM A706 Reinforcing Bar Splices (Caltrans MTD 20-9)

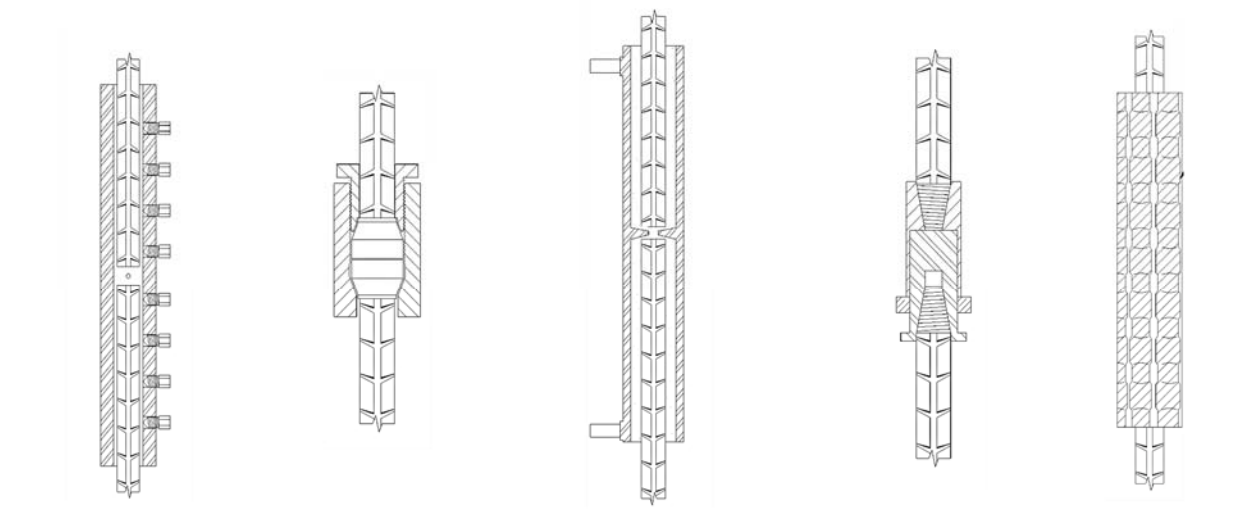

Figure 1-4. Mechanical Reinforcing Bar Couplers

(a) Specimens

(b) Test Setup

(c) SMA Failure at threads

Figure 1-5. Shear Screw Coupler to Connect SMA Bars to Steel Bars (Hillis and Saiidi, 2009)

(a) Slow-Strain Rate Tests

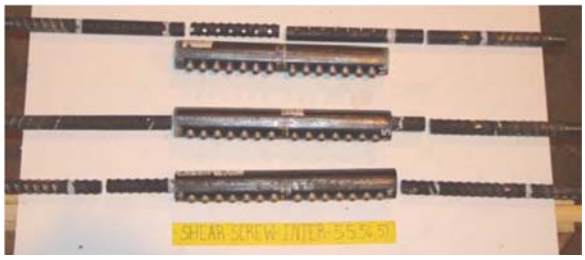

(b) Intermediate-Strain Rate Tests

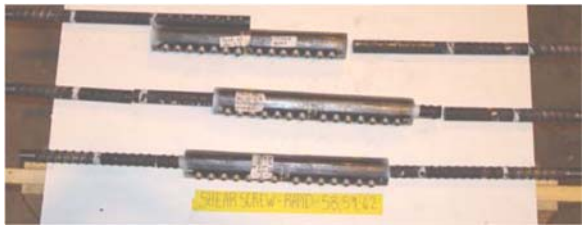

(c) Rapid-Strain Rate Tests

Figure 1-6. Shear Screw Coupler Specimen Tests (Rowell et al., 2009)

(a) Three-Screw Coupler

(b) Four-Screw Coupler

Figure 1-7. Shear Screw Coupler Specimen Tests (Huaco, 2013)

(a) Nine-Screw Coupler

(b) Failure of SMA inside Coupler

Figure 1-8. Shear Screw Coupler Specimen For SMA Bars (Alam et al., 2010)

(a) Slow-Strain Rate Tests (failure shown on right-side of coupler)

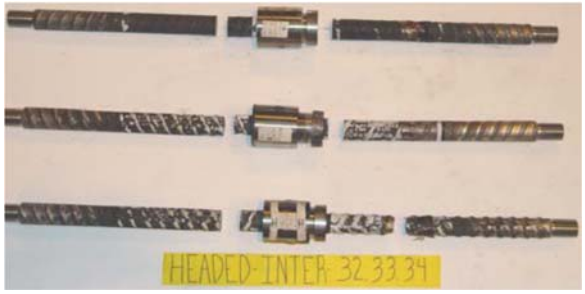

(b) Intermediate-Strain Rate Tests (failure shown on right-side of coupler)

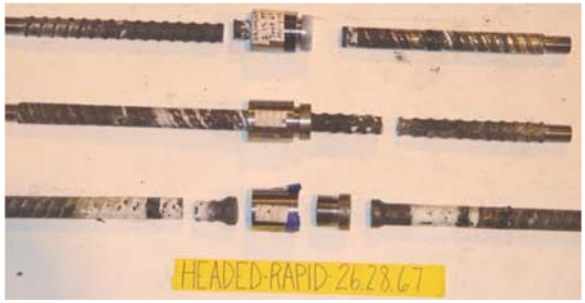

(c) Rapid-Strain Rate Tests (failure shown on right-side of coupler)

Figure 1-9. Headed Bar Coupler Specimen Tests (Rowell et al., 2009)

(a) Monotonic Test (b) Cyclic Test (c) Dynamic Test

Figure 1-10. Headed Bar Coupler Specimen Test (Haber et al., 2013)

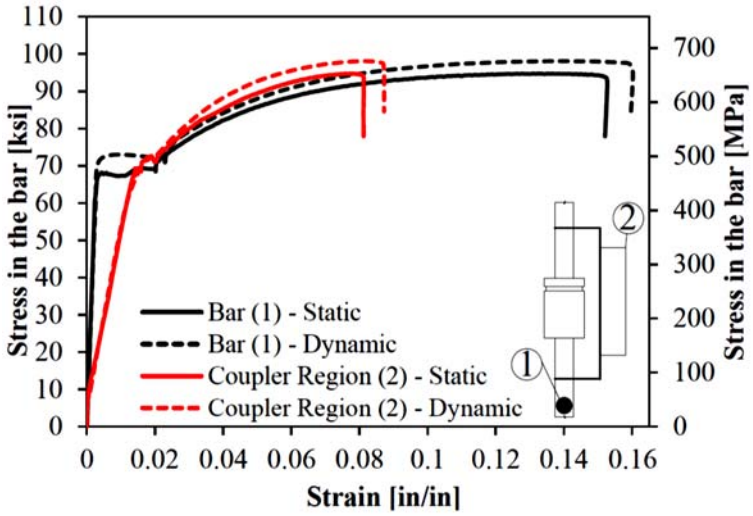

Figure 1-11. Stress-Strain Behavior of Headed Bar Coupler Specimen Tests (Haber et al., 2013)

Figure 1-12. Grouted Coupler Specimen Tests (Noureddine, 1996)

(a) Bar fracture in one of three Tests (b) Spalling in all three Tests

Figure 1-13. Thread-Grout Sleeve Coupler Tests with No. 6 Bars (Jansson, 2008)

(a) Bar fracture in one of three Tests

(b) Thread failure in all three Tests

(c) Thread failure in one of three Tests

(d) Spalling in all three Tests

Figure 1-14. Thread-Grout Sleeve Coupler Tests with No. 11 Bars (Jansson, 2008)

(a) Pull-out failure in one of three Tests

(b) Pull-out failure in one of three Tests

(c) Bar fracture in one of three Tests

Figure 1-15. Grouted Coupler Tests with No. 6 Bars (Jansson, 2008)

(a) Pull-out failure in one of three SSGCs

(b) Splice failure in one of three SSGCs

(c) Splice fracture in one of three SSGCs

Figure 1-16. Grouted Coupler Tests with No. 11 Bars (Jansson, 2008)

Figure 1-17. Grouted Coupler Specimen Tests under Low Strain Rate (Rowell et al., 2009)

Figure 1-18. Grouted Coupler Specimen Tests under Intermediate Strain Rate (Rowell et al., 2009)

Figure 1-19. Grouted Coupler Specimen Tests under High Strain Rate (Rowell et al., 2009)

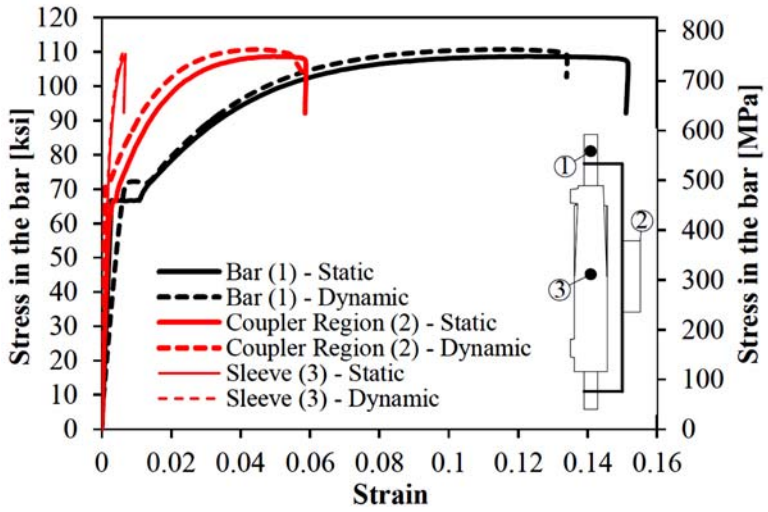

Figure 1-20. Stress-Strain Behavior of Grouted Coupler Specimen Tests (Haber et al., 2013)

Figure 1-21. Grouted Sleeve Coupler Specimens Tests (Haber et al., 2013)

(a) Test Setup and Failure

(a) Bar pull-out

Figure 1-22. Grouted Sleeve Coupler Specimens Tests (Ameli et al., 2015)

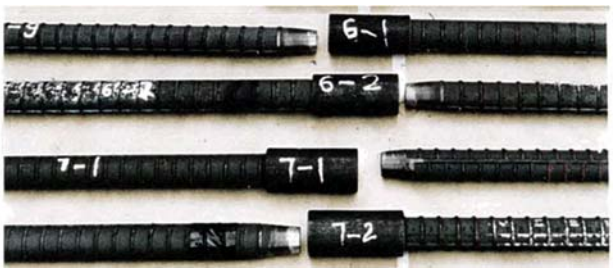

Figure 1-23. Taper Threaded Coupler Specimen Tests (Noureddine, 1996)

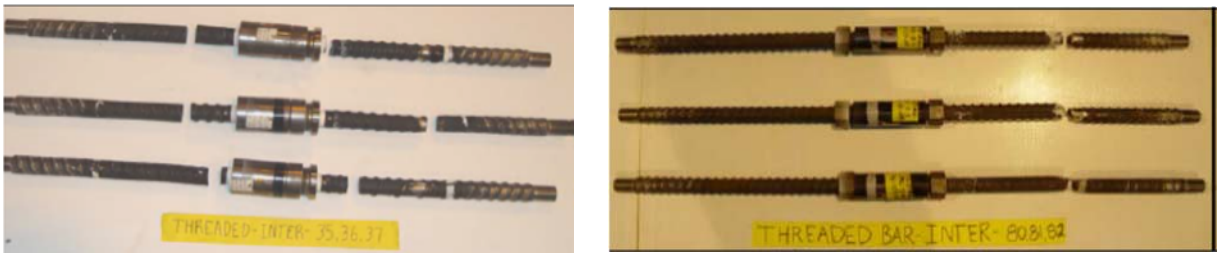

(a) Taper Threaded Coupler (b) Straight Threaded Coupler

Figure 1-24. Threaded Coupler Specimen Tests under Intermediate Strain Rate (Rowell et al., 2009)

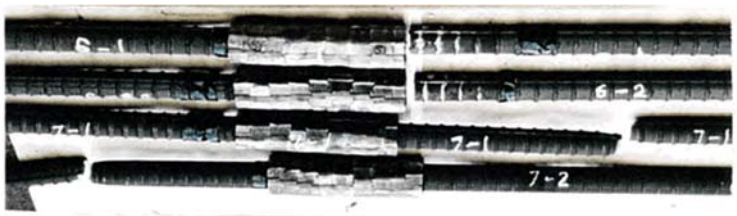

Figure 1-25. Swaged Sleeve Coupler Specimen Tests (Noureddine, 1996)

Figure 1-26. Swaged Sleeve Coupler Specimen Tests (Yang et al., 2014)

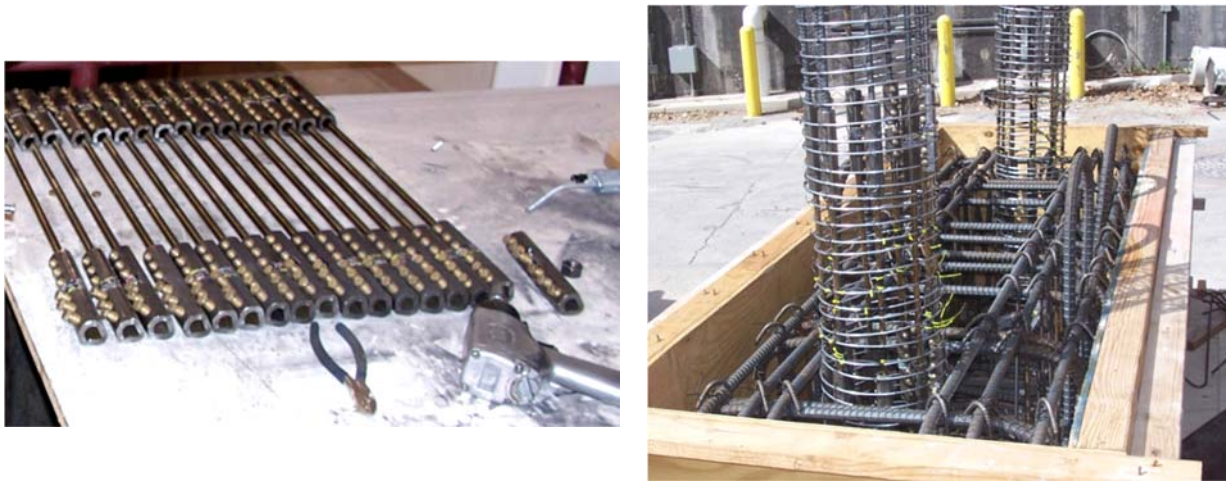

(a) SMA Bars Connected to Couplers (b) Shear Screw Couplers

Figure 1-27. Two-Column Bent with Shear Screw Couplers (Hillis and Saiidi, 2009)

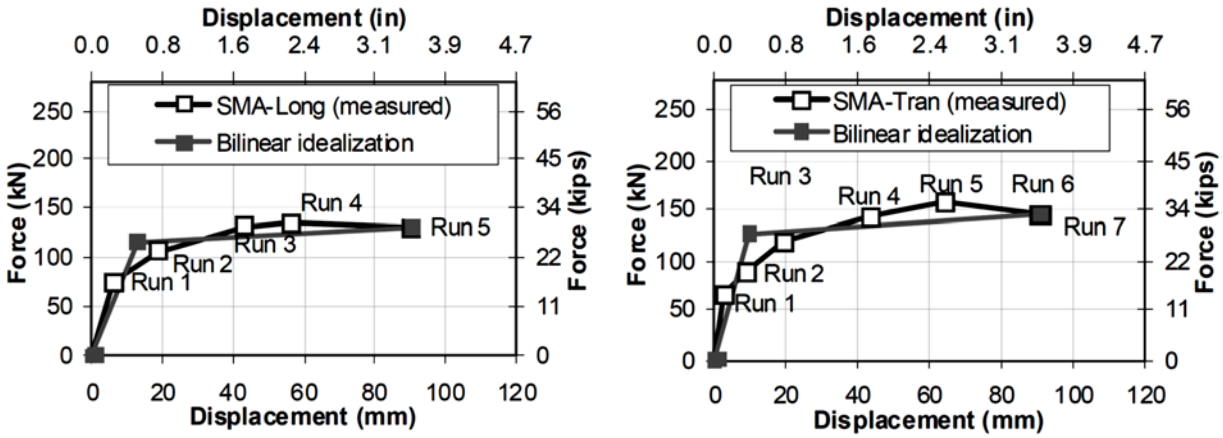

(a) Longitudinal Direction (b) Transverse Direction

Figure 1-28. Force-Displacement Envelope for Two-Column Bent with Shear Screw Couplers (Cruz and Saiidi, 2012)

Figure 1-29. Double-Curvature Column Test (Huaco, 2013)

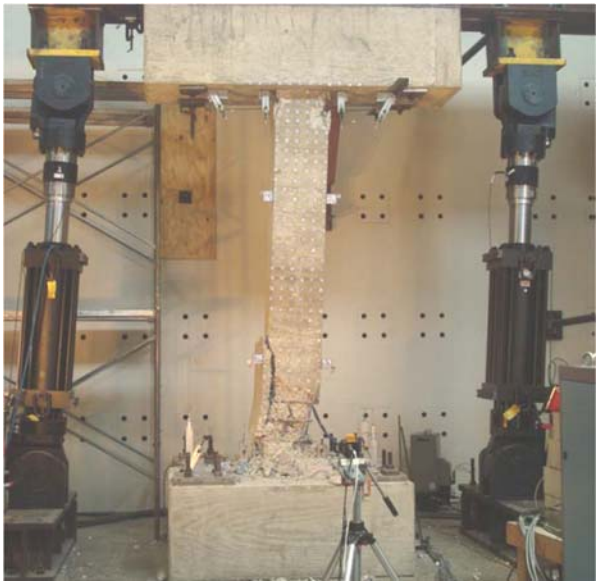

(a) Original Column after Testing

(b) Short Shear Screw Couplers at Base

(c) Repaired Column

Figure 1-30. First Repaired Columns with Short Shear Screw Couplers and GFRP (Huaco, 2013)

(a) Original Column after Testing

(b) Short Shear Screw Couplers at Base

(c) Long Shear Screw Couplers at Base

(d) Repaired Columns

Figure 1-31. Second Repaired Columns with Shear Screw Couplers (Huaco, 2013)

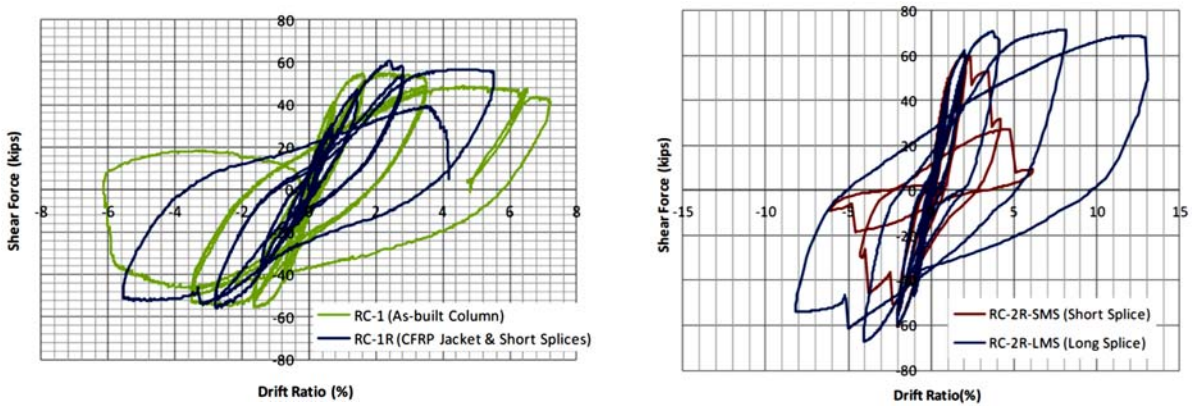

(a) First Column (b) Short SSC vs. Long SSC Columns

Figure 1-32. Force-Drift Hysteresis of Repaired Columns with Shear Screw Couplers (Huaco, 2013)

(a) Original Column after Testing

(b) Plastic Hinge of Original Column after Testing

(c) Long Shear Screw Couplers at Base

(d) Repaired Column

Figure 1-33. Repaired Column with Shear Screw Couplers (Yang et al., 2014)

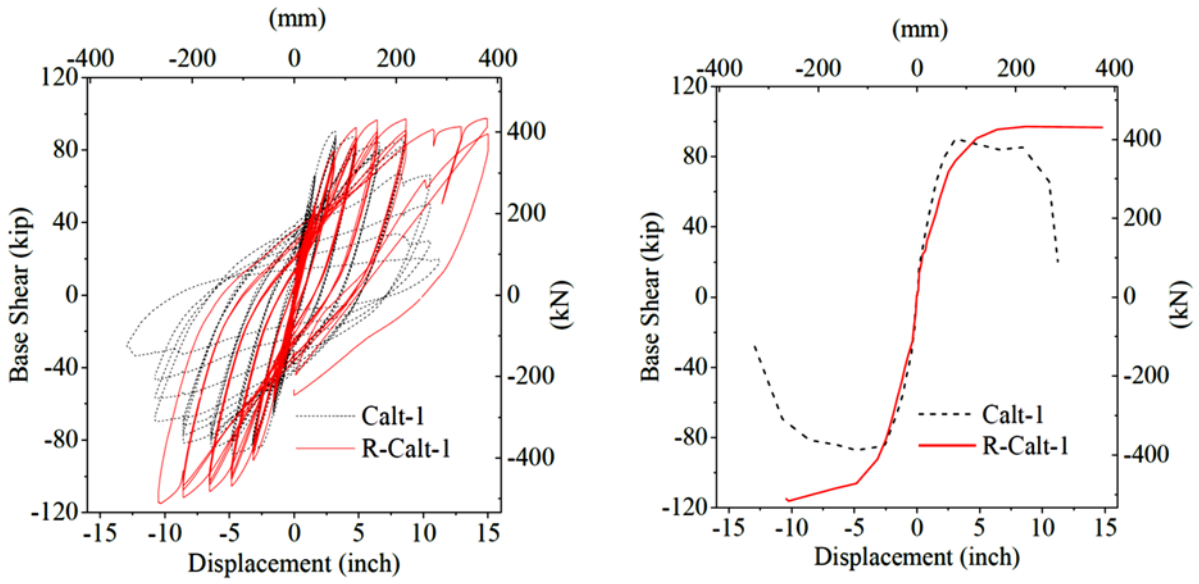

(a) Force-Displacement Hysteresis (b) Force-Displacement Envelope

Figure 1-34. Response of Repaired Column with Shear Screw Couplers (Yang et al., 2014)

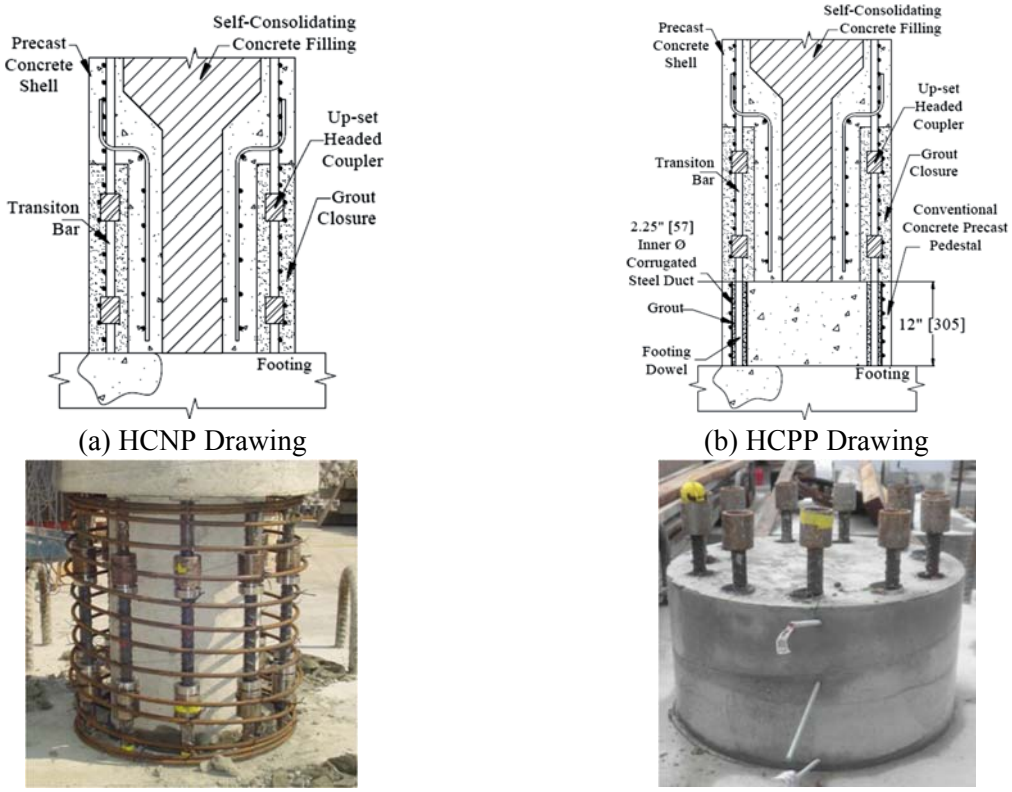

(a) HCNP Drawing (b) HCPP Drawing

(c) HCNP Plastic Hinge Region (d) HCPP Pedestal

Figure 1-35. Precast Columns with Headed Bar Couplers (Haber et al., 2013)

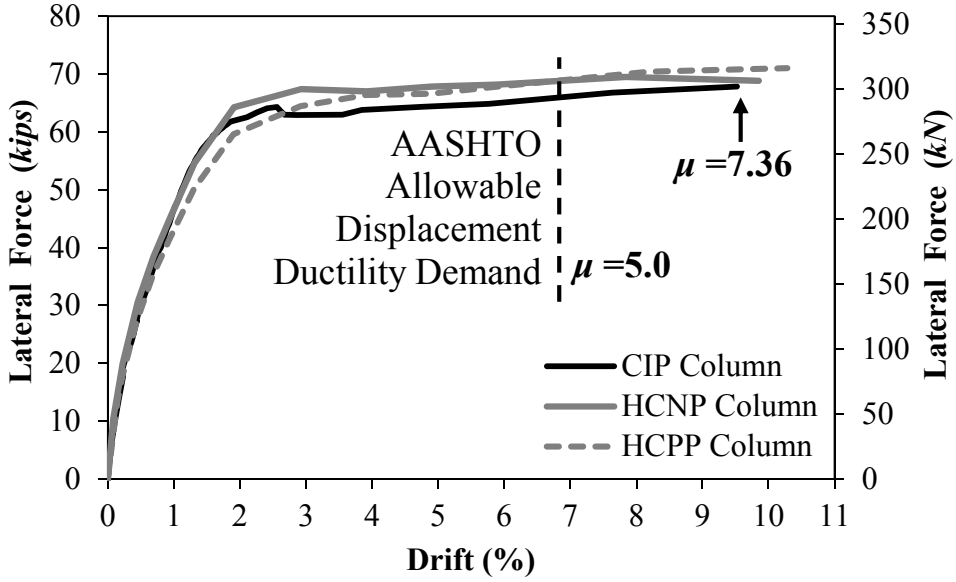

Figure 1-36. Force- Drift Envelope for Headed Bar Coupler Columns (Haber et al., 2013)

(a) SMA-Steel Bar Cage (b) Test Model

Figure 1-37. Precast Columns with Headed Bar Couplers (Tazarv and Saiidi, 2014)

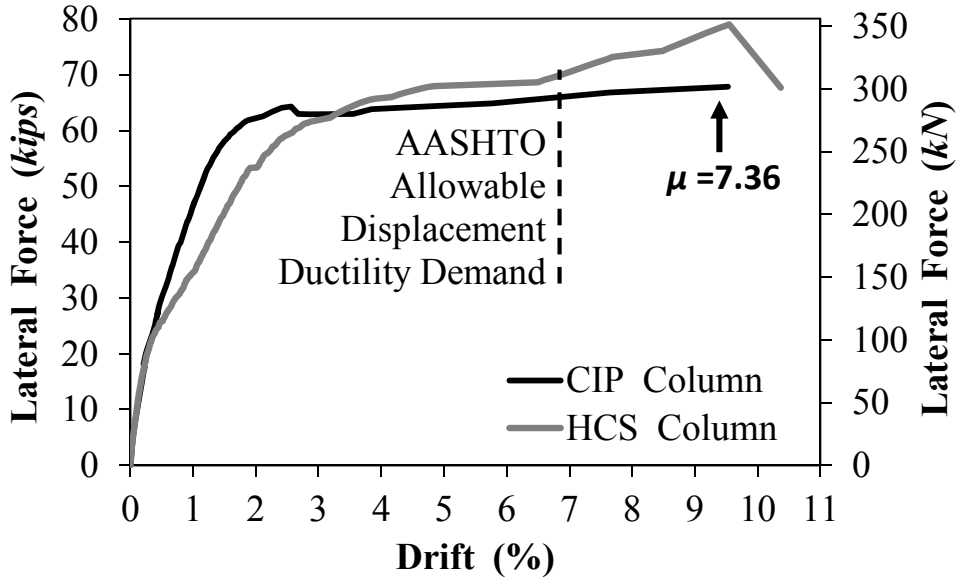

Figure 1-38. Force- Drift Envelope for Headed Bar Coupler Column (Tazarv and Saiidi, 2014)

(a) Short SMA Column

(d) Long SMA Column

(c) Test Models

Figure 1-39. Cast-in-Place Columns with Headed Bar Couplers (Nakashoji and Saiidi, 2014)

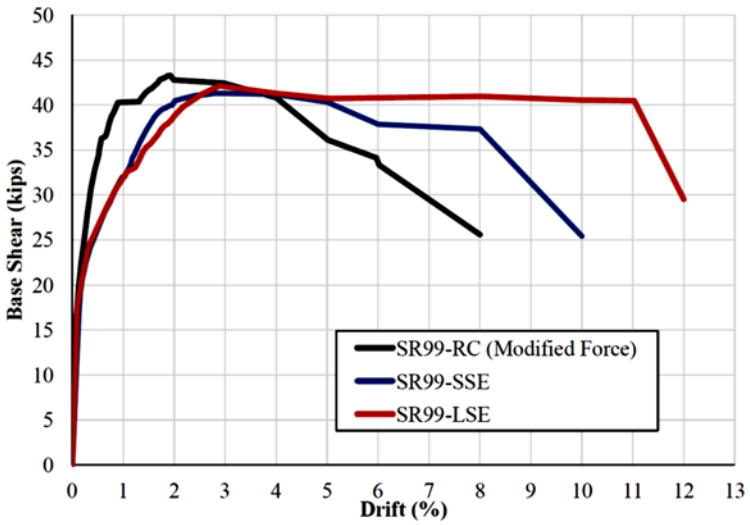

Figure 1-40. Force- Drift Envelope for Headed Bar Coupler Columns (Nakashoji and Saiidi, 2014)

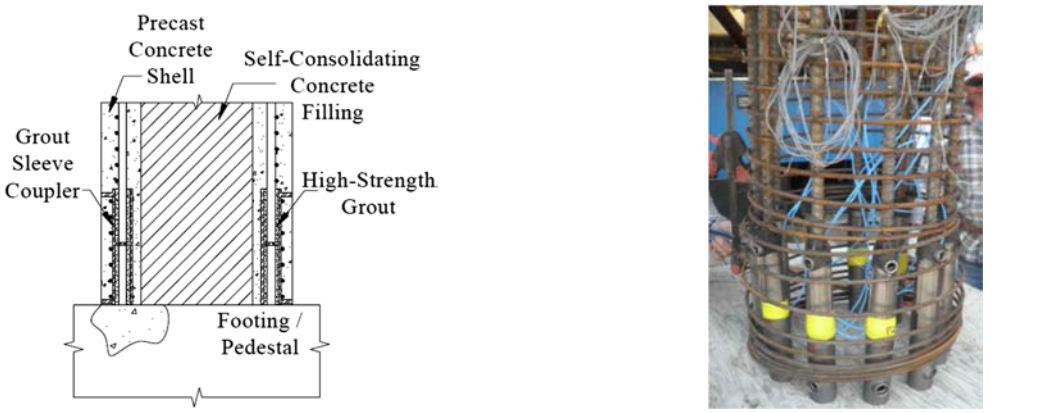

(a) GCNP or GCPP Drawing (b) Steel Cage w/ Grouted Couplers

Figure 1-41. Precast Columns with Grouted Couplers (Haber et al., 2013)

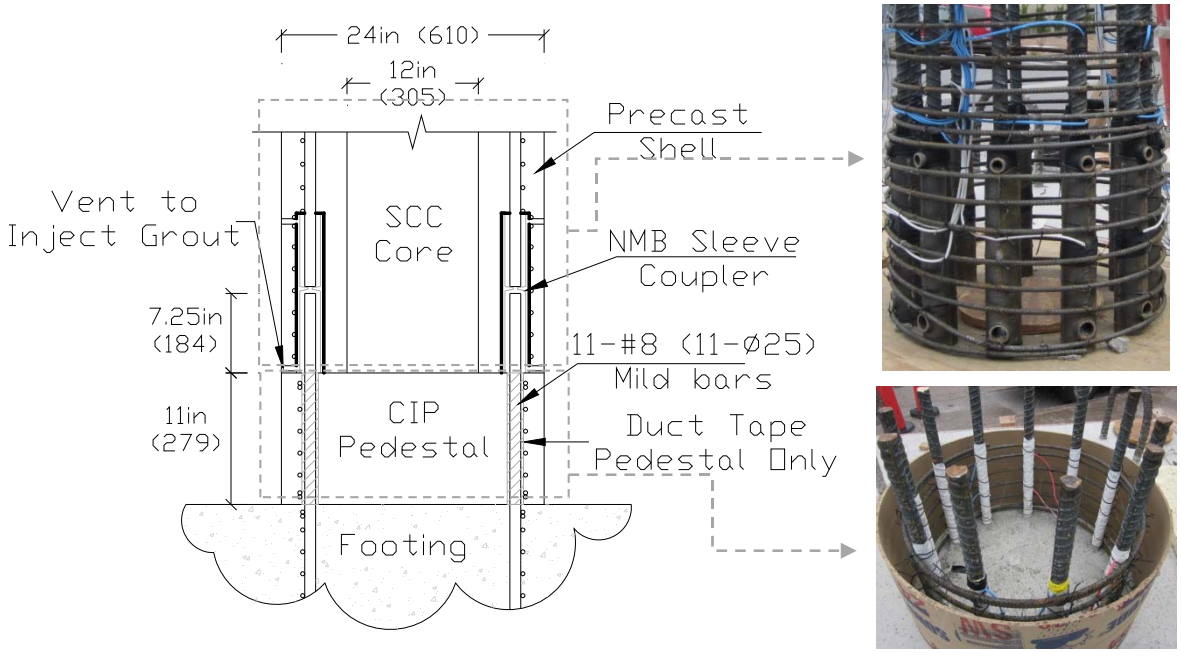

(a) Drawing (b) photographs

Figure 1-42. Precast Columns with Grouted Couplers (Tazarv and Saiidi, 2014)

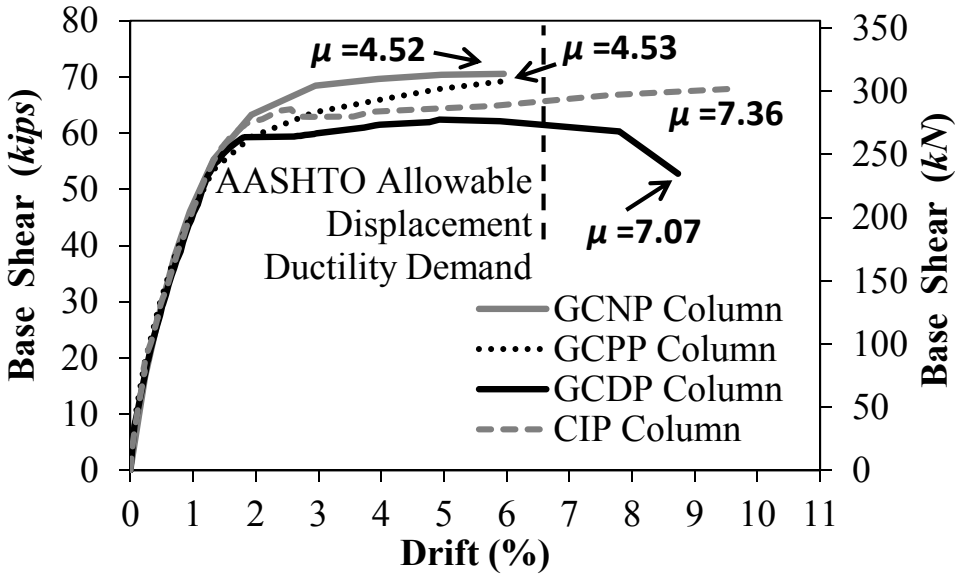

Figure 1-43. Force-Drift Envelope for Grouted Coupler Columns

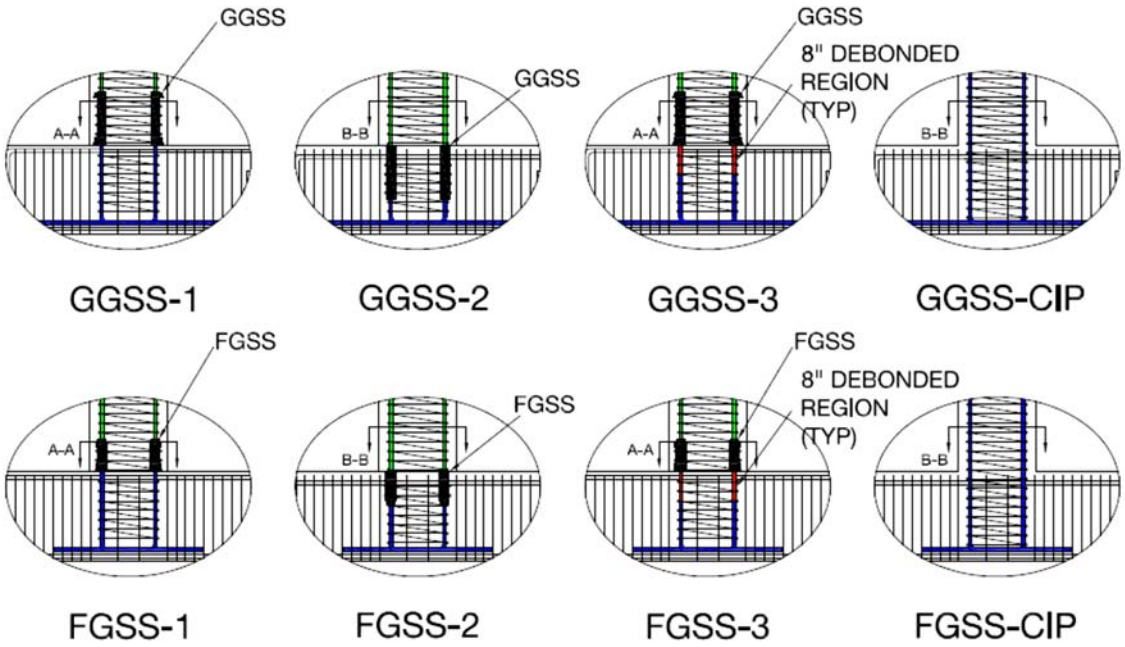

(a) Top Models are Column-to-Footing Connections, Bottom are Column-to-Cap Beam Connections

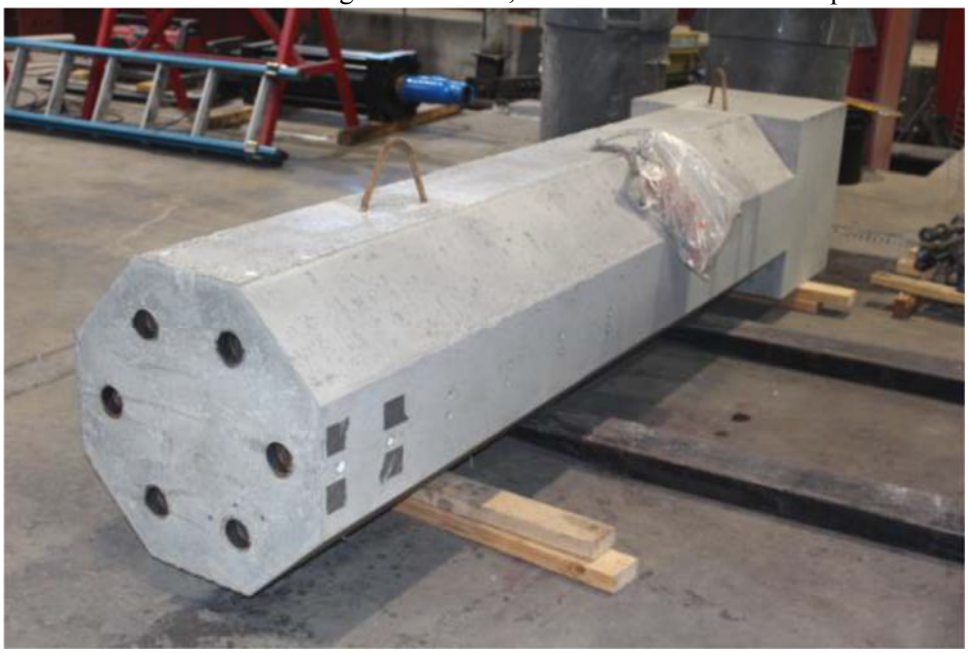

(b) Precast Column Section

Figure 1-44. Precast Columns with Grouted Couplers (Pantelides et al., 2014)

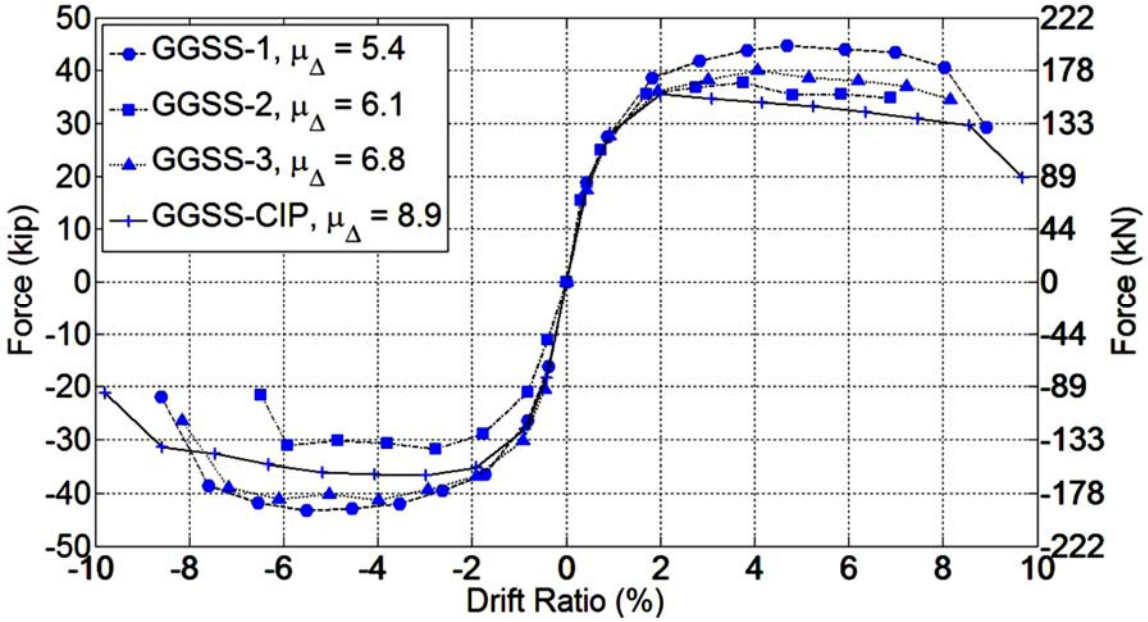

Figure 1-45. Force-Drift Envelope for Footing Grouted Coupler Columns (Pantelides et al., 2014)

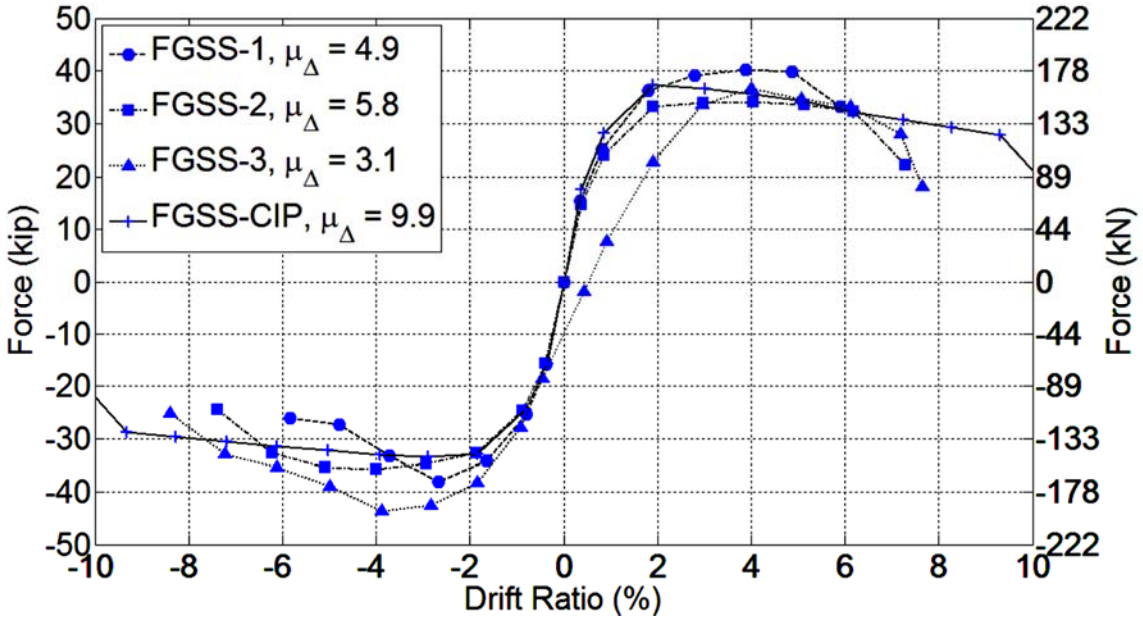

Figure 1-46. Force-Drift Envelope for Cap Beam Grouted Coupler Columns (Pantelides et al., 2014)

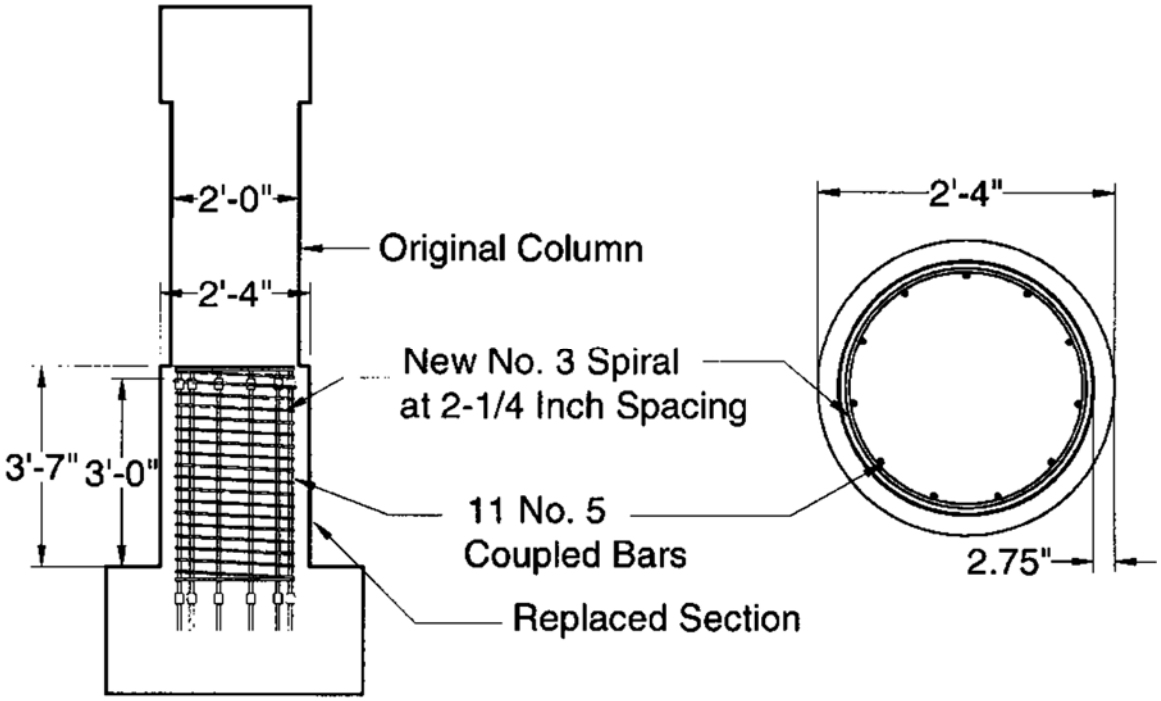

Figure 1-47. Repaired Column with Threaded Bar Couplers (Lehman et al., 2001)

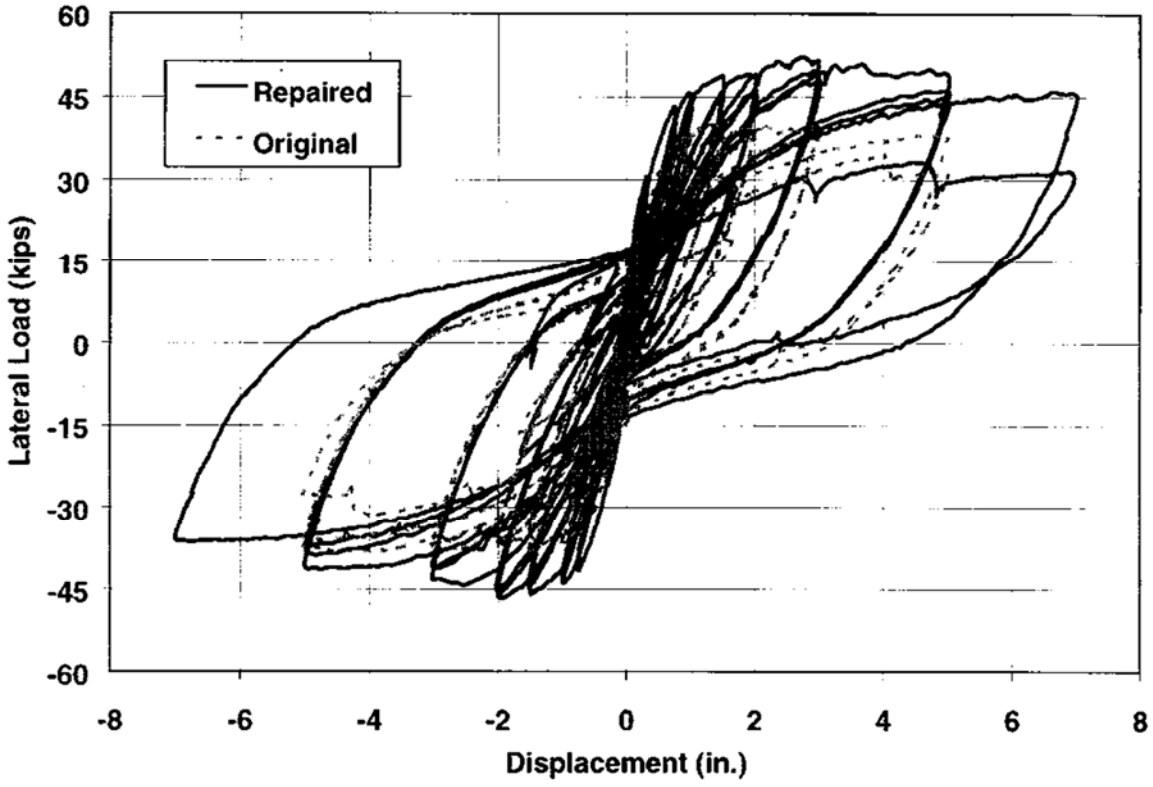

Figure 1-48. Force-Displacement Hysteresis of Repaired Column with Threaded Bar Couplers (Lehman et al., 2001)

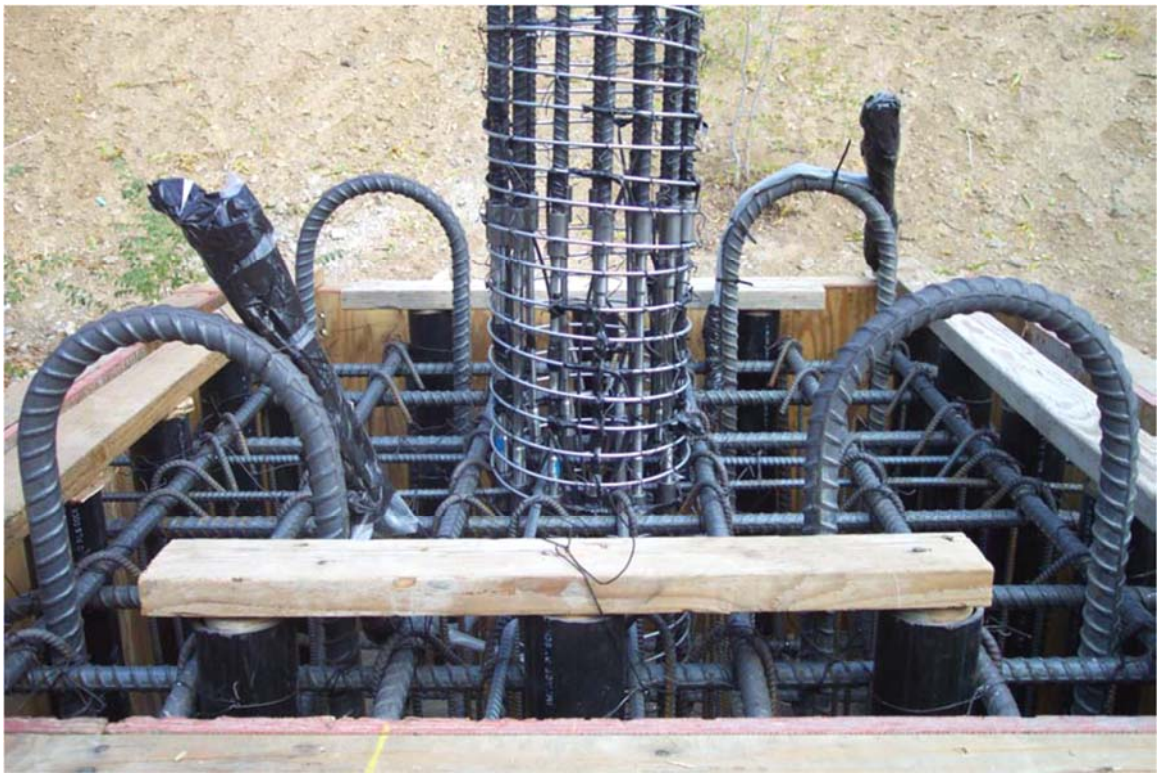

Figure 1-49. Column with Threaded Bar Couplers (Wang and Saiidi, 2006)

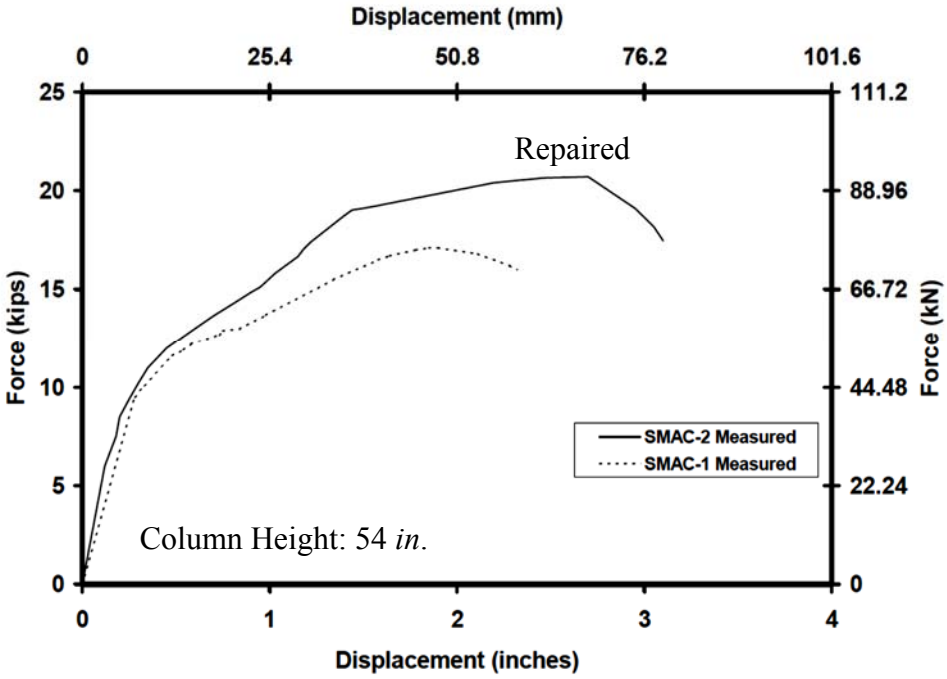

Figure 1-50. Force-Displacement Envelope for Threaded Coupler Columns (Wang and Saiidi, 2006)

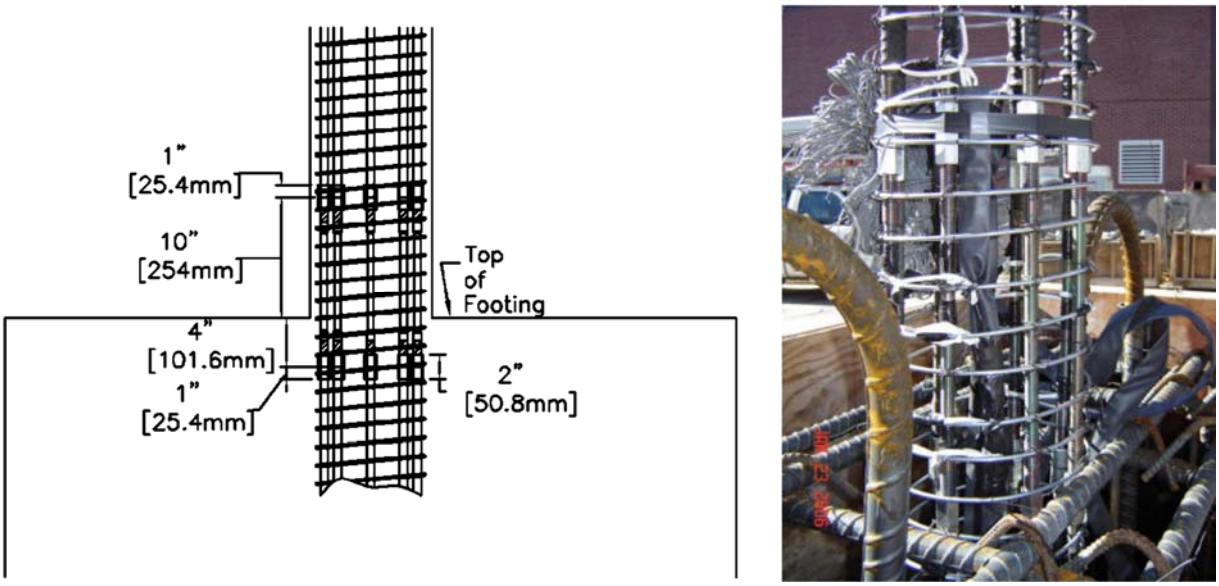

(a) Column-to-Footing Drawing (b) Cage w/ Threaded Couplers

Figure 1-51. Cast-in-Place Columns with Threaded Couplers (O'Brien et al., 2006)

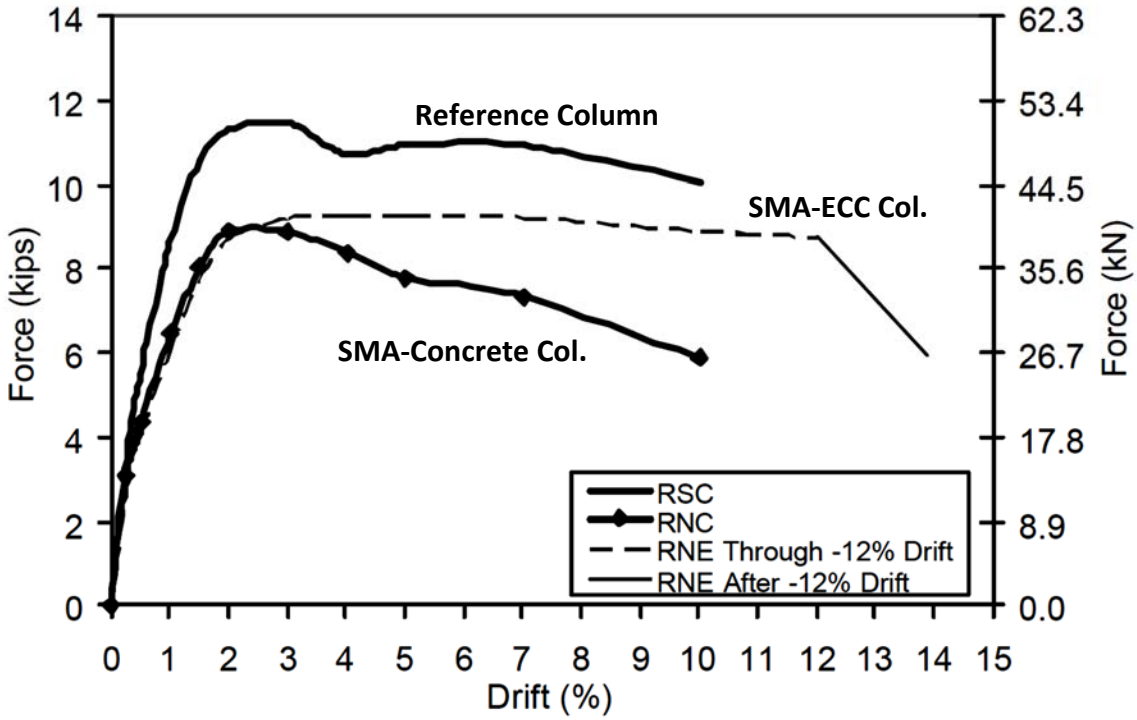

Figure 1-52. Force-Displacement Envelope for Threaded Coupler Columns (O'Brien et al., 2006)

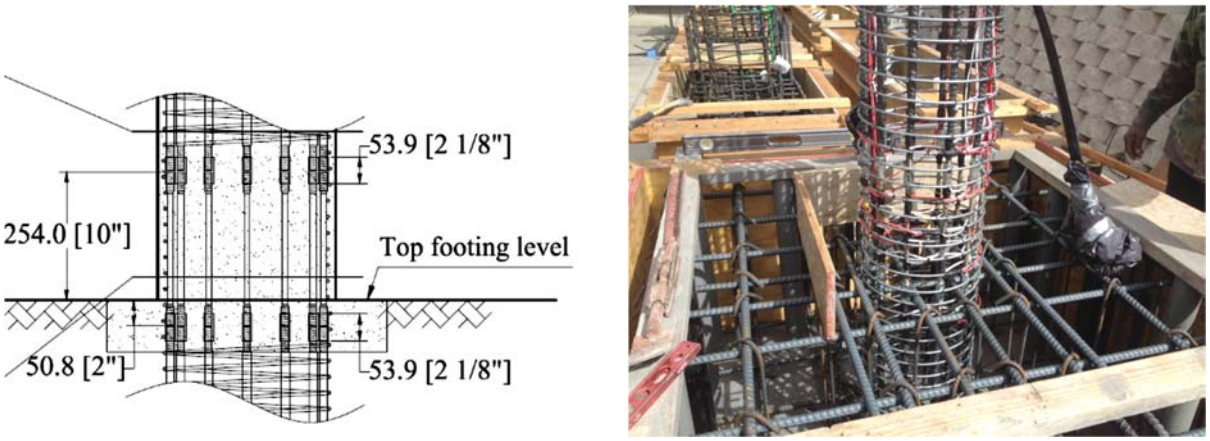

(a) Column-to-Footing Drawing (b) Cage w/ Threaded Couplers

Figure 1-53. Cast-in-Place Column with Threaded Couplers (Varela and Saiidi, 2014)

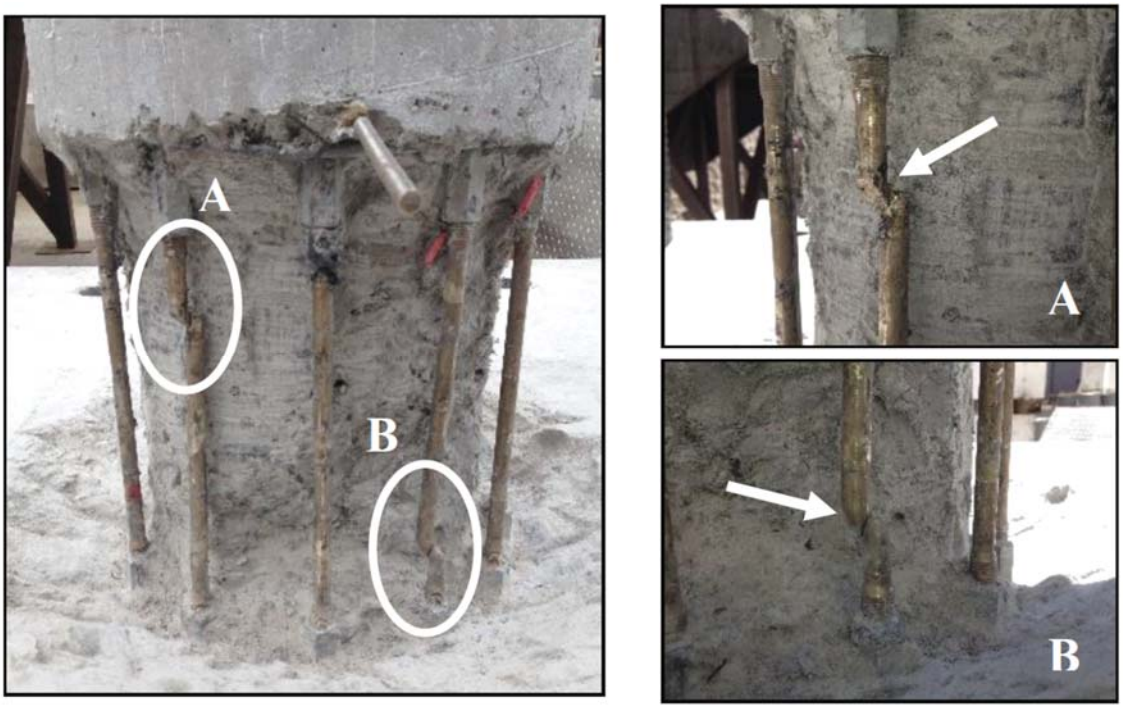

Figure 1-54. Location of SMA Bar Fracture in Threaded Coupler Column (Varela and Saiidi, 2014)

(a) Original Column after Testing

(b) Plastic Hinge of Original Column after Testing

(c) Swaged Couplers at Base

(d) Repaired Columns

Figure 1-55. Repaired Column with Swaged Couplers (Yang et al., 2014)

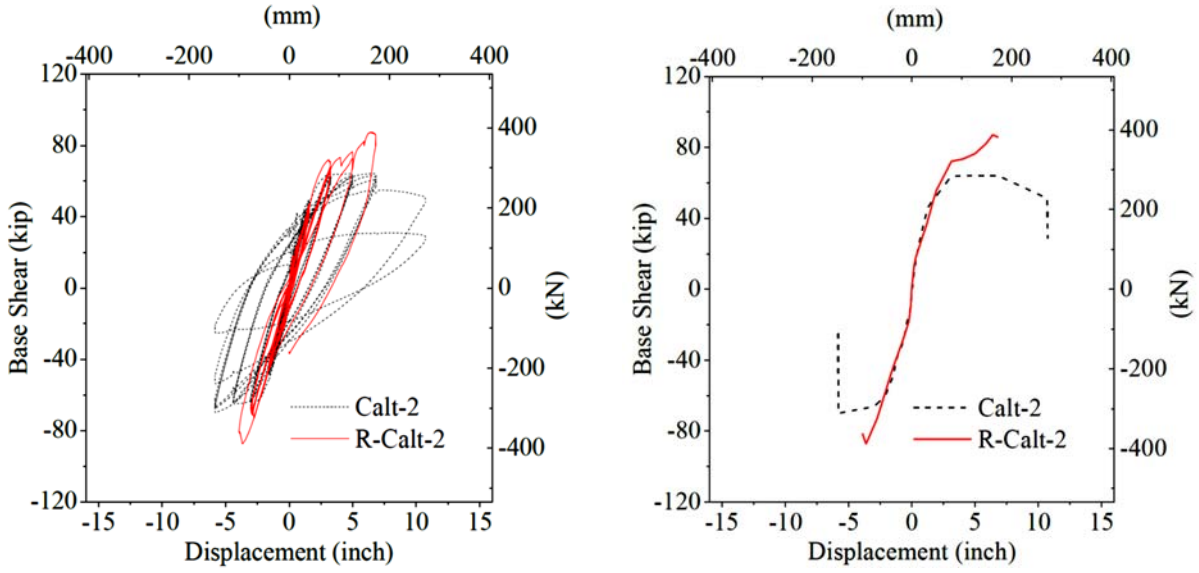

(a) Force-Displacement Hysteresis (b) Force-Displacement Envelope

Figure 1-56. Response of Repaired Column with Swaged Couplers (Yang et al., 2014)

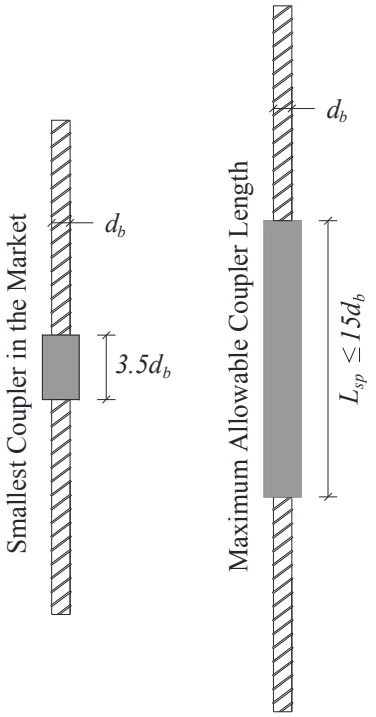

(a) Coupler Length

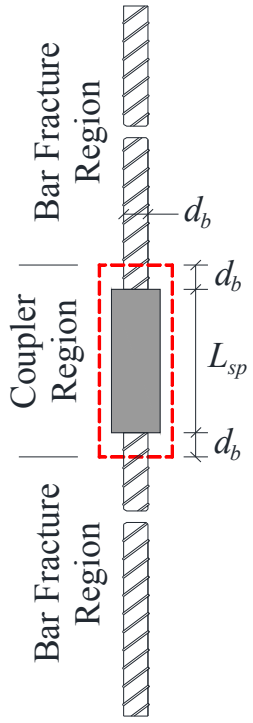

(b) Coupler and Fracture Regions

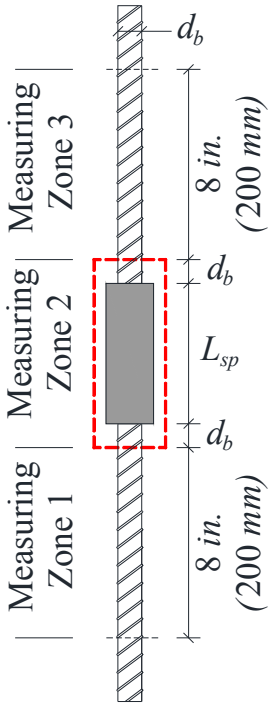

(c) Modified Strain Measurement for "California Test 670"

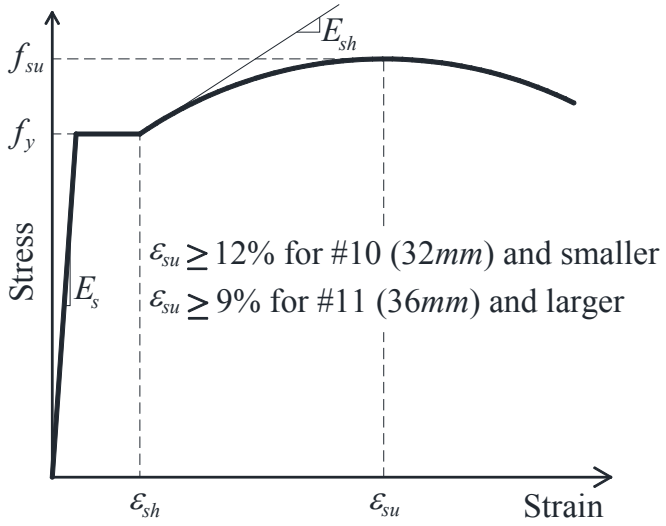

(d) Strain Requirements for Spliced Bars

Figure 2-1. Mechanical Bar Splice Length and Measuring Zones

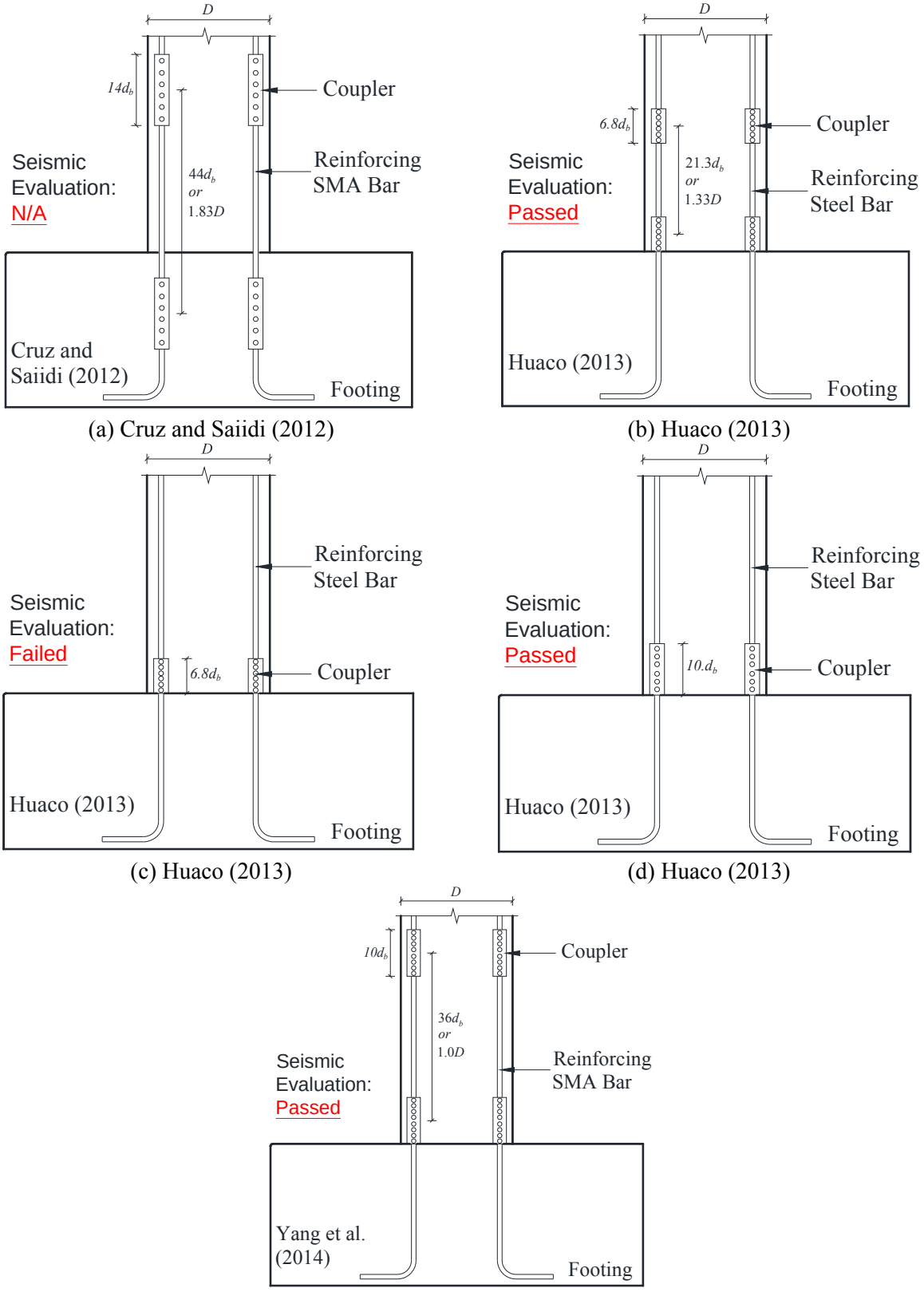

Figure 2-2. Evaluation of Columns Incorporating Shear Screw Couplers

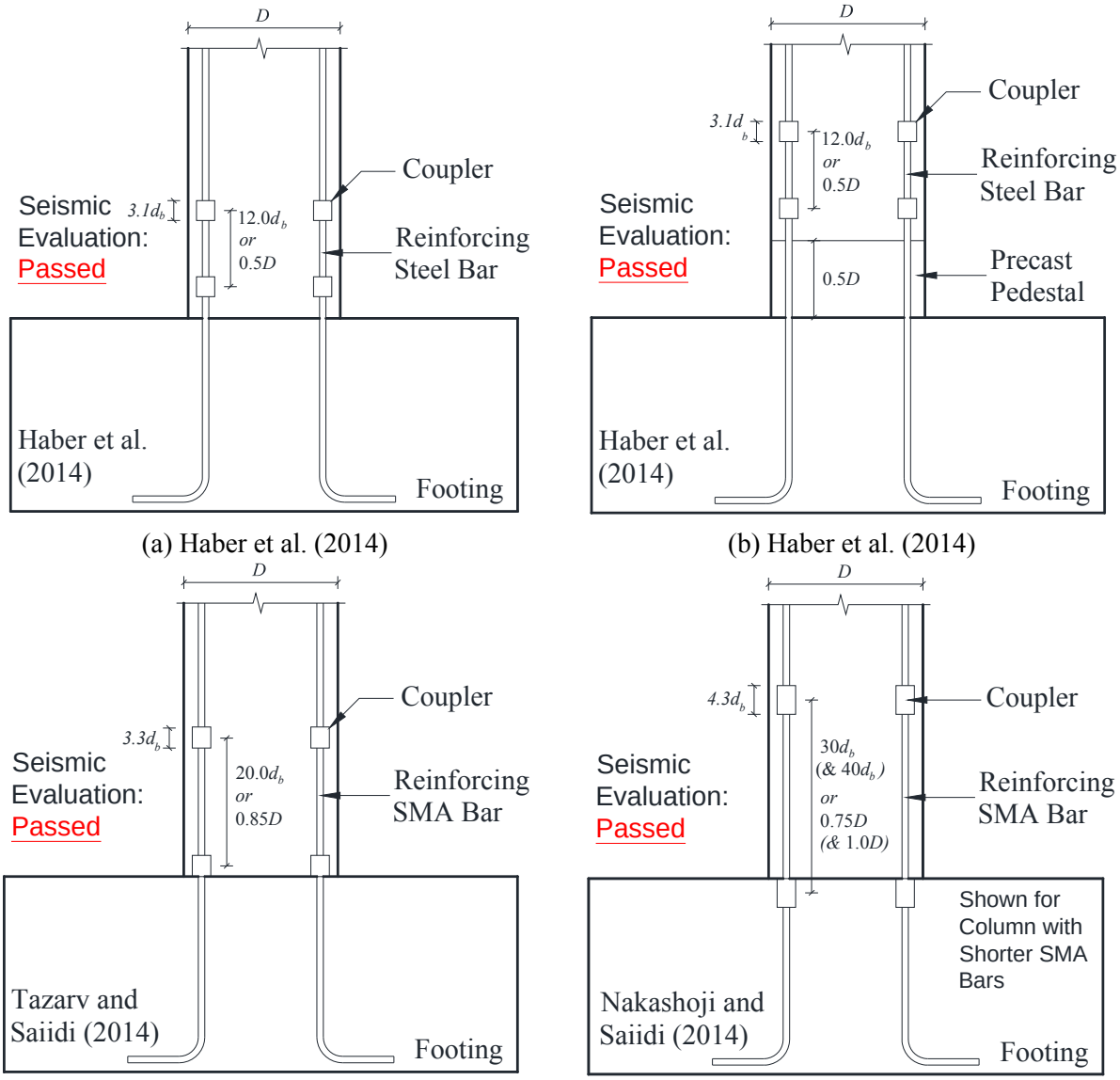

(a) Haber et al. (2014)

(b) Haber et al. (2014)

(c) Tazarv and Saiidi (2014)

(d) Nakashoji and Saiidi (2014)

Figure 2-3. Evaluation of Columns Incorporating Headed Bar Couplers

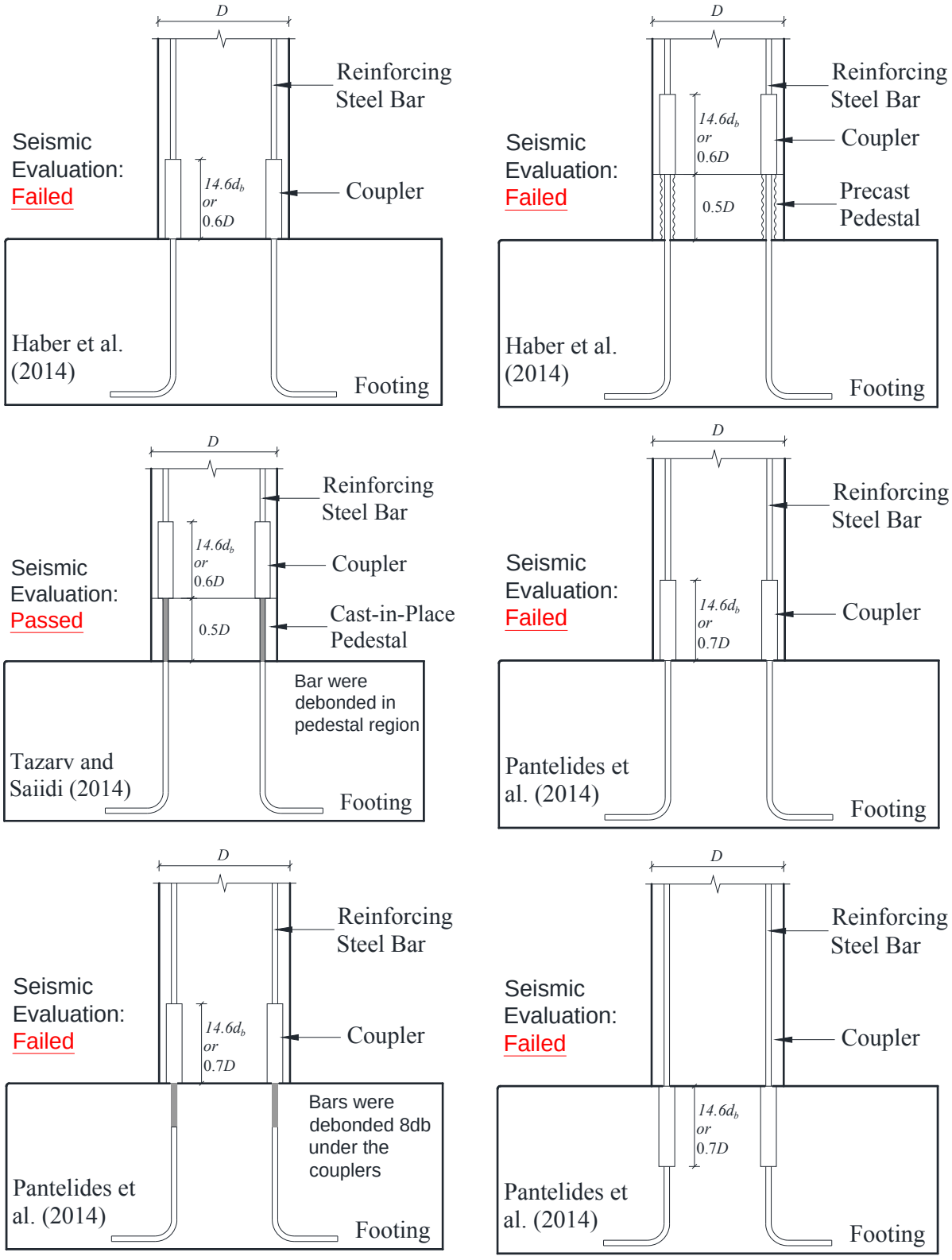

Figure 2-4. Evaluation of Columns Incorporating Grouted Couplers

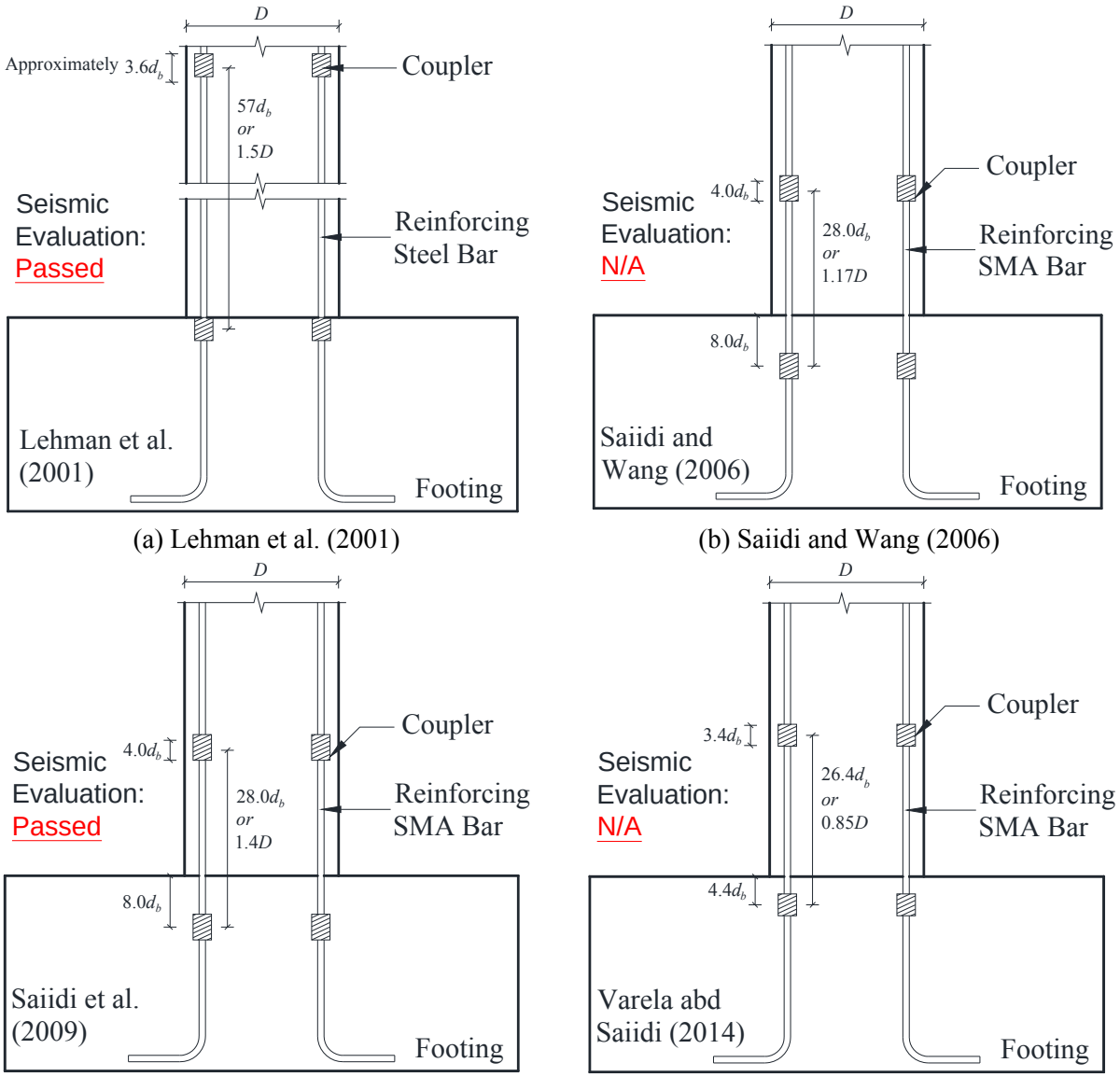

(a) Lehman et al. (2001)

(b) Saiidi and Wang (2006)

(c) Saiidi et al. (2009)

(d) Varela and Saiidi (2014)

Figure 2-5. Evaluation of Columns Incorporating Threaded Couplers

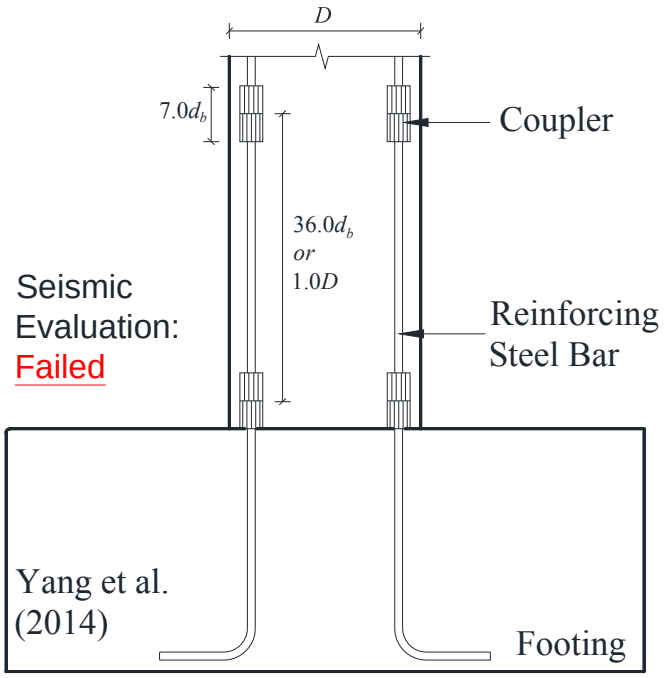

Figure 2-6. Evaluation of Columns Incorporating Swaged Couplers

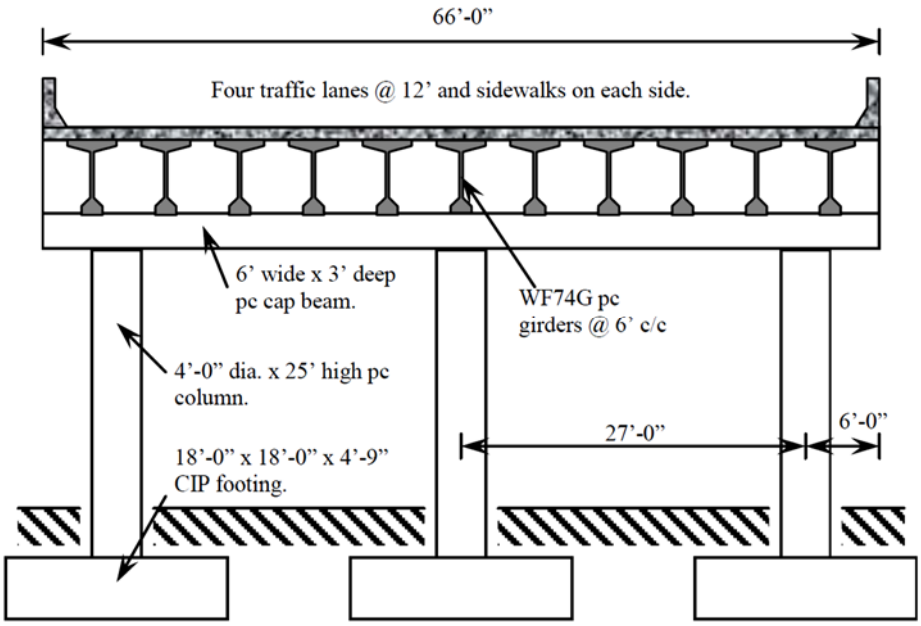

Figure 3-1. Reference Cast-in-Place Bent (Marsh et al. 2011)

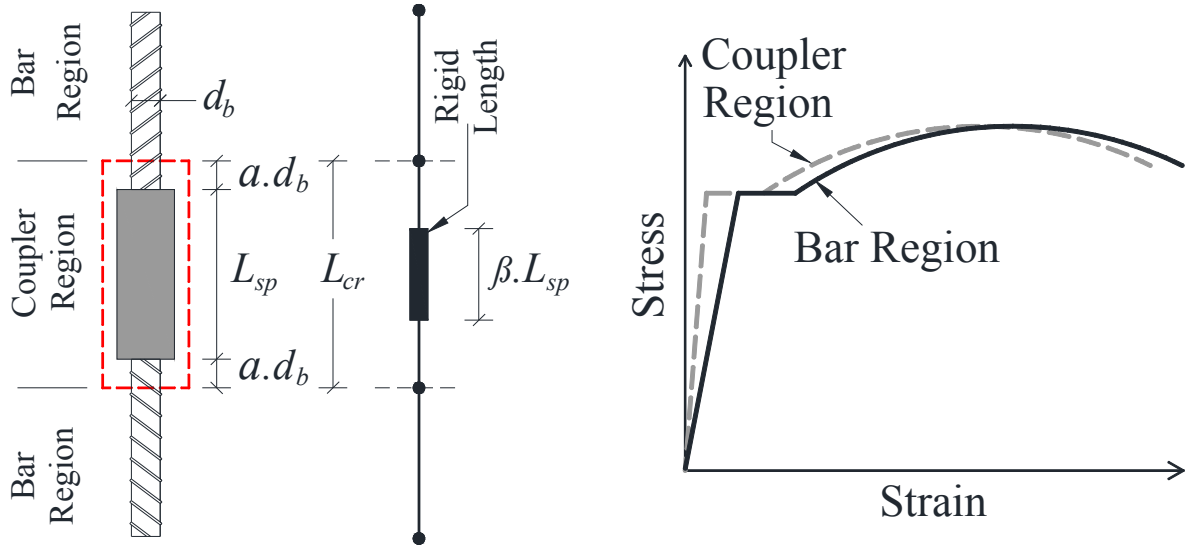

(a) Coupler Region (b) Stress-Strain Model for Couplers

Figure 4-1. Stress-Strain Model for Mechanical Bar Splices

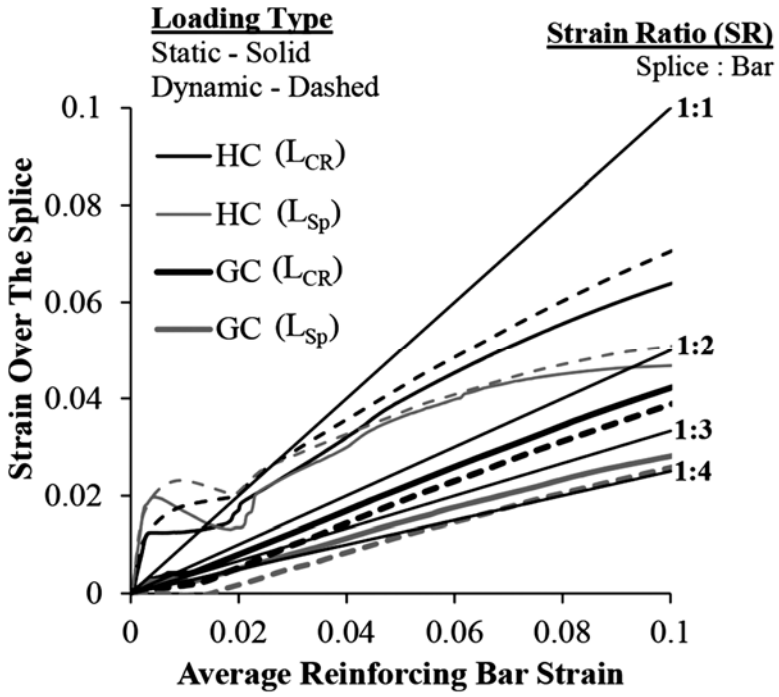

Figure 4-2. Measured Coupler Strain versus Measured Connecting Steel Bar Strains (Haber et al., 2015)

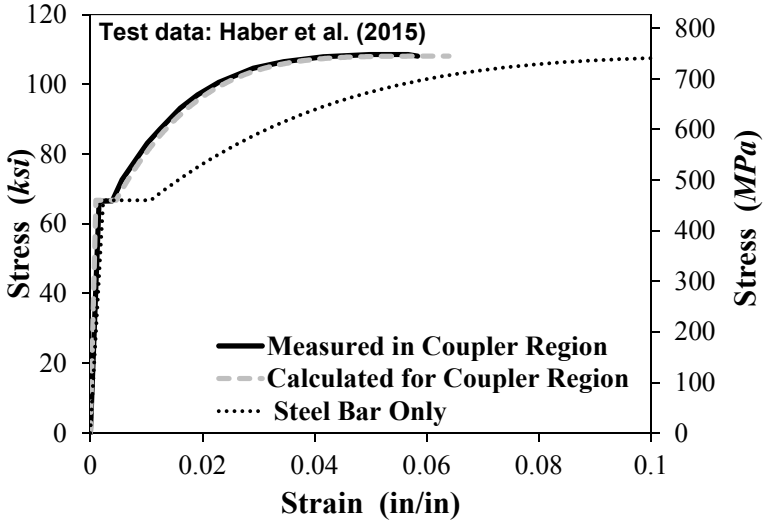

Figure 4-3. Measured and Calculated Stress-Strain Relationship for Grouted Couplers

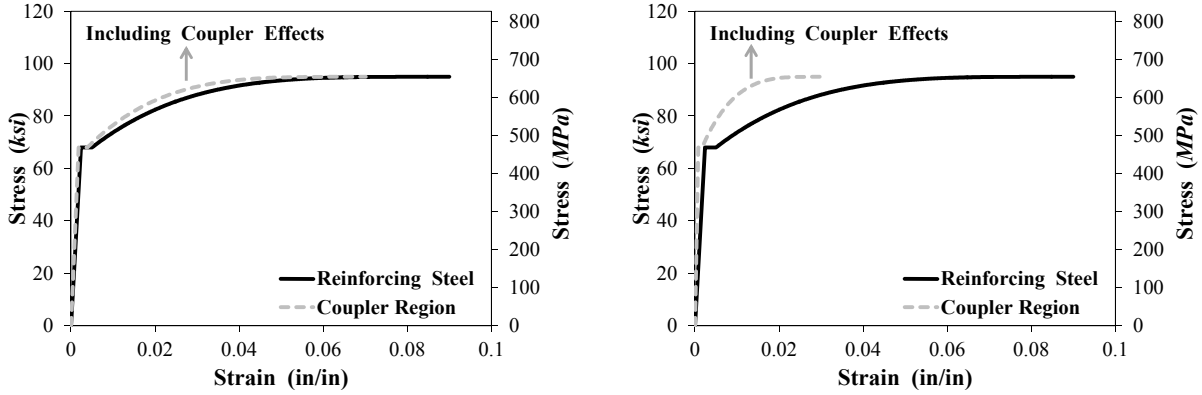

(a) Low Rigid Length Factor ($\beta = 0.25$) (b) High Rigid Length Factor ($\beta = 0.75$)

Figure 4-4. Effect of Coupler Rigid Length Factor on Stress-Strain Relationship

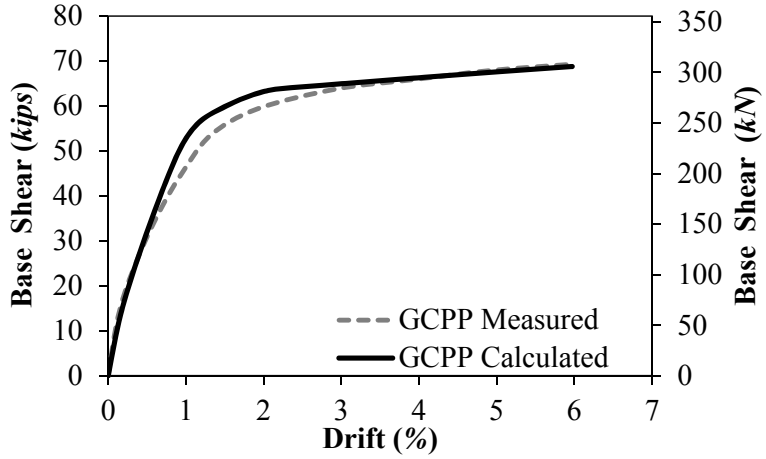

Figure 4-5. Measured and Calculated Force-Drift for GCPP Using Proposed Coupler Model

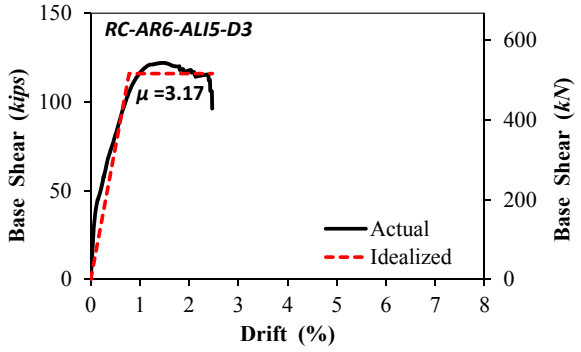

(a) Aspect Ratio 6, Axial Load Index 5%, Ductility 3

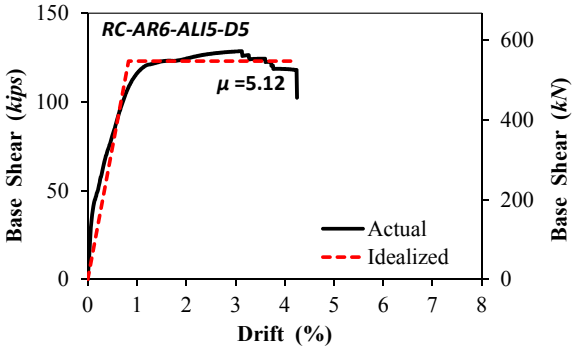

(b) Aspect Ratio 6, Axial Load Index 5%, Ductility 5

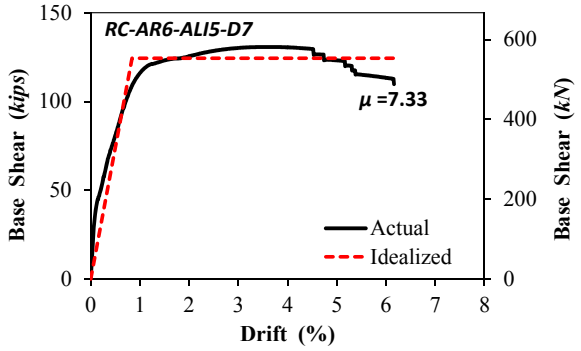

(c) Aspect Ratio 6, Axial Load Index 5%, Ductility 7

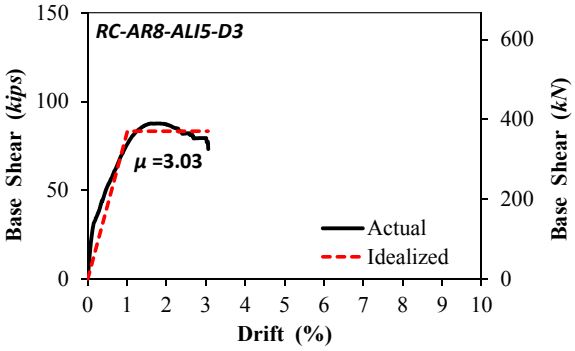

(d) Aspect Ratio 8, Axial Load Index 5%, Ductility 3

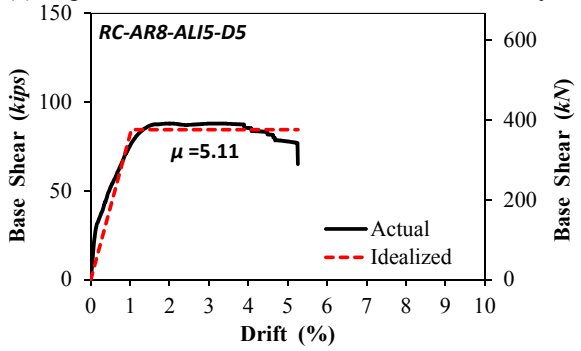

(e) Aspect Ratio 8, Axial Load Index 5%, Ductility 5

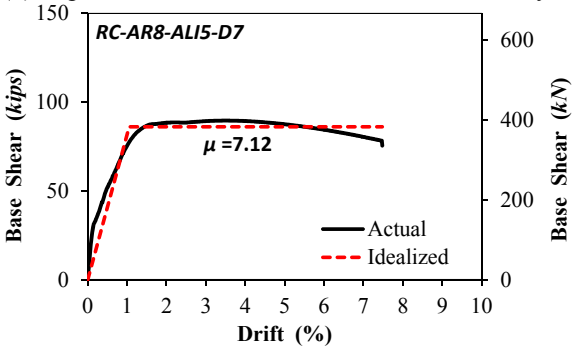

(f) Aspect Ratio 8, Axial Load Index 5%, Ductility 7

Figure 4-6. Reference RC Column Pushover Curves

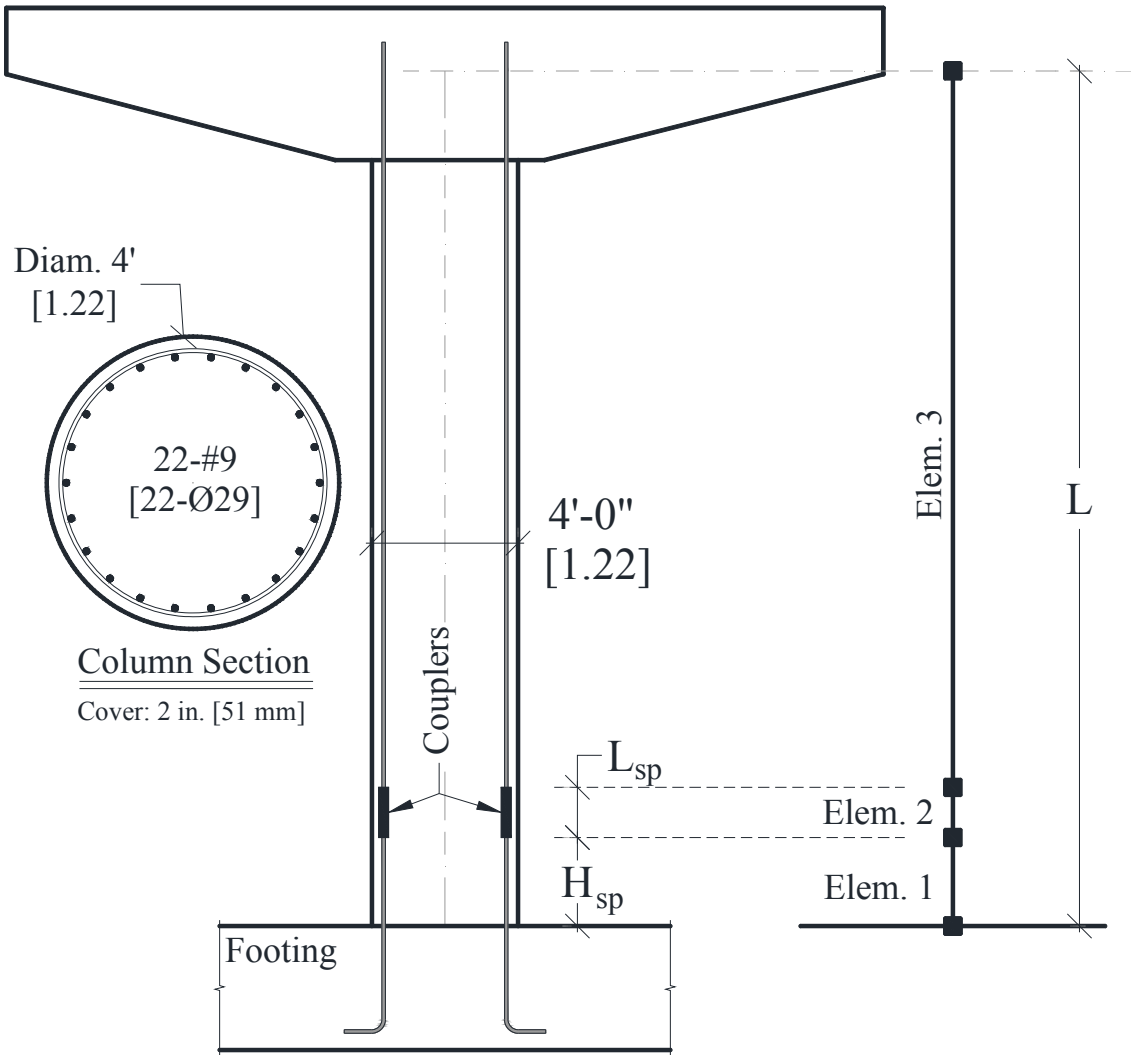

Figure 4-7. Analytical Model Details for Columns with Mechanical Bar Splices

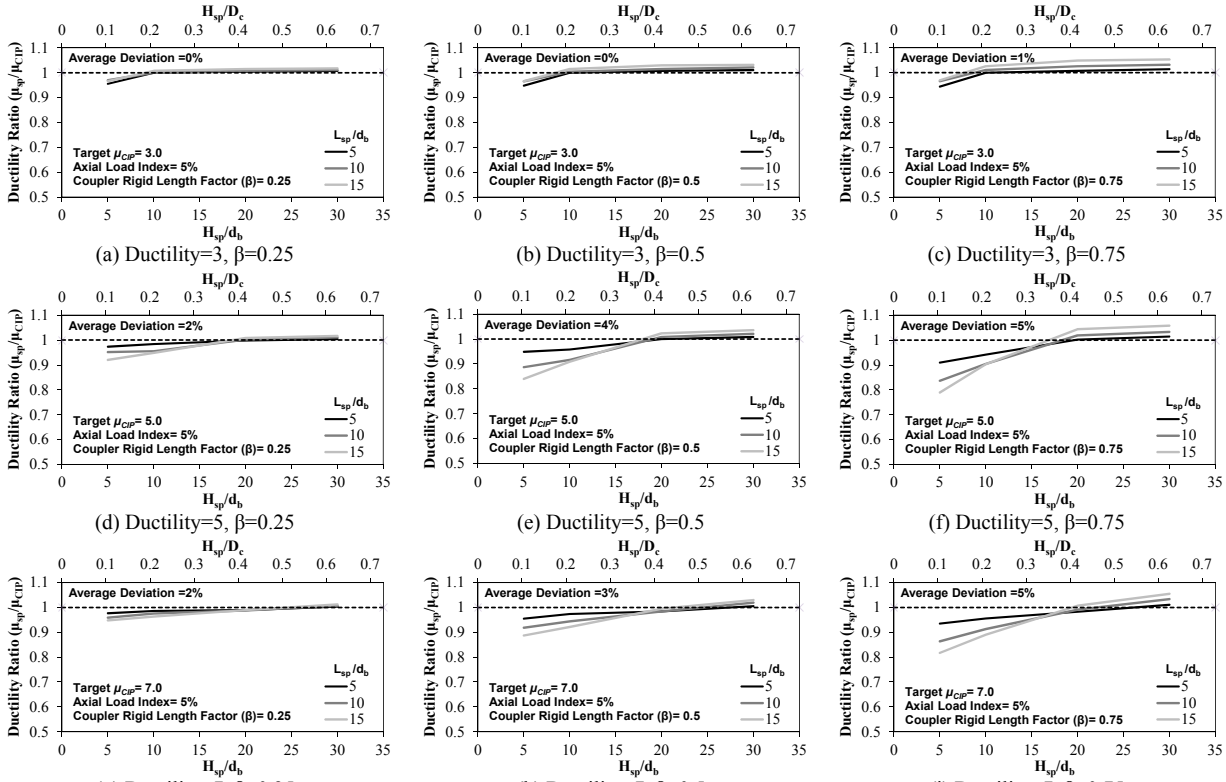

(a) Ductility=3, β=0.25 (b) Ductility=3, β=0.5 (c) Ductility=3, β=0.75

(d) Ductility=5, β=0.25 (e) Ductility=5, β=0.5 (f) Ductility=5, β=0.75

(g) Ductility=7, β=0.25 (h) Ductility=7, β=0.5 (i) Ductility=7, β=0.75

Figure 4-8. Effect of Coupler Lengh on Ductility of Columns with AR=4 and ALI=5%

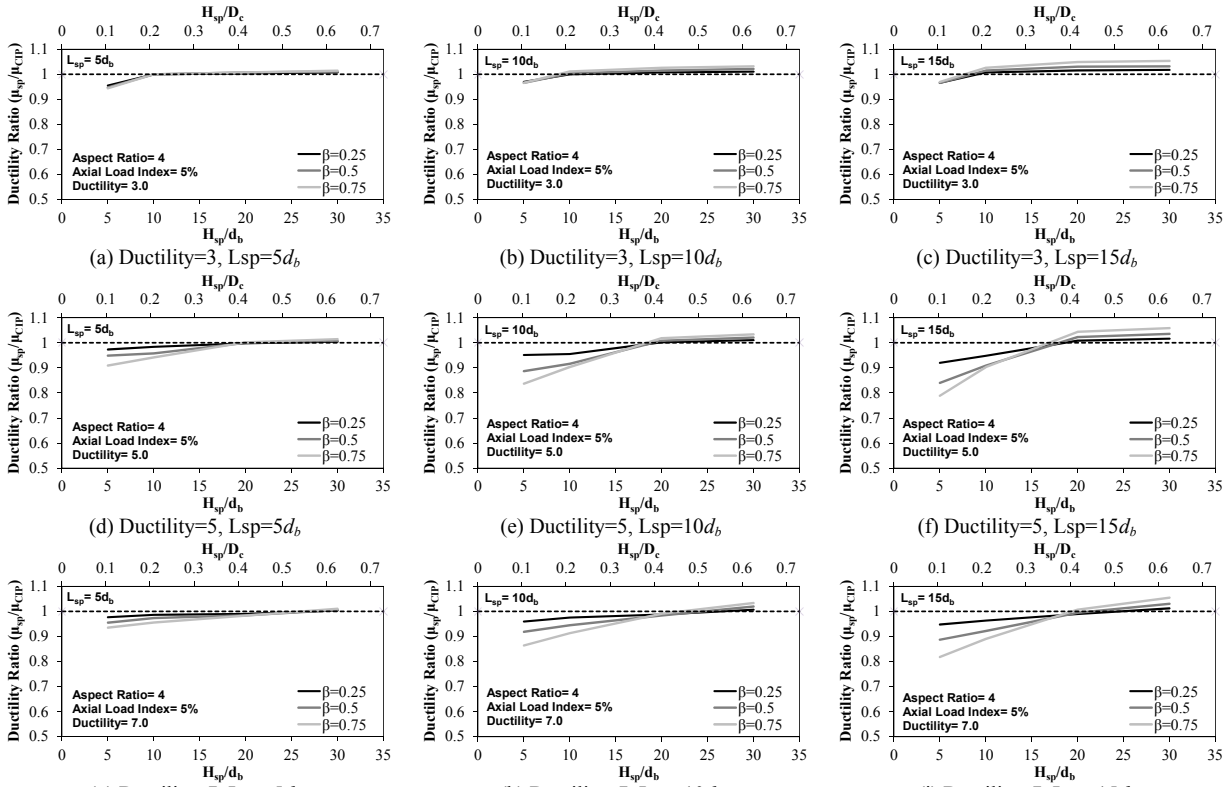

(a) Ductility=3, Lsp=5d_b (b) Ductility=3, Lsp=10d_b (c) Ductility=3, Lsp=15d_b

(d) Ductility=5, Lsp=5d_b (e) Ductility=5, Lsp=10d_b (f) Ductility=5, Lsp=15d_b

(g) Ductility=7, Lsp=5d_b (h) Ductility=7, Lsp=10d_b (i) Ductility=7, Lsp=15d_b

Figure 4-9. Effect of Coupler Rigid Length Factor on Ductility of Columns with AR=4 and ALI=5%

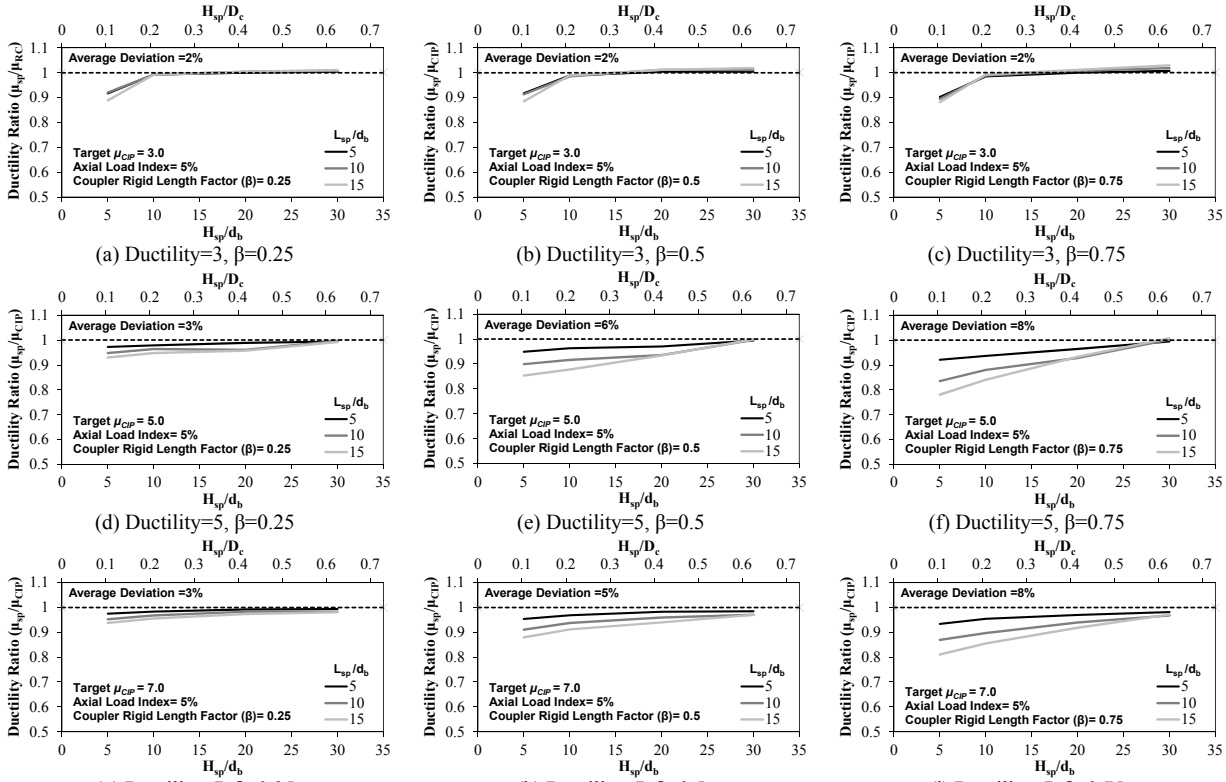

(a) Ductility=3, β=0.25 (b) Ductility=3, β=0.5 (c) Ductility=3, β=0.75

(d) Ductility=5, β=0.25 (e) Ductility=5, β=0.5 (f) Ductility=5, β=0.75

(g) Ductility=7, β=0.25 (h) Ductility=7, β=0.5 (i) Ductility=7, β=0.75

Figure 4-10. Effect of Coupler Lengh on Ductility of Columns with AR=6 and ALI=5%

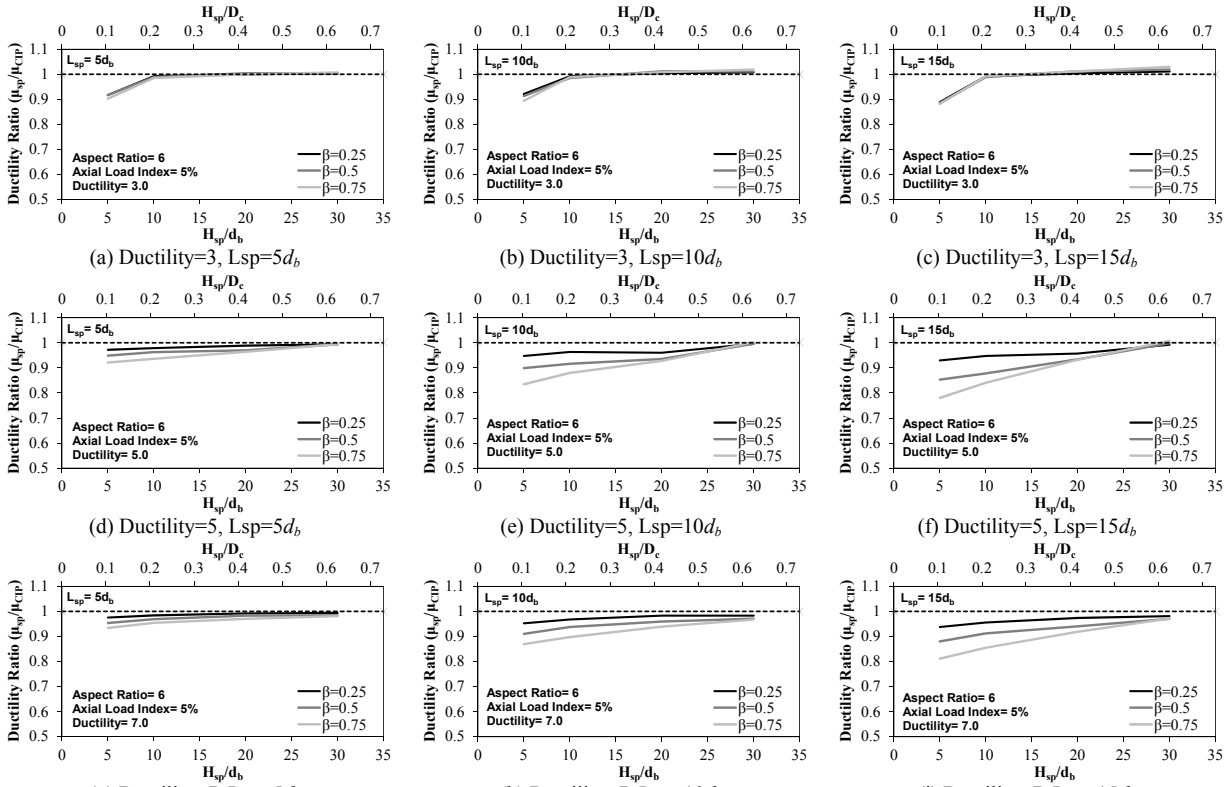

(a) Ductility=3, Lsp=5d_b (b) Ductility=3, Lsp=10d_b (c) Ductility=3, Lsp=15d_b

(d) Ductility=5, Lsp=5d_b (e) Ductility=5, Lsp=10d_b (f) Ductility=5, Lsp=15d_b

(g) Ductility=7, Lsp=5d_b (h) Ductility=7, Lsp=10d_b (i) Ductility=7, Lsp=15d_b

Figure 4-11. Effect of Coupler Rigid Length Factor on Ductility of Columns with AR=6 and ALI=5%

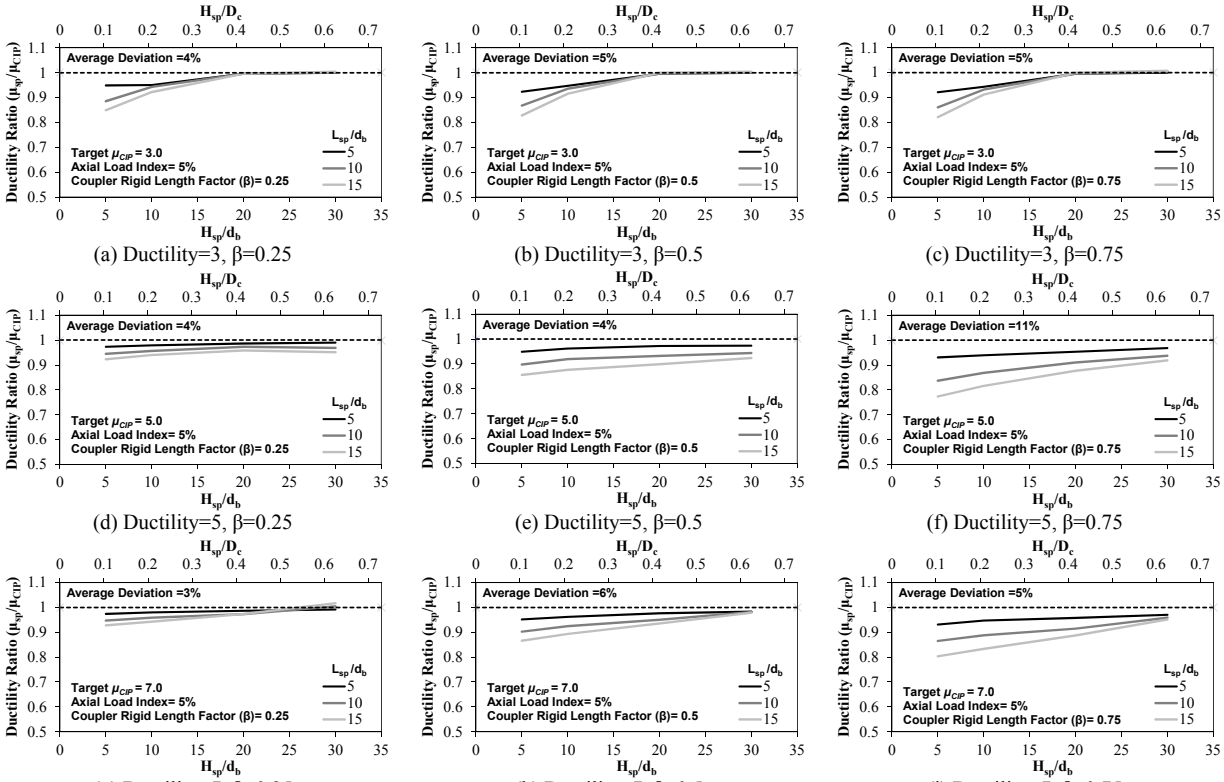

(a) Ductility=3, β=0.25 (b) Ductility=3, β=0.5 (c) Ductility=3, β=0.75

(d) Ductility=5, β=0.25 (e) Ductility=5, β=0.5 (f) Ductility=5, β=0.75

(g) Ductility=7, β=0.25 (h) Ductility=7, β=0.5 (i) Ductility=7, β=0.75

Figure 4-12. Effect of Coupler Lengh on Ductility of Columns with AR=8 and ALI=5%

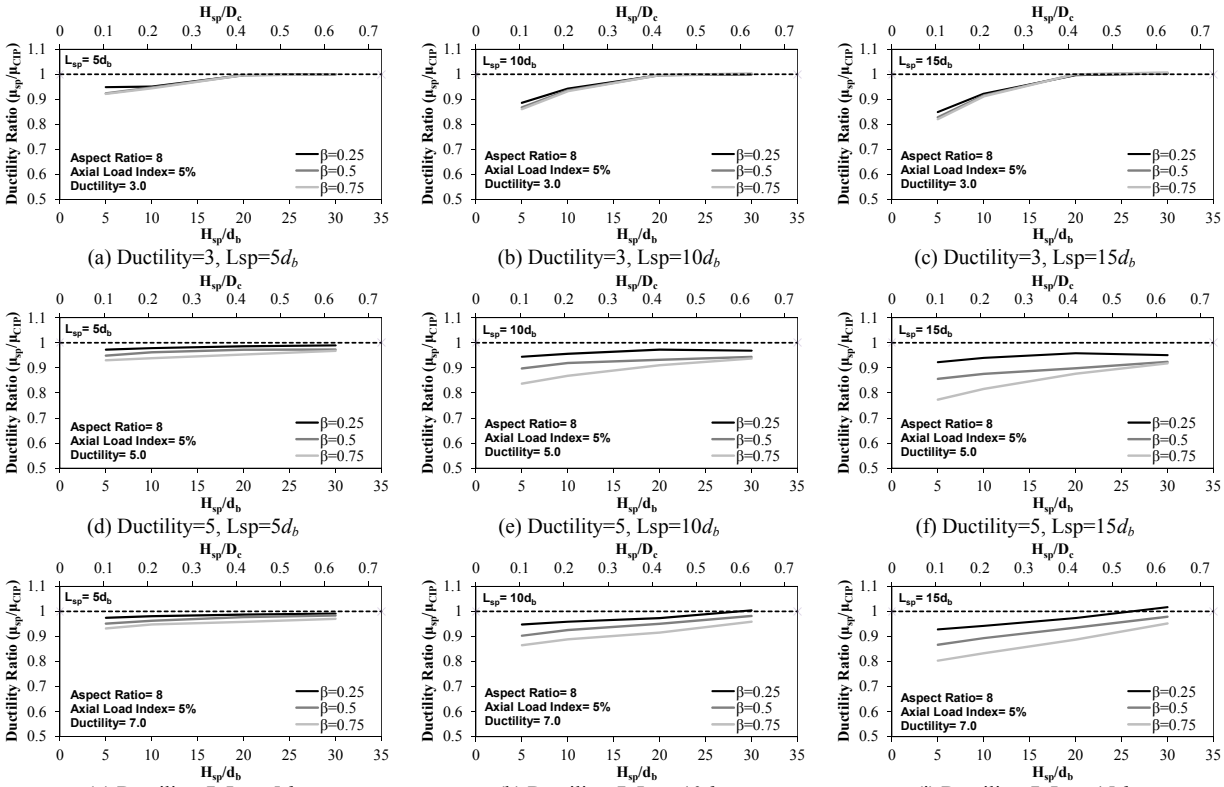

(a) Ductility=3, Lsp=5d_b (b) Ductility=3, Lsp=10d_b (c) Ductility=3, Lsp=15d_b

(d) Ductility=5, Lsp=5d_b (e) Ductility=5, Lsp=10d_b (f) Ductility=5, Lsp=15d_b

(g) Ductility=7, Lsp=5d_b (h) Ductility=7, Lsp=10d_b (i) Ductility=7, Lsp=15d_b

Figure 4-13. Effect of Coupler Rigid Length Factor on Ductility of Columns with AR=8 and ALI=5%

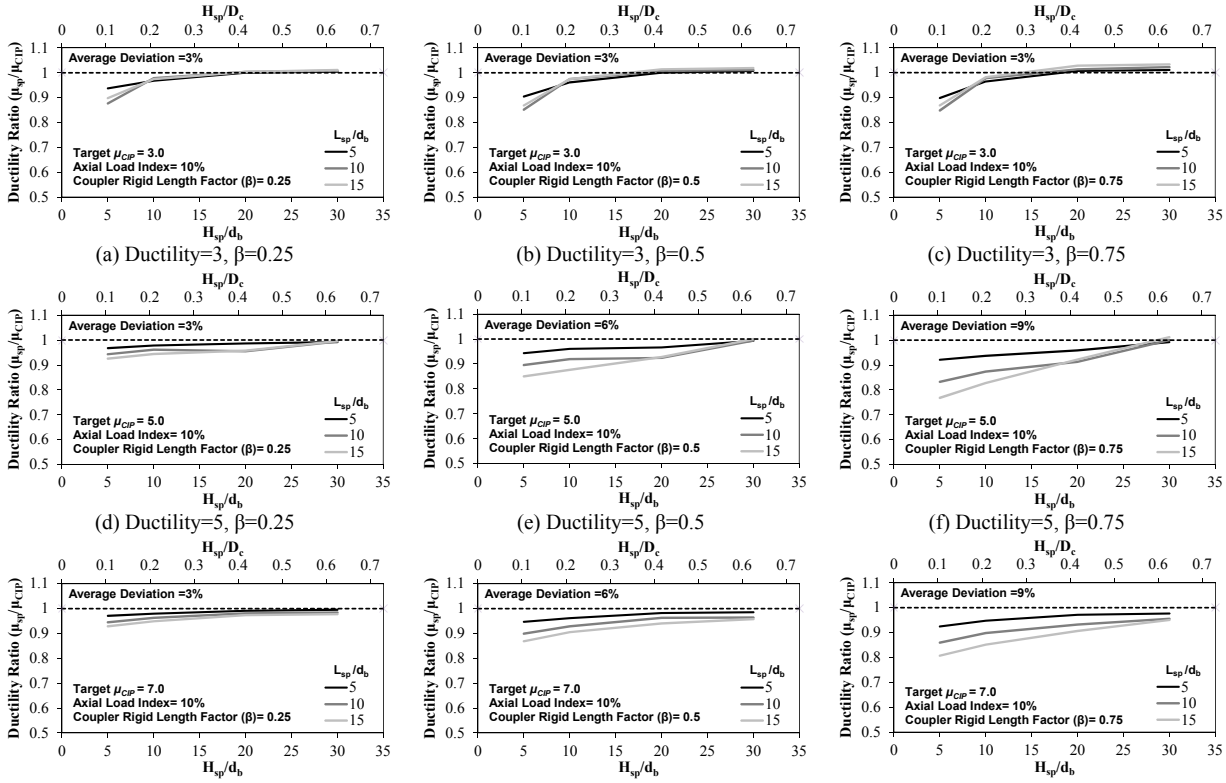

(a) Ductility=3, β=0.25 (b) Ductility=3, β=0.5 (c) Ductility=3, β=0.75

(d) Ductility=5, β=0.25 (e) Ductility=5, β=0.5 (f) Ductility=5, β=0.75

(g) Ductility=7, β=0.25 (h) Ductility=7, β=0.5 (i) Ductility=7, β=0.75

Figure 4-14. Effect of Coupler Lengh on Ductility of Columns with AR=6 and ALI=10%

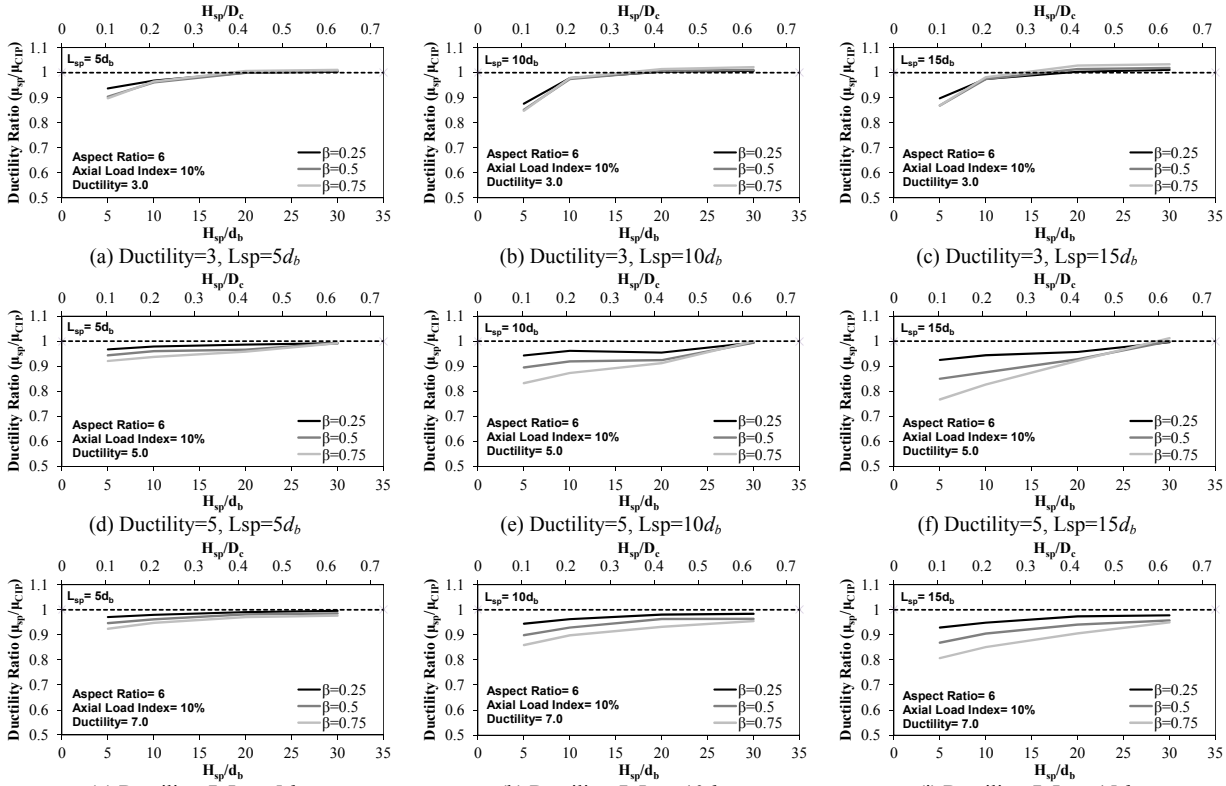

(a) Ductility=3, Lsp=5d_b (b) Ductility=3, Lsp=10d_b (c) Ductility=3, Lsp=15d_b

(d) Ductility=5, Lsp=5d_b (e) Ductility=5, Lsp=10d_b (f) Ductility=5, Lsp=15d_b

(g) Ductility=7, Lsp=5d_b (h) Ductility=7, Lsp=10d_b (i) Ductility=7, Lsp=15d_b

Figure 4-15. Effect of Coupler Rigid Length Factor on Ductility of Columns with AR=6 and ALI=10%

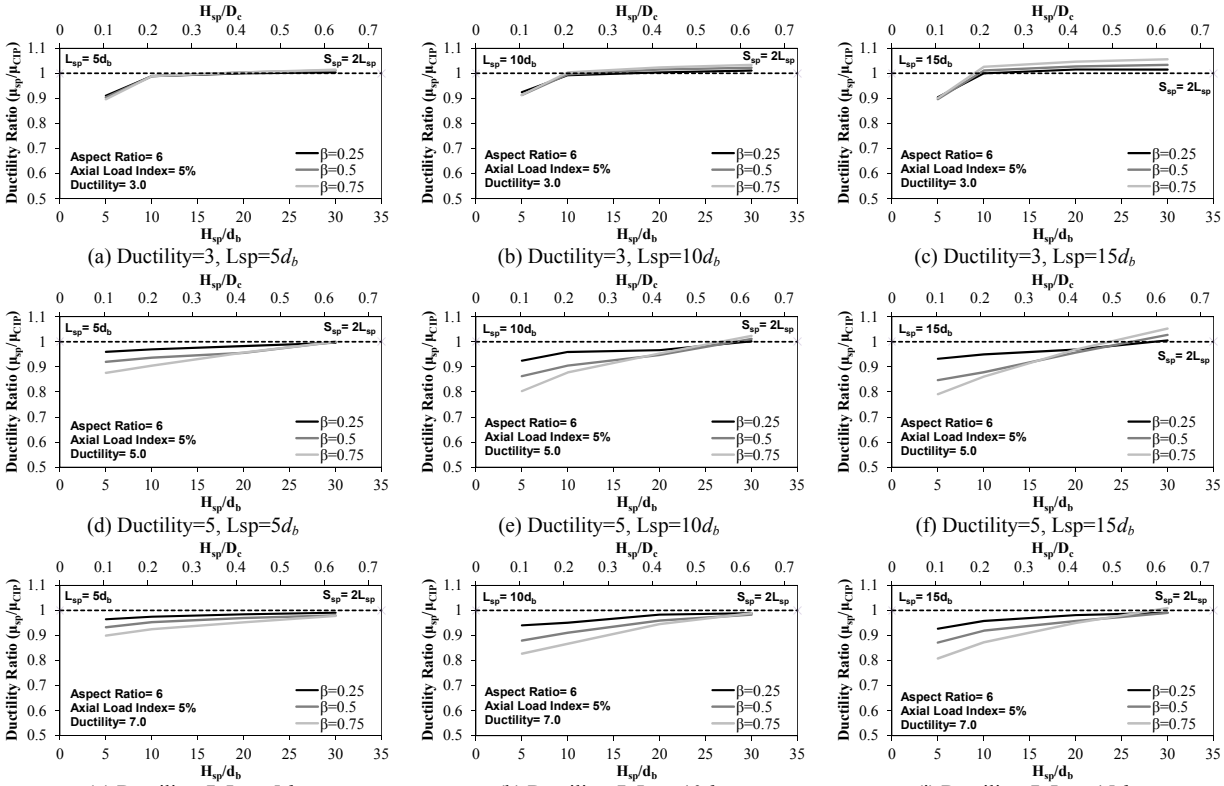

(a) Ductility=3, Lsp=5d_b (b) Ductility=3, Lsp=10d_b (c) Ductility=3, Lsp=15d_b

(d) Ductility=5, Lsp=5d_b (e) Ductility=5, Lsp=10d_b (f) Ductility=5, Lsp=15d_b

(g) Ductility=7, Lsp=5d_b (h) Ductility=7, Lsp=10d_b (i) Ductility=7, Lsp=15d_b

Figure 4-16. Effect of Coupler Spacing on Ductility of Columns with AR=6 and ALI=5%

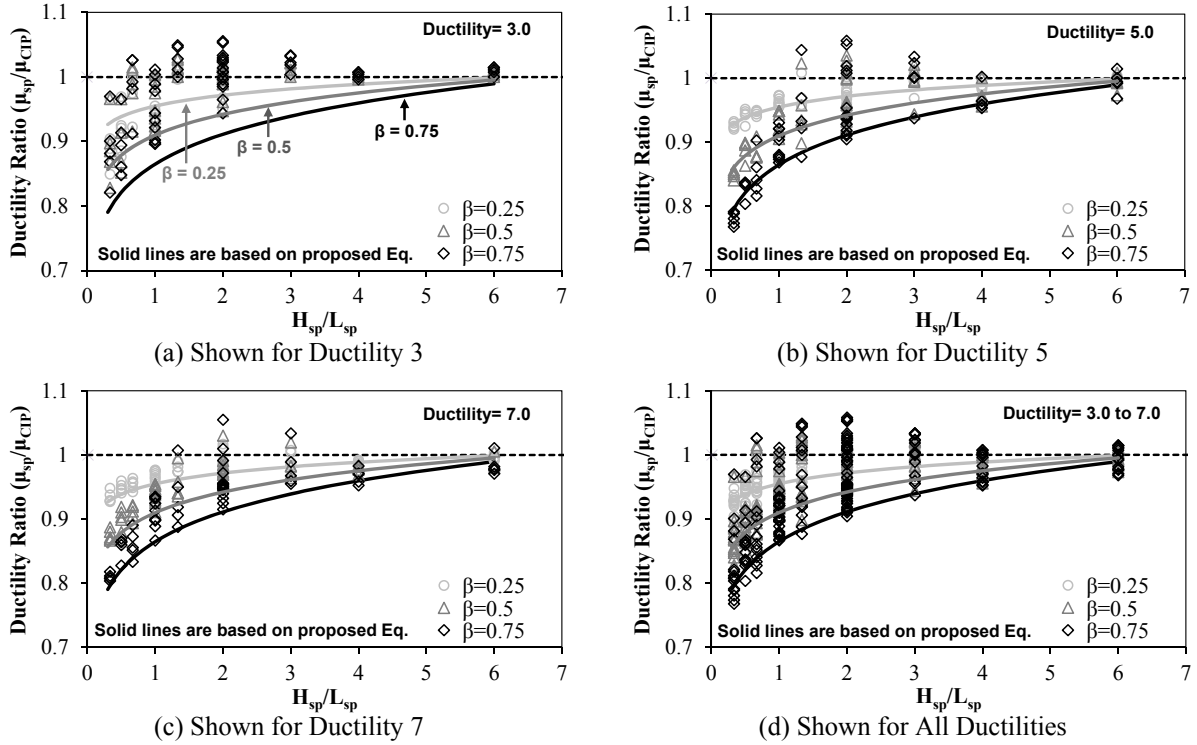

(a) Shown for Ductility 3 (b) Shown for Ductility 5

(c) Shown for Ductility 7 (d) Shown for All Ductilities

Figure 4-17. Proposed Design Equation Accounting for Coupler Effects versus Analysis Results

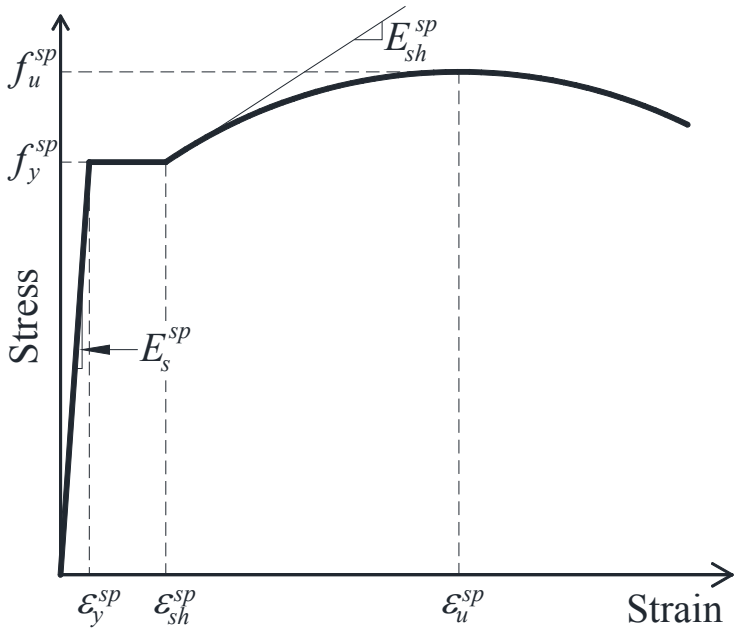

Figure R-1. Stress-Strain Model for Mechanical Bar Splices

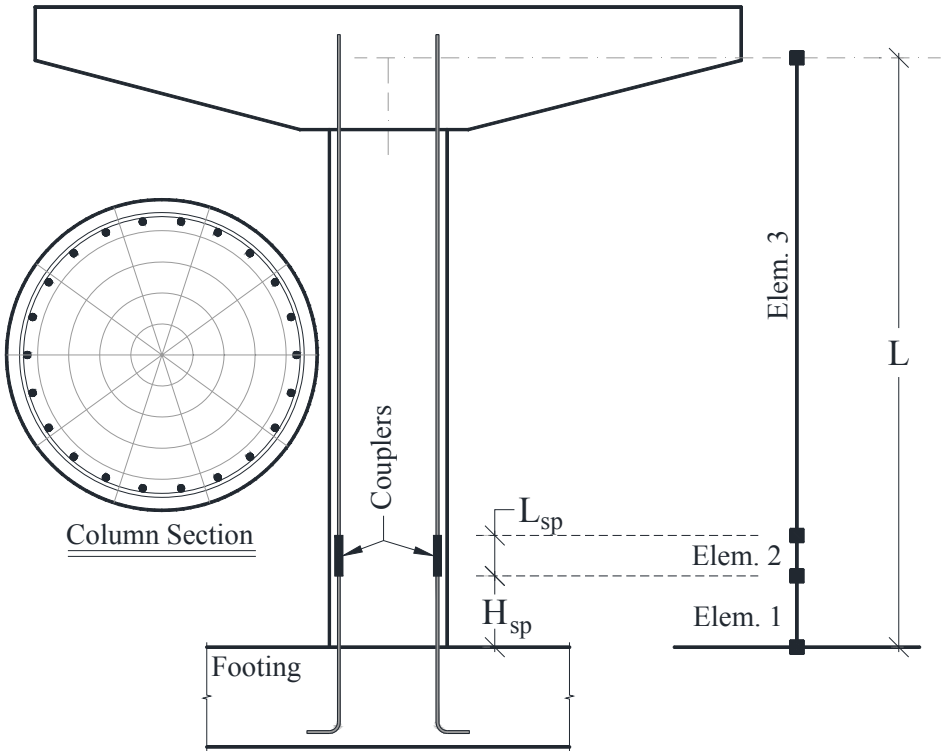

Figure C-1. Analytical Model Details for Columns with Mechanical Bar Splices

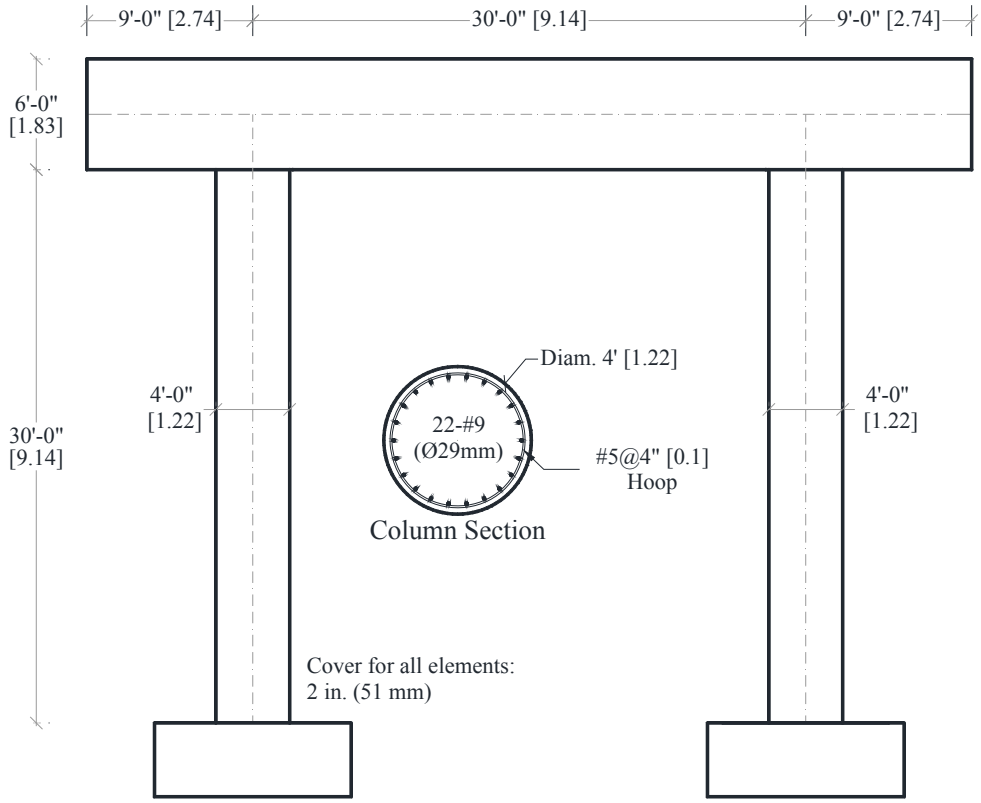

Figure 6-1. CIP Two-Column Bent Details, units: *ft* [*m*]

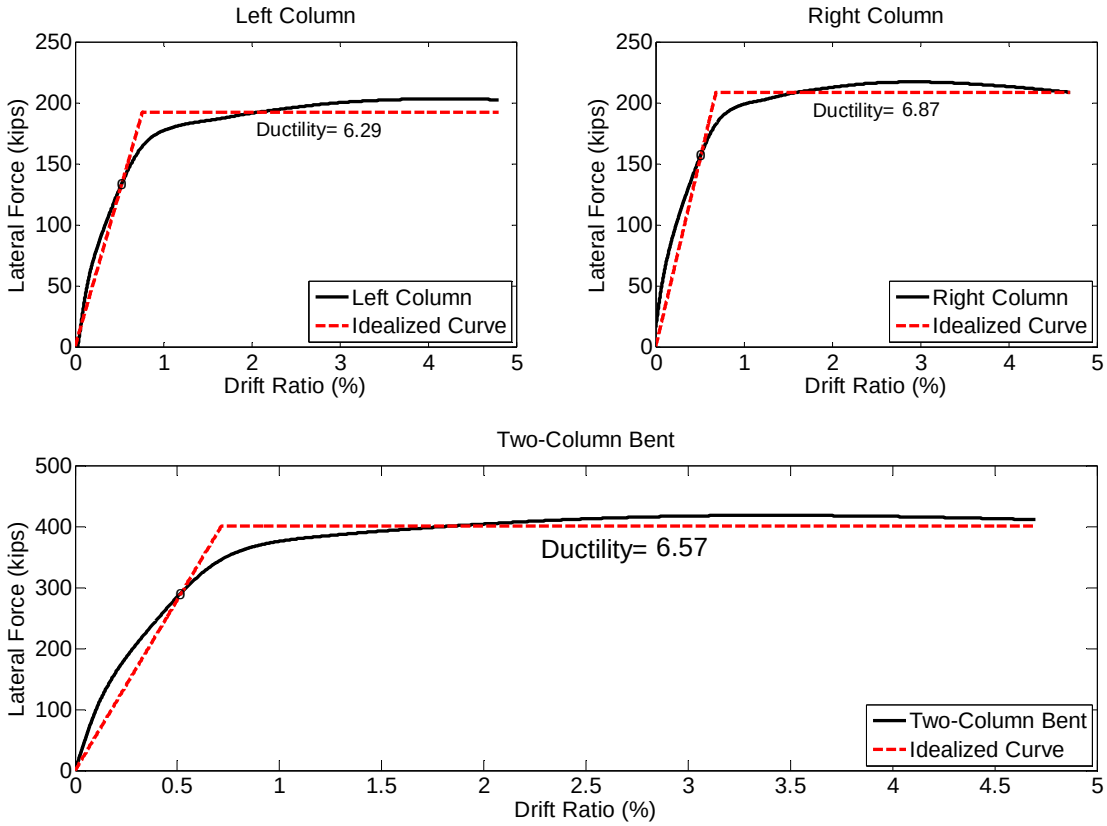

Figure 6-2. Pushover Response of CIP Bent for Loading from Left

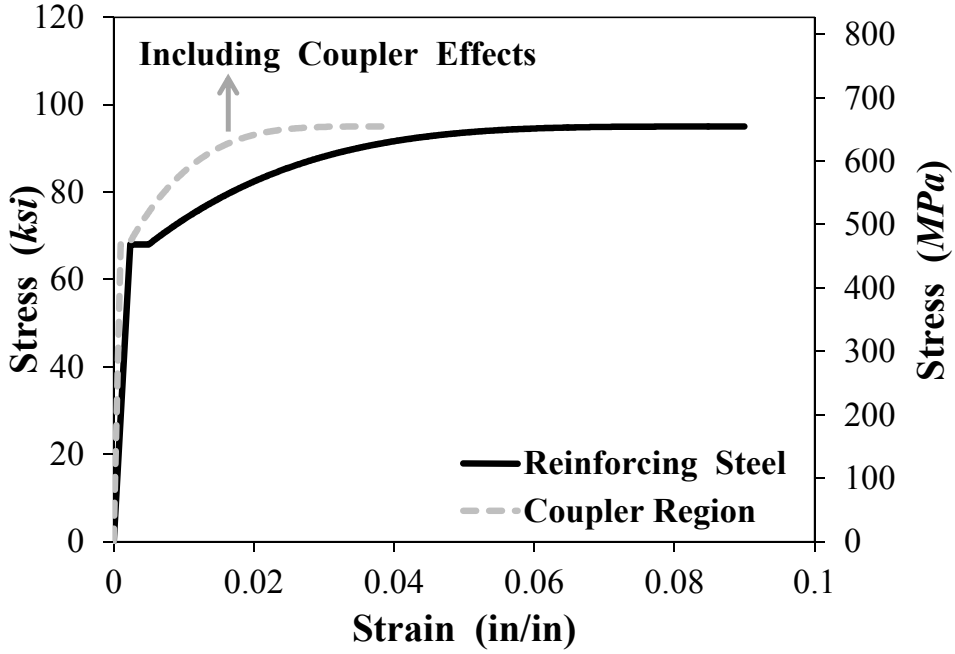

Figure 6-3. Grouted Coupler Stress-Strain Relationship

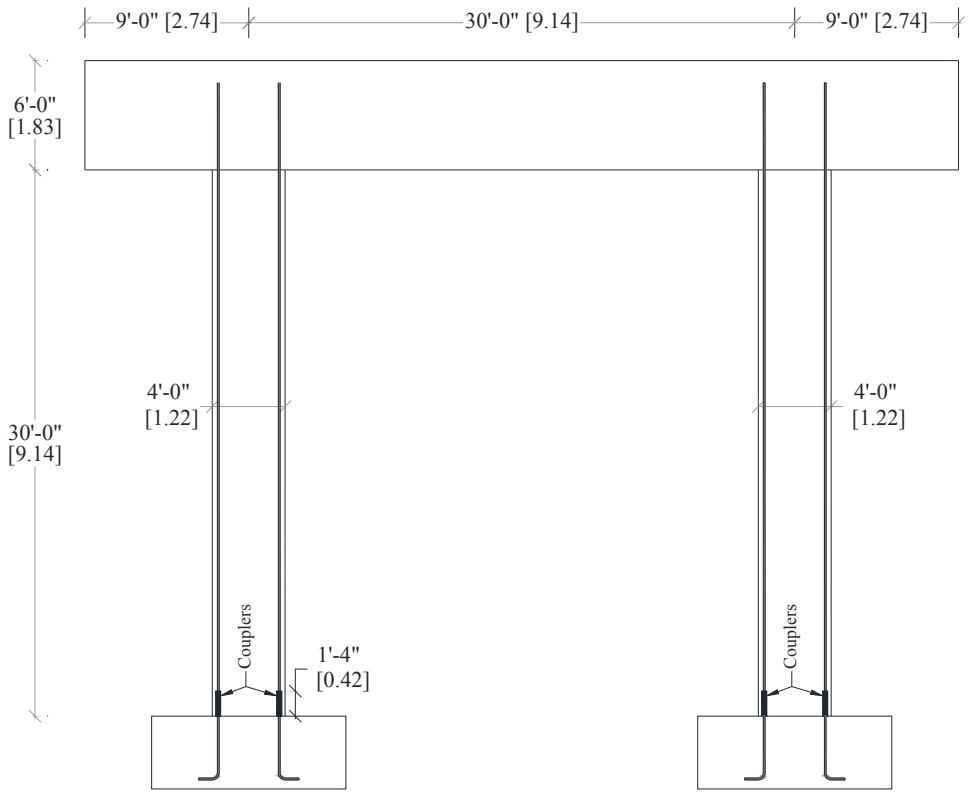

Figure 6-4. Bent with Grouted Couplers at Column Base, units: *ft* [*m*]

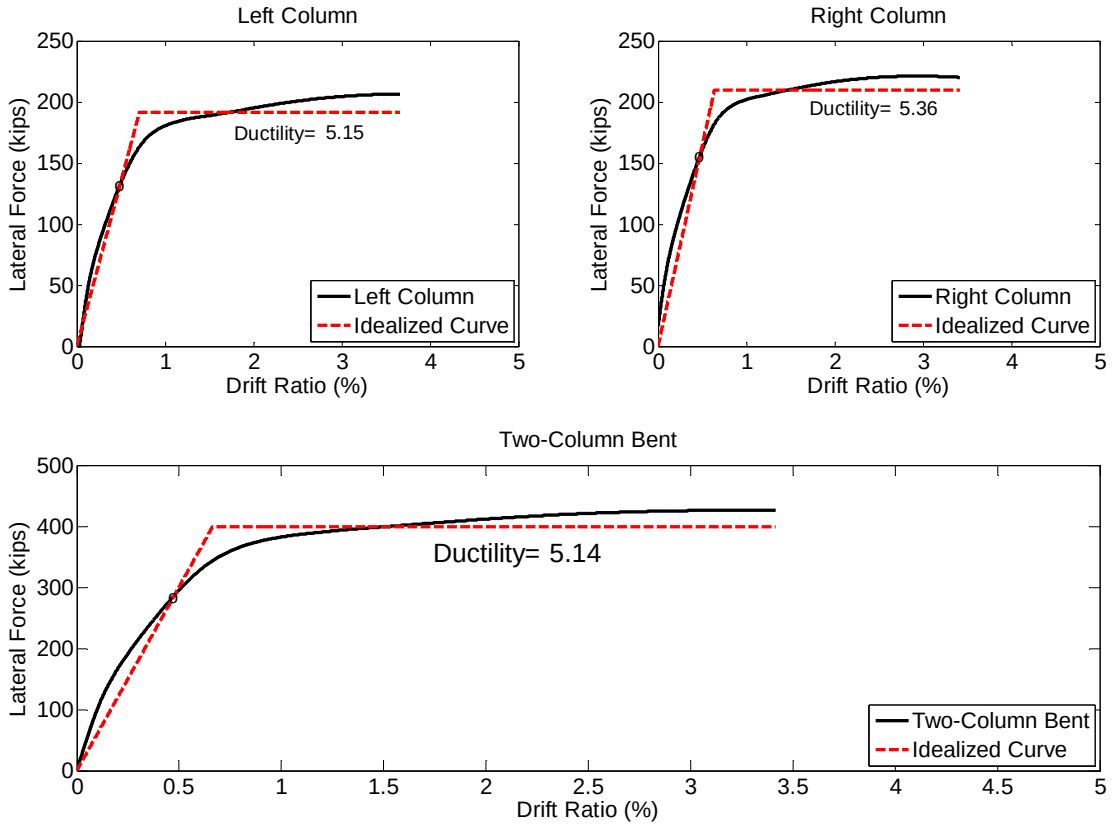

Figure 6-5. Pushover Response of Bent with Grouted Couplers at Column Base for Loading from Left

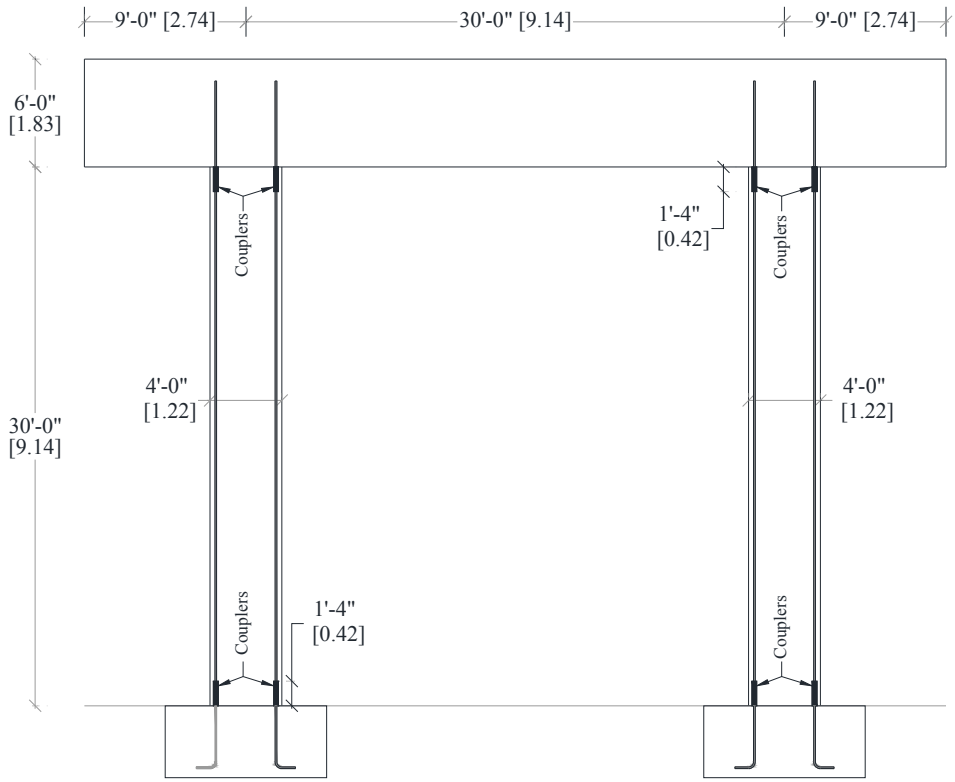

Figure 6-6. Bent with Grouted Couplers at Both Ends of Column, units: *ft* [*m*]

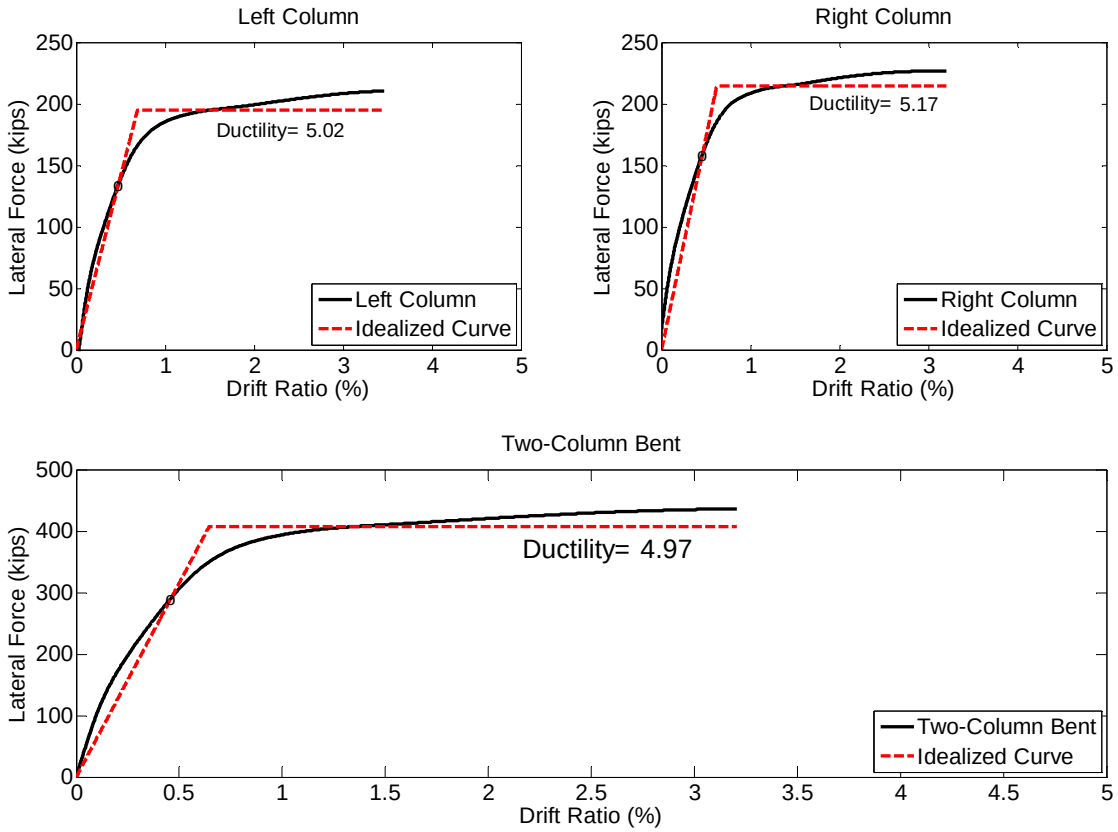

Figure 6-7. Pushover Response of Bent with Grouted Couplers at Both Ends of Columns

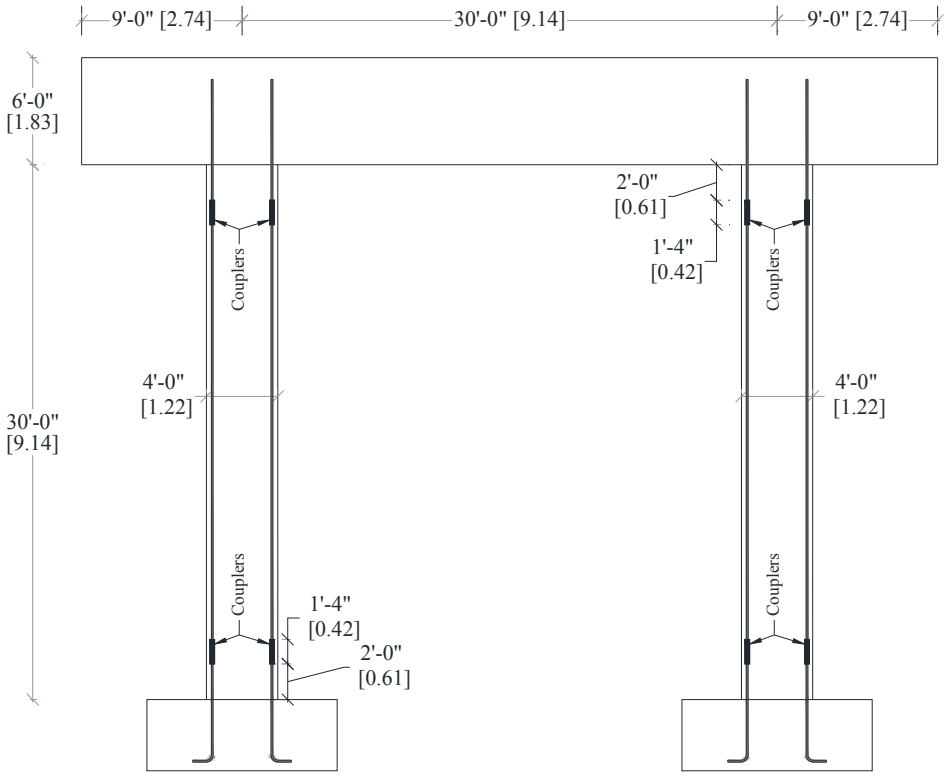

Figure 6-8. Bent with Shifted Grouted Couplers at Both Ends of Column, units: *ft* [*m*]

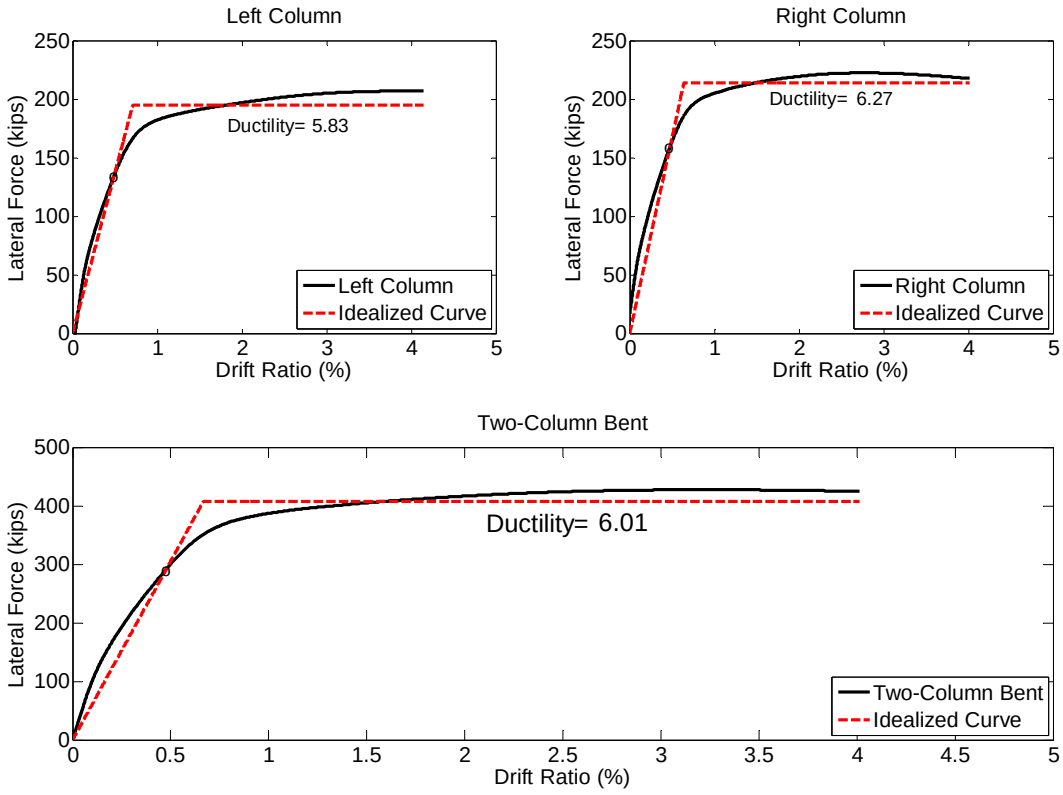

Figure 6-9. Pushover Response of Bent with Shifted Grouted Couplers at Both Ends of Columns

List of CCEER Publications

Report No.	Publication
CCEER-84-1	Saiidi, M., and R. Lawver, "User's Manual for LZAK-C64, A Computer Program to Implement the Q-Model on Commodore 64," Civil Engineering Department, Report No. CCEER-84-1, University of Nevada, Reno, January 1984.
CCEER-84-1 Reprint	Douglas, B., Norris, G., Saiidi, M., Dodd, L., Richardson, J. and Reid, W., "Simple Bridge Models for Earthquakes and Test Data," Civil Engineering Department, Report No. CCEER-84-1 Reprint, University of Nevada, Reno, January 1984.
CCEER-84-2	Douglas, B. and T. Iwasaki, "Proceedings of the First USA-Japan Bridge Engineering Workshop," held at the Public Works Research Institute, Tsukuba, Japan, Civil Engineering Department, Report No. CCEER-84-2, University of Nevada, Reno, April 1984.
CCEER-84-3	Saiidi, M., J. Hart, and B. Douglas, "Inelastic Static and Dynamic Analysis of Short R/C Bridges Subjected to Lateral Loads," Civil Engineering Department, Report No. CCEER-84-3, University of Nevada, Reno, July 1984.
CCEER-84-4	Douglas, B., "A Proposed Plan for a National Bridge Engineering Laboratory," Civil Engineering Department, Report No. CCEER-84-4, University of Nevada, Reno, December 1984.
CCEER-85-1	Norris, G. and P. Abdollaholiaee, "Laterally Loaded Pile Response: Studies with the Strain Wedge Model," Civil Engineering Department, Report No. CCEER-85-1, University of Nevada, Reno, April 1985.
CCEER-86-1	Ghusn, G. and M. Saiidi, "A Simple Hysteretic Element for Biaxial Bending of R/C in NEABS-86," Civil Engineering Department, Report No. CCEER-86-1, University of Nevada, Reno, July 1986.
CCEER-86-2	Saiidi, M., R. Lawver, and J. Hart, "User's Manual of ISADAB and SIBA, Computer Programs for Nonlinear Transverse Analysis of Highway Bridges Subjected to Static and Dynamic Lateral Loads," Civil Engineering Department, Report No. CCEER-86-2, University of Nevada, Reno, September 1986.
CCEER-87-1	Siddharthan, R., "Dynamic Effective Stress Response of Surface and Embedded Footings in Sand," Civil Engineering Department, Report No. CCEER-86-2, University of Nevada, Reno, June 1987.
CCEER-87-2	Norris, G. and R. Sack, "Lateral and Rotational Stiffness of Pile Groups for Seismic Analysis of Highway Bridges," Civil Engineering Department, Report No. CCEER-87-2, University of Nevada, Reno, June 1987.
CCEER-88-1	Orie, J. and M. Saiidi, "A Preliminary Study of One-Way Reinforced Concrete Pier Hinges

Subjected to Shear and Flexure," Civil Engineering Department, Report No. CCEER-88-1, University of Nevada, Reno, January 1988.

CCEER-88-2 Orie, D., M. Saiidi, and B. Douglas, "A Micro-CAD System for Seismic Design of Regular Highway Bridges," Civil Engineering Department, Report No. CCEER-88-2, University of Nevada, Reno, June 1988.

CCEER-88-3 Orie, D. and M. Saiidi, "User's Manual for Micro-SARB, a Microcomputer Program for Seismic Analysis of Regular Highway Bridges," Civil Engineering Department, Report No. CCEER-88-3, University of Nevada, Reno, October 1988.

CCEER-89-1 Douglas, B., M. Saiidi, R. Hayes, and G. Holcomb, "A Comprehensive Study of the Loads and Pressures Exerted on Wall Forms by the Placement of Concrete," Civil Engineering Department, Report No. CCEER-89-1, University of Nevada, Reno, February 1989.

CCEER-89-2 Richardson, J. and B. Douglas, "Dynamic Response Analysis of the Dominion Road Bridge Test Data," Civil Engineering Department, Report No. CCEER-89-2, University of Nevada, Reno, March 1989.

CCEER-89-2 Vrontinos, S., M. Saiidi, and B. Douglas, "A Simple Model to Predict the Ultimate Response of R/C Beams with Concrete Overlays," Civil Engineering Department, Report NO. CCEER-89-2, University of Nevada, Reno, June 1989.

CCEER-89-3 Ebrahimpour, A. and P. Jagadish, "Statistical Modeling of Bridge Traffic Loads - A Case Study," Civil Engineering Department, Report No. CCEER-89-3, University of Nevada, Reno, December 1989.

CCEER-89-4 Shields, J. and M. Saiidi, "Direct Field Measurement of Prestress Losses in Box Girder Bridges," Civil Engineering Department, Report No. CCEER-89-4, University of Nevada, Reno, December 1989.

CCEER-90-1 Saiidi, M., E. Maragakis, G. Ghusn, Y. Jiang, and D. Schwartz, "Survey and Evaluation of Nevada's Transportation Infrastructure, Task 7.2 - Highway Bridges, Final Report," Civil Engineering Department, Report No. CCEER 90-1, University of Nevada, Reno, October 1990.

CCEER-90-2 Abdel-Ghaffar, S., E. Maragakis, and M. Saiidi, "Analysis of the Response of Reinforced Concrete Structures During the Whittier Earthquake 1987," Civil Engineering Department, Report No. CCEER 90-2, University of Nevada, Reno, October 1990.

CCEER-91-1 Saiidi, M., E. Hwang, E. Maragakis, and B. Douglas, "Dynamic Testing and the Analysis of the Flamingo Road Interchange," Civil Engineering Department, Report No. CCEER-91-1, University of Nevada, Reno, February 1991.

CCEER-91-2 Norris, G., R. Siddharthan, Z. Zafir, S. Abdel-Ghaffar, and P. Gowda, "Soil-Foundation-Structure Behavior at the Oakland Outer Harbor Wharf," Civil Engineering Department, Report No. CCEER-91-2, University of Nevada, Reno, July 1991.

CCEER-91-3 Norris, G., "Seismic Lateral and Rotational Pile Foundation Stiffnesses at Cypress," Civil Engineering Department, Report No. CCEER-91-3, University of Nevada, Reno, August 1991.

CCEER-91-4 O'Connor, D. and M. Saiidi, "A Study of Protective Overlays for Highway Bridge Decks in Nevada, with Emphasis on Polyester-Styrene Polymer Concrete," Civil Engineering Department, Report No. CCEER-91-4, University of Nevada, Reno, October 1991.

CCEER-91-5 O'Connor, D.N. and M. Saiidi, "Laboratory Studies of Polyester-Styrene Polymer Concrete Engineering Properties," Civil Engineering Department, Report No. CCEER-91-5, University of Nevada, Reno, November 1991.

CCEER-92-1 Straw, D.L. and M. Saiidi, "Scale Model Testing of One-Way Reinforced Concrete Pier Hinges Subject to Combined Axial Force, Shear and Flexure," edited by D.N. O'Connor, Civil Engineering Department, Report No. CCEER-92-1, University of Nevada, Reno, March 1992.

CCEER-92-2 Wehbe, N., M. Saiidi, and F. Gordaninejad, "Basic Behavior of Composite Sections Made of Concrete Slabs and Graphite Epoxy Beams," Civil Engineering Department, Report No. CCEER-92-2, University of Nevada, Reno, August 1992.

CCEER-92-3 Saiidi, M. and E. Hutchens, "A Study of Prestress Changes in A Post-Tensioned Bridge During the First 30 Months," Civil Engineering Department, Report No. CCEER-92-3, University of Nevada, Reno, April 1992.

CCEER-92-4 Saiidi, M., B. Douglas, S. Feng, E. Hwang, and E. Maragakis, "Effects of Axial Force on Frequency of Prestressed Concrete Bridges," Civil Engineering Department, Report No. CCEER-92-4, University of Nevada, Reno, August 1992.

CCEER-92-5 Siddharthan, R., and Z. Zafir, "Response of Layered Deposits to Traveling Surface Pressure Waves," Civil Engineering Department, Report No. CCEER-92-5, University of Nevada, Reno, September 1992.

CCEER-92-6 Norris, G., and Z. Zafir, "Liquefaction and Residual Strength of Loose Sands from Drained Triaxial Tests," Civil Engineering Department, Report No. CCEER-92-6, University of Nevada, Reno, September 1992.

CCEER-92-6-A Norris, G., Siddharthan, R., Zafir, Z. and Madhu, R. "Liquefaction and Residual Strength of Sands from Drained Triaxial Tests," Civil Engineering Department, Report No. CCEER-92-6-A, University of Nevada, Reno, September 1992.

CCEER-92-7 Douglas, B., "Some Thoughts Regarding the Improvement of the University of Nevada, Reno's National Academic Standing," Civil Engineering Department, Report No. CCEER-92-7, University of Nevada, Reno, September 1992.

CCEER-92-8 Saiidi, M., E. Maragakis, and S. Feng, "An Evaluation of the Current Caltrans Seismic Restrainer Design Method," Civil Engineering Department, Report No. CCEER-92-8, University of Nevada, Reno, October 1992.

CCEER-92-9 O'Connor, D., M. Saiidi, and E. Maragakis, "Effect of Hinge Restrainers on the Response of the Madrone Drive Undercrossing During the Loma Prieta Earthquake," Civil Engineering Department, Report No. CCEER-92-9, University of Nevada, Reno, February 1993.

CCEER-92-10 O'Connor, D., and M. Saiidi, "Laboratory Studies of Polyester Concrete: Compressive Strength at Elevated Temperatures and Following Temperature Cycling, Bond Strength to Portland Cement Concrete, and Modulus of Elasticity," Civil Engineering Department, Report No. CCEER-92-10, University of Nevada, Reno, February 1993.

CCEER-92-11 Wehbe, N., M. Saiidi, and D. O'Connor, "Economic Impact of Passage of Spent Fuel Traffic on Two Bridges in Northeast Nevada," Civil Engineering Department, Report No. CCEER-92-11, University of Nevada, Reno, December 1992.

CCEER-93-1 Jiang, Y., and M. Saiidi, "Behavior, Design, and Retrofit of Reinforced Concrete One-way Bridge Column Hinges," edited by D. O'Connor, Civil Engineering Department, Report

No. CCEER-93-1, University of Nevada, Reno, March 1993.

CCEER-93-2 Abdel-Ghaffar, S., E. Maragakis, and M. Saiidi, "Evaluation of the Response of the Aptos Creek Bridge During the 1989 Loma Prieta Earthquake," Civil Engineering Department, Report No. CCEER-93-2, University of Nevada, Reno, June 1993.

CCEER-93-3 Sanders, D.H., B.M. Douglas, and T.L. Martin, "Seismic Retrofit Prioritization of Nevada Bridges," Civil Engineering Department, Report No. CCEER-93-3, University of Nevada, Reno, July 1993.

CCEER-93-4 Abdel-Ghaffar, S., E. Maragakis, and M. Saiidi, "Performance of Hinge Restrainers in the Huntington Avenue Overhead During the 1989 Loma Prieta Earthquake," Civil Engineering Department, Report No. CCEER-93-4, University of Nevada, Reno, June 1993 (in final preparation).

CCEER-93-5 Maragakis, E., M. Saiidi, S. Feng, and L. Flournoy, "Effects of Hinge Restrainers on the Response of the San Gregorio Bridge during the Loma Prieta Earthquake," (in final preparation) Civil Engineering Department, Report No. CCEER-93-5, University of Nevada, Reno.

CCEER-93-6 Saiidi, M., E. Maragakis, S. Abdel-Ghaffar, S. Feng, and D. O'Connor, "Response of Bridge Hinge Restrainers during Earthquakes -Field Performance, Analysis, and Design," Civil Engineering Department, Report No. CCEER-93-6, University of Nevada, Reno, May 1993.

CCEER-93-7 Wehbe, N., Saiidi, M., Maragakis, E., and Sanders, D., "Adequacy of Three Highway Structures in Southern Nevada for Spent Fuel Transportation," Civil Engineering Department, Report No. CCEER-93-7, University of Nevada, Reno, August 1993.

CCEER-93-8 Roybal, J., Sanders, D.H., and Maragakis, E., "Vulnerability Assessment of Masonry in the Reno-Carson City Urban Corridor," Civil Engineering Department, Report No. CCEER-93-8, University of Nevada, Reno, May 1993.

CCEER-93-9 Zafir, Z. and Siddharthan, R., "MOVLOAD: A Program to Determine the Behavior of Nonlinear Horizontally Layered Medium Under Moving Load," Civil Engineering Department, Report No. CCEER-93-9, University of Nevada, Reno, August 1993.

CCEER-93-10 O'Connor, D.N., Saiidi, M., and Maragakis, E.A., "A Study of Bridge Column Seismic Damage Susceptibility at the Interstate 80/U.S. 395 Interchange in Reno, Nevada," Civil Engineering Department, Report No. CCEER-93-10, University of Nevada, Reno, October 1993.

CCEER-94-1 Maragakis, E., B. Douglas, and E. Abdelwahed, "Preliminary Dynamic Analysis of a Railroad Bridge," Report CCEER-94-1, January 1994.

CCEER-94-2 Douglas, B.M., Maragakis, E.A., and Feng, S., "Stiffness Evaluation of Pile Foundation of Cazenovia Creek Overpass," Civil Engineering Department, Report No. CCEER-94-2, University of Nevada, Reno, March 1994.

CCEER-94-3 Douglas, B.M., Maragakis, E.A., and Feng, S., "Summary of Pretest Analysis of Cazenovia Creek Bridge," Civil Engineering Department, Report No. CCEER-94-3, University of Nevada, Reno, April 1994.

CCEER-94-4 Norris, G.M., Madhu, R., Valceschini, R., and Ashour, M., "Liquefaction and Residual Strength of Loose Sands from Drained Triaxial Tests," Report 2, Vol. 1&2, Civil Engineering Department, Report No. CCEER-94-4, University of Nevada, Reno, August 1994.

CCEER-94-5 Saiidi, M., Hutchens, E., and Gardella, D., "Prestress Losses in a Post-Tensioned R/C Box Girder Bridge in Southern Nevada," Civil Engineering Department, CCEER-94-5, University of Nevada, Reno, August 1994.

CCEER-95-1 Siddharthan, R., El-Gamal, M., and Maragakis, E.A., "Nonlinear Bridge Abutment , Verification, and Design Curves," Civil Engineering Department, CCEER-95-1, University of Nevada, Reno, January 1995.

CCEER-95-2 Ashour, M. and Norris, G., "Liquefaction and Undrained Response Evaluation of Sands from Drained Formulation," Civil Engineering Department, Report No. CCEER-95-2, University of Nevada, Reno, February 1995.

CCEER-95-3 Wehbe, N., Saiidi, M., Sanders, D. and Douglas, B., "Ductility of Rectangular Reinforced Concrete Bridge Columns with Moderate Confinement," Civil Engineering Department, Report No. CCEER-95-3, University of Nevada, Reno, July 1995.

CCEER-95-4 Martin, T.., Saiidi, M. and Sanders, D., "Seismic Retrofit of Column-Pier Cap Connections in Bridges in Northern Nevada," Civil Engineering Department, Report No. CCEER-95-4, University of Nevada, Reno, August 1995.

CCEER-95-5 Darwish, I., Saiidi, M. and Sanders, D., "Experimental Study of Seismic Susceptibility Column-Footing Connections in Bridges in Northern Nevada," Civil Engineering Department, Report No. CCEER-95-5, University of Nevada, Reno, September 1995.

CCEER-95-6 Griffin, G., Saiidi, M. and Maragakis, E., "Nonlinear Seismic Response of Isolated Bridges and Effects of Pier Ductility Demand," Civil Engineering Department, Report No. CCEER-95-6, University of Nevada, Reno, November 1995.

CCEER-95-7 Acharya, S.., Saiidi, M. and Sanders, D., "Seismic Retrofit of Bridge Footings and Column-Footing Connections," Civil Engineering Department, Report No. CCEER-95-7, University of Nevada, Reno, November 1995.

CCEER-95-8 Maragakis, E., Douglas, B., and Sandirasegaram, U., "Full-Scale Field Resonance Tests of a Railway Bridge," A Report to the Association of American Railroads, Civil Engineering Department, Report No. CCEER-95-8, University of Nevada, Reno, December 1995.

CCEER-95-9 Douglas, B., Maragakis, E. and Feng, S., "System Identification Studies on Cazenovia Creek Overpass," Report for the National Center for Earthquake Engineering Research, Civil Engineering Department, Report No. CCEER-95-9, University of Nevada, Reno, October 1995.

CCEER-96-1 El-Gamal, M.E. and Siddharthan, R.V., "Programs to Computer Translational Stiffness of Seat-Type Bridge Abutment," Civil Engineering Department, Report No. CCEER-96-1, University of Nevada, Reno, March 1996.

CCEER-96-2 Labia, Y., Saiidi, M. and Douglas, B., "Evaluation and Repair of Full-Scale Prestressed Concrete Box Girders," A Report to the National Science Foundation, Research Grant CMS-9201908, Civil Engineering Department, Report No. CCEER-96-2, University of Nevada, Reno, May 1996.

CCEER-96-3 Darwish, I., Saiidi, M. and Sanders, D., "Seismic Retrofit of R/C Oblong Tapered Bridge Columns with Inadequate Bar Anchorage in Columns and Footings," A Report to the Nevada Department of Transportation, Civil Engineering Department, Report No. CCEER-96-3, University of Nevada, Reno, May 1996.

CCEER-96-4 Ashour, M., Pilling, R., Norris, G. and Perez, H., "The Prediction of Lateral Load Behavior

of Single Piles and Pile Groups Using the Strain Wedge Model," A Report to the California Department of Transportation, Civil Engineering Department, Report No. CCEER-96-4, University of Nevada, Reno, June 1996.

CCEER-97-1-A Rimal, P. and Itani, A. "Sensitivity Analysis of Fatigue Evaluations of Steel Bridges," Center for Earthquake Research, Department of Civil Engineering, University of Nevada, Reno, Nevada Report No. CCEER-97-1-A, September, 1997.

CCEER-97-1-B Maragakis, E., Douglas, B., and Sandirasegaram, U. "Full-Scale Field Resonance Tests of a Railway Bridge," A Report to the Association of American Railroads, Civil Engineering Department, University of Nevada, Reno, May, 1996.

CCEER-97-2 Wehbe, N., Saiidi, M., and D. Sanders, "Effect of Confinement and Flares on the Seismic Performance of Reinforced Concrete Bridge Columns," Civil Engineering Department, Report No. CCEER-97-2, University of Nevada, Reno, September 1997.

CCEER-97-3 Darwish, I., M. Saiidi, G. Norris, and E. Maragakis, "Determination of In-Situ Footing Stiffness Using Full-Scale Dynamic Field Testing," A Report to the Nevada Department of Transportation, Structural Design Division, Carson City, Nevada, Report No. CCEER-97-3, University of Nevada, Reno, October 1997.

CCEER-97-4-A Itani, A. "Cyclic Behavior of Richmond-San Rafael Tower Links," Center for Civil Engineering Earthquake Research, Department of Civil Engineering, University of Nevada, Reno, Nevada, Report No. CCEER-97-4, August 1997.

CCEER-97-4-B Wehbe, N., and M. Saiidi, "User's Manual for RCMC v. 1.2 : A Computer Program for Moment-Curvature Analysis of Confined and Unconfined Reinforced Concrete Sections," Center for Civil Engineering Earthquake Research, Department of Civil Engineering, University of Nevada, Reno, Nevada, Report No. CCEER-97-4, November, 1997.

CCEER-97-5 Isakovic, T., M. Saiidi, and A. Itani, "Influence of new Bridge Configurations on Seismic Performance," Department of Civil Engineering, University of Nevada, Reno, Report No. CCEER-97-5, September, 1997.

CCEER-98-1 Itani, A., Vesco, T. and Dietrich, A., "Cyclic Behavior of "as Built" Laced Members With End Gusset Plates on the San Francisco Bay Bridge," Center for Civil Engineering Earthquake Research, Department of Civil Engineering, University of Nevada, Reno, Nevada Report No. CCEER-98-1, March, 1998.

CCEER-98-2 G. Norris and M. Ashour, "Liquefaction and Undrained Response Evaluation of Sands from Drained Formulation," Center for Civil Engineering Earthquake Research, Department of Civil Engineering, University of Nevada, Reno, Nevada, Report No. CCEER-98-2, May, 1998.

CCEER-98-3 Qingbin, Chen, B. M. Douglas, E. Maragakis, and I. G. Buckle, "Extraction of Nonlinear Hysteretic Properties of Seismically Isolated Bridges from Quick-Release Field Tests," Center for Civil Engineering Earthquake Research, Department of Civil Engineering, University of Nevada, Reno, Nevada, Report No. CCEER-98-3, June, 1998.

CCEER-98-4 Maragakis, E., B. M. Douglas, and C. Qingbin, "Full-Scale Field Capacity Tests of a Railway Bridge," Center for Civil Engineering Earthquake Research, Department of Civil Engineering, University of Nevada, Reno, Nevada, Report No. CCEER-98-4, June, 1998.

CCEER-98-5 Itani, A., Douglas, B., and Woodgate, J., "Cyclic Behavior of Richmond-San Rafael Retrofitted Tower Leg," Center for Civil Engineering Earthquake Research, Department

of Civil Engineering, University of Nevada, Reno. Report No. CCEER-98-5, June 1998

CCEER-98-6 Moore, R., Saiidi, M., and Itani, A., "Seismic Behavior of New Bridges with Skew and Curvature," Center for Civil Engineering Earthquake Research, Department of Civil Engineering, University of Nevada, Reno. Report No. CCEER-98-6, October, 1998.

CCEER-98-7 Itani, A and Dietrich, A, "Cyclic Behavior of Double Gusset Plate Connections," Center for Civil Engineering Earthquake Research, Department of Civil Engineering, University of Nevada, Reno, Nevada, Report No. CCEER-98-5, December, 1998.

CCEER-99-1 Caywood, C., M. Saiidi, and D. Sanders, "Seismic Retrofit of Flared Bridge Columns with Steel Jackets," Civil Engineering Department, University of Nevada, Reno, Report No. CCEER-99-1, February 1999.

CCEER-99-2 Mangoba, N., M. Mayberry, and M. Saiidi, "Prestress Loss in Four Box Girder Bridges in Northern Nevada," Civil Engineering Department, University of Nevada, Reno, Report No. CCEER-99-2, March 1999.

CCEER-99-3 Abo-Shadi, N., M. Saiidi, and D. Sanders, "Seismic Response of Bridge Pier Walls in the Weak Direction," Civil Engineering Department, University of Nevada, Reno, Report No. CCEER-99-3, April 1999.

CCEER-99-4 Buzick, A., and M. Saiidi, "Shear Strength and Shear Fatigue Behavior of Full-Scale Prestressed Concrete Box Girders," Civil Engineering Department, University of Nevada, Reno, Report No. CCEER-99-4, April 1999.

CCEER-99-5 Randall, M., M. Saiidi, E. Maragakis and T. Isakovic, "Restrainer Design Procedures For Multi-Span Simply-Supported Bridges," Civil Engineering Department, University of Nevada, Reno, Report No. CCEER-99-5, April 1999.

CCEER-99-6 Wehbe, N. and M. Saiidi, "User's Manual for RCMC v. 1.2, A Computer Program for Moment-Curvature Analysis of Confined and Unconfined Reinforced Concrete Sections," Civil Engineering Department, University of Nevada, Reno, Report No. CCEER-99-6, May 1999.

CCEER-99-7 Burda, J. and A. Itani, "Studies of Seismic Behavior of Steel Base Plates," Civil Engineering Department, University of Nevada, Reno, Report No. CCEER-99-7, May 1999.

CCEER-99-8 Ashour, M. and G. Norris, "Refinement of the Strain Wedge Model Program," Civil Engineering Department, University of Nevada, Reno, Report No. CCEER-99-8, March 1999.

CCEER-99-9 Dietrich, A., and A. Itani, "Cyclic Behavior of Laced and Perforated Steel Members on the San Francisco-Oakland Bay Bridge," Civil Engineering Department, University, Reno, Report No. CCEER-99-9, December 1999.

CCEER 99-10 Itani, A., A. Dietrich, "Cyclic Behavior of Built Up Steel Members and their Connections," Civil Engineering Department, University of Nevada, Reno, Report No. CCEER-99-10, December 1999.

CCEER 99-10-A Itani, A., E. Maragakis and P. He, "Fatigue Behavior of Riveted Open Deck Railroad Bridge Girders," Civil Engineering Department, University of Nevada, Reno, Report No. CCEER-99-10-A, August 1999.

CCEER 99-11 Itani, A., J. Woodgate, "Axial and Rotational Ductility of Built Up Structural Steel Members," Civil Engineering Department, University of Nevada, Reno, Report No.

CCEER-99-11, December 1999.

CCEER-99-12 Sgambelluri, M., Sanders, D.H., and Saiidi, M.S., "Behavior of One-Way Reinforced Concrete Bridge Column Hinges in the Weak Direction," Department of Civil Engineering, University of Nevada, Reno, Report No. CCEER-99-12, December 1999.

CCEER-99-13 Laplace, P., Sanders, D.H., Douglas, B, and Saiidi, M, "Shake Table Testing of Flexure Dominated Reinforced Concrete Bridge Columns", Department of Civil Engineering, University of Nevada, Reno, Report No. CCEER-99-13, December 1999.

CCEER-99-14 Ahmad M. Itani, Jose A. Zepeda, and Elizabeth A. Ware "Cyclic Behavior of Steel Moment Frame Connections for the Moscone Center Expansion," Department of Civil Engineering, University of Nevada, Reno, Report No. CCEER-99-14, December 1999.

CCEER 00-1 Ashour, M., and Norris, G. "Undrained Lateral Pile and Pile Group Response in Saturated Sand," Civil Engineering Department, University of Nevada, Reno, Report No. CCEER-00-1, May 1999. January 2000.

CCEER 00-2 Saiidi, M. and Wehbe, N., "A Comparison of Confinement Requirements in Different Codes for Rectangular, Circular, and Double-Spiral RC Bridge Columns," Civil Engineering Department, University of Nevada, Reno, Report No. CCEER-00-2, January 2000.

CCEER 00-3 McElhaney, B., M. Saiidi, and D. Sanders, "Shake Table Testing of Flared Bridge Columns With Steel Jacket Retrofit," Civil Engineering Department, University of Nevada, Reno, Report No. CCEER-00-3, January 2000.

CCEER 00-4 Martinovic, F., M. Saiidi, D. Sanders, and F. Gordaninejad, "Dynamic Testing of Non-Prismatic Reinforced Concrete Bridge Columns Retrofitted with FRP Jackets," Civil Engineering Department, University of Nevada, Reno, Report No. CCEER-00-4, January 2000.

CCEER 00-5 Itani, A., and M. Saiidi, "Seismic Evaluation of Steel Joints for UCLA Center for Health Science Westwood Replacement Hospital," Civil Engineering Department, University of Nevada, Reno, Report No. CCEER-00-5, February 2000.

CCEER 00-6 Will, J. and D. Sanders, "High Performance Concrete Using Nevada Aggregates," Civil Engineering Department, University of Nevada, Reno, Report No. CCEER-00-6, May 2000.

CCEER 00-7 French, C., and M. Saiidi, "A Comparison of Static and Dynamic Performance of Models of Flared Bridge Columns," Civil Engineering Department, University of Nevada, Reno, Report No. CCEER-00-7, October 2000.

CCEER 00-8 Itani, A., H. Sedarat, "Seismic Analysis of the AISI LRFD Design Example of Steel Highway Bridges," Civil Engineering Department, University of Nevada, Reno, Report No. CCEER 00-08, November 2000.

CCEER 00-9 Moore, J., D. Sanders, and M. Saiidi, "Shake Table Testing of 1960's Two Column Bent with Hinges Bases," Civil Engineering Department, University of Nevada, Reno, Report No. CCEER 00-09, December 2000.

CCEER 00-10 Asthana, M., D. Sanders, and M. Saiidi, "One-Way Reinforced Concrete Bridge Column Hinges in the Weak Direction," Civil Engineering Department, University of Nevada, Reno, Report No. CCEER 00-10, April 2001.

CCEER 01-1 Ah Sha, H., D. Sanders, M. Saiidi, "Early Age Shrinkage and Cracking of Nevada Concrete Bridge Decks," Civil Engineering Department, University of Nevada, Reno, Report No. CCEER 01-01, May 2001.

CCEER 01-2 Ashour, M. and G. Norris, "Pile Group program for Full Material Modeling a Progressive Failure," Civil Engineering Department, University of Nevada, Reno, Report No. CCEER 01-02, July 2001.

CCEER 01-3 Itani, A., C. Lanaud, and P. Dusicka, "Non-Linear Finite Element Analysis of Built-Up Shear Links," Civil Engineering Department, University of Nevada, Reno, Report No. CCEER 01-03, July 2001.

CCEER 01-4 Saiidi, M., J. Mortensen, and F. Martinovic, "Analysis and Retrofit of Fixed Flared Columns with Glass Fiber-Reinforced Plastic Jacketing," Civil Engineering Department, University of Nevada, Reno, Report No. CCEER 01-4, August 2001

CCEER 01-5 Not Published

CCEER 01-6 Laplace, P., D. Sanders, and M. Saiidi, "Experimental Study and Analysis of Retrofitted Flexure and Shear Dominated Circular Reinforced Concrete Bridge Columns Subjected to Shake Table Excitation," Civil Engineering Department, University of Nevada, Reno, Report No. CCEER 01-6, June 2001.

CCEER 01-7 Reppi, F., and D. Sanders, "Removal and Replacement of Cast-in-Place, Post-tensioned, Box Girder Bridge," Civil Engineering Department, University of Nevada, Reno, Report No. CCEER 01-7, December 2001.

CCEER 02-1 Pulido, C., M. Saiidi, D. Sanders, and A. Itani, "Seismic Performance and Retrofitting of Reinforced Concrete Bridge Bents," Civil Engineering Department, University of Nevada, Reno, Report No. CCEER 02-1, January 2002.

CCEER 02-2 Yang, Q., M. Saiidi, H. Wang, and A. Itani, "Influence of Ground Motion Incoherency on Earthquake Response of Multi-Support Structures," Civil Engineering Department, University of Nevada, Reno, Report No. CCEER 02-2, May 2002.

CCEER 02-3 M. Saiidi, B. Gopalakrishnan, E. Reinhardt, and R. Siddharthan, "A Preliminary Study of Shake Table Response of A Two-Column Bridge Bent on Flexible Footings," Civil Engineering Department, University of Nevada, Reno, Report No. CCEER 02-03, June 2002.

CCEER 02-4 Not Published

CCEER 02-5 Banghart, A., Sanders, D., Saiidi, M., "Evaluation of Concrete Mixes for Filling the Steel Arches in the Galena Creek Bridge," Civil Engineering Department, University of Nevada, Reno, Report No. CCEER 02-05, June 2002.

CCEER 02-6 Dusicka, P., Itani, A., Buckle, I. G., "Cyclic Behavior of Shear Links and Tower Shaft Assembly of San Francisco – Oakland Bay Bridge Tower," Civil Engineering Department, University of Nevada, Reno, Report No. CCEER 02-06, July 2002.

CCEER 02-7 Mortensen, J., and M. Saiidi, "A Performance-Based Design Method for Confinement in Circular Columns," Civil Engineering Department, University of Nevada, Reno, Report No. CCEER 02-07, November 2002.

CCEER 03-1 Wehbe, N., and M. Saiidi, "User's manual for SPMC v. 1.0 : A Computer Program for Moment-Curvature Analysis of Reinforced Concrete Sections with Interlocking Spirals,"

Center for Civil Engineering Earthquake Research, Department of Civil Engineering, University of Nevada, Reno, Nevada, Report No. CCEER-03-1, May, 2003.

CCEER 03-2 Wehbe, N., and M. Saiidi, "User's manual for RCMC v. 2.0 : A Computer Program for Moment-Curvature Analysis of Confined and Unconfined Reinforced Concrete Sections," Center for Civil Engineering Earthquake Research, Department of Civil Engineering, University of Nevada, Reno, Nevada, Report No. CCEER-03-2, June, 2003.

CCEER 03-3 Nada, H., D. Sanders, and M. Saiidi, "Seismic Performance of RC Bridge Frames with Architectural-Flared Columns," Civil Engineering Department, University of Nevada, Reno, Report No. CCEER 03-3, January 2003.

CCEER 03-4 Reinhardt, E., M. Saiidi, and R. Siddharthan, "Seismic Performance of a CFRP/ Concrete Bridge Bent on Flexible Footings," Civil Engineering Department, University of Nevada, Reno, Report No. CCEER 03-4, August 2003.

CCEER 03-5 Johnson, N., M. Saiidi, A. Itani, and S. Ladkany, "Seismic Retrofit of Octagonal Columns with Pedestal and One-Way Hinge at the Base," Center for Civil Engineering Earthquake Research, Department of Civil Engineering, University of Nevada, Reno, Nevada, and Report No. CCEER-03-5, August 2003.

CCEER 03-6 Mortensen, C., M. Saiidi, and S. Ladkany, "Creep and Shrinkage Losses in Highly Variable Climates," Center for Civil Engineering Earthquake Research, Department of Civil Engineering, University of Nevada, Reno, Report No. CCEER-03-6, September 2003.

CCEER 03- 7 Ayoub, C., M. Saiidi, and A. Itani, "A Study of Shape-Memory-Alloy-Reinforced Beams and Cubes," Center for Civil Engineering Earthquake Research, Department of Civil Engineering, University of Nevada, Reno, Nevada, Report No. CCEER-03-7, October 2003.

CCEER 03-8 Chandane, S., D. Sanders, and M. Saiidi, "Static and Dynamic Performance of RC Bridge Bents with Architectural-Flared Columns," Center for Civil Engineering Earthquake Research, Department of Civil Engineering, University of Nevada, Reno, Nevada, Report No. CCEER-03-8, November 2003.

CCEER 04-1 Olaegbe, C., and Saiidi, M., "Effect of Loading History on Shake Table Performance of A Two-Column Bent with Infill Wall," Center for Civil Engineering Earthquake Research, Department of Civil Engineering, University of Nevada, Reno, Nevada, Report No. CCEER-04-1, January 2004.

CCEER 04-2 Johnson, R., Maragakis, E., Saiidi, M., and DesRoches, R., "Experimental Evaluation of Seismic Performance of SMA Bridge Restrainers," Center for Civil Engineering Earthquake Research, Department of Civil Engineering, University of Nevada, Reno, Nevada, Report No. CCEER-04-2, February 2004.

CCEER 04-3 Moustafa, K., Sanders, D., and Saiidi, M., "Impact of Aspect Ratio on Two-Column Bent Seismic Performance," Center for Civil Engineering Earthquake Research, Department of Civil Engineering, University of Nevada, Reno, Nevada, Report No. CCEER-04-3, February 2004.

CCEER 04-4 Maragakis, E., Saiidi, M., Sanchez-Camargo, F., and Elfass, S., "Seismic Performance of Bridge Restrainers At In-Span Hinges," Center for Civil Engineering Earthquake Research, Department of Civil Engineering, University of Nevada, Reno, Nevada, Report No. CCEER-04-4, March 2004.

CCEER 04-5 Ashour, M., Norris, G. and Elfass, S., "Analysis of Laterally Loaded Long or Intermediate Drilled Shafts of Small or Large Diameter in Layered Soil," Center for Civil Engineering Earthquake Research, Department of Civil Engineering, University of Nevada, Reno, Nevada, Report No. CCEER-04-5, June 2004.

CCEER 04-6 Correal, J., Saiidi, M. and Sanders, D., "Seismic Performance of RC Bridge Columns Reinforced with Two Interlocking Spirals," Center for Civil Engineering Earthquake Research, Department of Civil Engineering, University of Nevada, Reno, Nevada, Report No. CCEER-04-6, August 2004.

CCEER 04-7 Dusicka, P., Itani, A. and Buckle, I., "Cyclic Response and Low Cycle Fatigue Characteristics of Plate Steels," Center for Civil Engineering Earthquake Research, Department of Civil Engineering, University of Nevada, Reno, Nevada, Report No. CCEER-04-7, November 2004.

CCEER 04-8 Dusicka, P., Itani, A. and Buckle, I., "Built-up Shear Links as Energy Dissipaters for Seismic Protection of Bridges," Center for Civil Engineering Earthquake Research, Department of Civil Engineering, University of Nevada, Reno, Nevada, Report No. CCEER-04-8, November 2004.

CCEER 04-9 Sureshkumar, K., Saiidi, S., Itani, A. and Ladkany, S., "Seismic Retrofit of Two-Column Bents with Diamond Shape Columns," Center for Civil Engineering Earthquake Research, Department of Civil Engineering, University of Nevada, Reno, Nevada, Report No. CCEER-04-9, November 2004.

CCEER 05-1 Wang, H. and Saiidi, S., "A Study of RC Columns with Shape Memory Alloy and Engineered Cementitious Composites," Center for Civil Engineering Earthquake Research, Department of Civil Engineering, University of Nevada, Reno, Nevada, Report No. CCEER-05-1, January 2005.

CCEER 05-2 Johnson, R., Saiidi, S. and Maragakis, E., "A Study of Fiber Reinforced Plastics for Seismic Bridge Restrainers," Center for Civil Engineering Earthquake Research, Department of Civil Engineering, University of Nevada, Reno, Nevada, Report No. CCEER-05-2, January 2005.

CCEER 05-3 Carden, L.P., Itani, A.M., Buckle, I.G, "Seismic Load Path in Steel Girder Bridge Superstructures," Center for Civil Engineering Earthquake Research, Department of Civil Engineering, University of Nevada, Reno, Nevada, Report No. CCEER-05-3, January 2005.

CCEER 05-4 Carden, L.P., Itani, A.M., Buckle, I.G, "Seismic Performance of Steel Girder Bridge Superstructures with Ductile End Cross Frames and Seismic Isolation," Center for Civil Engineering Earthquake Research, Department of Civil Engineering, University of Nevada, Reno, Nevada, Report No. CCEER-05-4, January 2005.

CCEER 05-5 Goodwin, E., Maragakis, M., Itani, A. and Luo, S., "Experimental Evaluation of the Seismic Performance of Hospital Piping Subassemblies," Center for Civil Engineering Earthquake Research, Department of Civil Engineering, University of Nevada, Reno, Nevada, Report No. CCEER-05-5, February 2005.

CCEER 05-6 Zadeh M. S., Saiidi, S, Itani, A. and Ladkany, S., "Seismic Vulnerability Evaluation and Retrofit Design of Las Vegas Downtown Viaduct," Center for Civil Engineering Earthquake Research, Department of Civil Engineering, University of Nevada, Reno, Nevada, Report No. CCEER-05-6, February 2005.

CCEER 05-7 Phan, V., Saiidi, S. and Anderson, J., "Near Fault (Near Field) Ground Motion Effects on Reinforced Concrete Bridge Columns," Center for Civil Engineering Earthquake Research, Department of Civil Engineering, University of Nevada, Reno, Nevada, Report No. CCEER-05-7, August 2005.

CCEER 05-8 Carden, L., Itani, A. and Laplace, P., "Performance of Steel Props at the UNR Fire Science Academy subjected to Repeated Fire," Center for Civil Engineering Earthquake Research, Department of Civil Engineering, University of Nevada, Reno, Nevada, Report No. CCEER-05-8, August 2005.

CCEER 05-9 Yamashita, R. and Sanders, D., "Shake Table Testing and an Analytical Study of Unbonded Prestressed Hollow Concrete Column Constructed with Precast Segments," Center for Civil Engineering Earthquake Research, Department of Civil Engineering, University of Nevada, Reno, Nevada, Report No. CCEER-05-9, August 2005.

CCEER 05-10 Not Published

CCEER 05-11 Carden, L., Itani., A., and Peckan, G., "Recommendations for the Design of Beams and Posts in Bridge Falsework," Center for Civil Engineering Earthquake Research, Department of Civil Engineering, University of Nevada, Reno, Nevada, Report No. CCEER-05-11, October 2005.

CCEER 06-01 Cheng, Z., Saiidi, M., and Sanders, D., "Development of a Seismic Design Method for Reinforced Concrete Two-Way Bridge Column Hinges," Center for Civil Engineering Earthquake Research, Department of Civil Engineering, University of Nevada, Reno, Nevada, Report No. CCEER-06-01, February 2006.

CCEER 06-02 Johnson, N., Saiidi, M., and Sanders, D., "Large-Scale Experimental and Analytical Studies of a Two-Span Reinforced Concrete Bridge System," Center for Civil Engineering Earthquake Research, Department of Civil Engineering, University of Nevada, Reno, Nevada, Report No. CCEER-06-02, March 2006.

CCEER 06-03 Saiidi, M., Ghasemi, H. and Tiras, A., "Seismic Design and Retrofit of Highway Bridges," Proceedings, Second US-Turkey Workshop, Center for Civil Engineering Earthquake Research, Department of Civil Engineering, University of Nevada, Reno, Nevada, Report No. CCEER-06-03, May 2006.

CCEER 07-01 O'Brien, M., Saiidi, M. and Sadrossadat-Zadeh, M., "A Study of Concrete Bridge Columns Using Innovative Materials Subjected to Cyclic Loading," Center for Civil Engineering Earthquake Research, Department of Civil Engineering, University of Nevada, Reno, Nevada, Report No. CCEER-07-01, January 2007.

CCEER 07-02 Sadrossadat-Zadeh, M. and Saiidi, M., "Effect of Strain rate on Stress-Strain Properties and Yield Propagation in Steel Reinforcing Bars," Center for Civil Engineering Earthquake Research, Department of Civil Engineering, University of Nevada, Reno, Nevada, Report No. CCEER-07-02, January 2007.

CCEER 07-03 Sadrossadat-Zadeh, M. and Saiidi, M., "Analytical Study of NEESR-SG 4-Span Bridge Model Using OpenSees," Center for Civil Engineering Earthquake Research, Department of Civil Engineering, University of Nevada, Reno, Nevada, Report No. CCEER-07-03, January 2007.

CCEER 07-04 Nelson, R., Saiidi, M. and Zadeh, S., "Experimental Evaluation of Performance of Conventional Bridge Systems," Center for Civil Engineering Earthquake Research, Department of Civil Engineering, University of Nevada, Reno, Nevada, Report No. CCEER-07-04, October 2007.

CCEER 07-05 Bahen, N. and Sanders, D., "Strut-and-Tie Modeling for Disturbed Regions in Structural Concrete Members with Emphasis on Deep Beams," Center for Civil Engineering Earthquake Research, Department of Civil Engineering, University of Nevada, Reno, Nevada, Report No. CCEER-07-05, December 2007.

CCEER 07-06 Choi, H., Saiidi, M. and Somerville, P., "Effects of Near-Fault Ground Motion and Fault-Rupture on the Seismic Response of Reinforced Concrete Bridges," Center for Civil Engineering Earthquake Research, Department of Civil Engineering, University of Nevada, Reno, Nevada, Report No. CCEER-07-06, December 2007.

CCEER 07-07 Ashour M. and Norris, G., "Report and User Manual on Strain Wedge Model Computer Program for Files and Large Diameter Shafts with LRFD Procedure," Center for Civil Engineering Earthquake Research, Department of Civil Engineering, University of Nevada, Reno, Nevada, Report No. CCEER-07-07, October 2007.

CCEER 08-01 Doyle, K. and Saiidi, M., "Seismic Response of Telescopic Pipe Pin Connections," Center for Civil Engineering Earthquake Research, Department of Civil Engineering, University of Nevada, Reno, Nevada, Report No. CCEER-08-01, February 2008.

CCEER 08-02 Taylor, M. and Sanders, D., "Seismic Time History Analysis and Instrumentation of the Galena Creek Bridge," Center for Civil Engineering Earthquake Research, Department of Civil Engineering, University of Nevada, Reno, Nevada, Report No. CCEER-08-02, April 2008.

CCEER 08-03 Abdel-Mohti, A. and Pekcan, G., "Seismic Response Assessment and Recommendations for the Design of Skewed Post-Tensioned Concrete Box-Girder Highway Bridges," Center for Civil Engineering Earthquake Research, Department of Civil and Environmental Engineering, University of Nevada, Reno, Nevada, Report No. CCEER-08-03, September 2008.

CCEER 08-04 Saiidi, M., Ghasemi, H. and Hook, J., "Long Term Bridge Performance Monitoring, Assessment & Management," Proceedings, FHWA/NSF Workshop on Future Directions," Center for Civil Engineering Earthquake Research, Department of Civil and Environmental Engineering, University of Nevada, Reno, Nevada, Report No. CCEER 08-04, September 2008.

CCEER 09-01 Brown, A., and Saiidi, M., "Investigation of Near-Fault Ground Motion Effects on Substandard Bridge Columns and Bents," Center for Civil Engineering Earthquake Research, Department of Civil and Environmental Engineering, University of Nevada, Reno, Nevada, Report No. CCEER-09-01, July 2009.

CCEER 09-02 Linke, C., Pekcan, G., and Itani, A., "Detailing of Seismically Resilient Special Truss Moment Frames," Center for Civil Engineering Earthquake Research, Department of Civil and Environmental Engineering, University of Nevada, Reno, Nevada, Report No. CCEER-09-02, August 2009.

CCEER 09-03 Hillis, D., and Saiidi, M., "Design, Construction, and Nonlinear Dynamic Analysis of Three Bridge Bents Used in a Bridge System Test," Center for Civil Engineering Earthquake Research, Department of Civil and Environmental Engineering, University of Nevada, Reno, Nevada, Report No. CCEER-09-03, August 2009.

CCEER 09-04 Bahrami, H., Itani, A., and Buckle, I., "Guidelines for the Seismic Design of Ductile End Cross Frames in Steel Girder Bridge Superstructures," Center for Civil Engineering Earthquake Research, Department of Civil and Environmental Engineering, University of Nevada, Reno, Nevada, Report No. CCEER-09-04, September 2so009.

CCEER 10-01 Zaghi, A. E., and Saiidi, M., "Seismic Design of Pipe-Pin Connections in Concrete Bridges," Center for Civil Engineering Earthquake Research, Department of Civil and Environmental Engineering, University of Nevada, Reno, Nevada, Report No. CCEER-10-01, January 2010.

CCEER 10-02 Pooranampillai, S., Elfass, S., and Norris, G., "Laboratory Study to Assess Load Capacity Increase of Drilled Shafts through Post Grouting," Center for Civil Engineering Earthquake Research, Department of Civil and Environmental Engineering, University of Nevada, Reno, Nevada, Report No. CCEER-10-02, January 2010.

CCEER 10-03 Itani, A., Grubb, M., and Monzon, E, "Proposed Seismic Provisions and Commentary for Steel Plate Girder Superstructures," Center for Civil Engineering Earthquake Research, Department of Civil and Environmental Engineering, University of Nevada, Reno, Nevada, Report No. CCEER-10-03, June 2010.

CCEER 10-04 Cruz-Noguez, C., Saiidi, M., "Experimental and Analytical Seismic Studies of a Four-Span Bridge System with Innovative Materials," Center for Civil Engineering Earthquake Research, Department of Civil and Environmental Engineering, University of Nevada, Reno, Nevada, Report No. CCEER-10-04, September 2010.

CCEER 10-05 Vosooghi, A., Saiidi, M., "Post-Earthquake Evaluation and Emergency Repair of Damaged RC Bridge Columns Using CFRP Materials," Center for Civil Engineering Earthquake Research, Department of Civil and Environmental Engineering, University of Nevada, Reno, Nevada, Report No. CCEER-10-05, September 2010.

CCEER 10-06 Ayoub, M., Sanders, D., "Testing of Pile Extension Connections to Slab Bridges," Center for Civil Engineering Earthquake Research, Department of Civil and Environmental Engineering, University of Nevada, Reno, Nevada, Report No. CCEER-10-06, October 2010.

CCEER 10-07 Builes-Mejia, J. C. and Itani, A., "Stability of Bridge Column Rebar Cages during Construction," Center for Civil Engineering Earthquake Research, Department of Civil and Environmental Engineering, University of Nevada, Reno, Nevada, Report No. CCEER-10-07, November 2010.

CCEER 10-08 Monzon, E.V., "Seismic Performance of Steel Plate Girder Bridges with Integral Abutments," Center for Civil Engineering Earthquake Research, Department of Civil and Environmental Engineering, University of Nevada, Reno, Nevada, Report No. CCEER-10-08, November 2010.

CCEER 11-01 Motaref, S., Saiidi, M., and Sanders, D., "Seismic Response of Precast Bridge Columns with Energy Dissipating Joints," Center for Civil Engineering Earthquake Research, Department of Civil and Environmental Engineering, University of Nevada, Reno, Nevada, Report No. CCEER-11-01, May 2011.

CCEER 11-02 Harrison, N. and Sanders, D., "Preliminary Seismic Analysis and Design of Reinforced Concrete Bridge Columns for Curved Bridge Experiments," Center for Civil Engineering Earthquake Research, Department of Civil and Environmental Engineering, University of Nevada, Reno, Nevada, Report No. CCEER-11-02, May 2011.

CCEER 11-03 Vallejera, J. and Sanders, D., "Instrumentation and Monitoring the Galena Creek Bridge," Center for Civil Engineering Earthquake Research, Department of Civil and Environmental Engineering, University of Nevada, Reno, Nevada, Report No. CCEER-11-03, September 2011.

CCEER 11-04 Levi, M., Sanders, D., and Buckle, I., "Seismic Response of Columns in Horizontally Curved Bridges," Center for Civil Engineering Earthquake Research, Department of Civil and Environmental Engineering, University of Nevada, Reno, Nevada, Report No. CCEER-11-04, December 2011.

CCEER 12-01 Saiidi, M., "NSF International Workshop on Bridges of the Future – Wide Spread Implementation of Innovation," Center for Civil Engineering Earthquake Research, Department of Civil and Environmental Engineering, University of Nevada, Reno, Nevada, Report No. CCEER-12-01, January 2012.

CCEER 12-02 Larkin, A.S., Sanders, D., and Saiidi, M., "Unbonded Prestressed Columns for Earthquake Resistance," Center for Civil Engineering Earthquake Research, Department of Civil and Environmental Engineering, University of Nevada, Reno, Nevada, Report No. CCEER-12-02, January 2012.

CCEER 12-03 Arias-Acosta, J. G., Sanders, D., "Seismic Performance of Circular and Interlocking Spirals RC Bridge Columns under Bidirectional Shake Table Loading Part 1," Center for Civil Engineering Earthquake Research, Department of Civil and Environmental Engineering, University of Nevada, Reno, Nevada, Report No. CCEER-12-03, September 2012.

CCEER 12-04 Cukrov, M.E., Sanders, D., "Seismic Performance of Prestressed Pile-To-Bent Cap Connections," Center for Civil Engineering Earthquake Research, Department of Civil and Environmental Engineering, University of Nevada, Reno, Nevada, Report No. CCEER-12-04, September 2012.

CCEER 13-01 Carr, T. and Sanders, D., "Instrumentation and Dynamic Characterization of the Galena Creek Bridge," Center for Civil Engineering Earthquake Research, Department of Civil and Environmental Engineering, University of Nevada, Reno, Nevada, Report No. CCEER-13-01, January 2013.

CCEER 13-02 Vosooghi, A. and Buckle, I., "Evaluation of the Performance of a Conventional Four-Span Bridge During Shake Table Tests," Center for Civil Engineering Earthquake Research, Department of Civil and Environmental Engineering, University of Nevada, Reno, Nevada, Report No. CCEER-13-02, January 2013.

CCEER 13-03 Amirihormozaki, E. and Pekcan, G., "Analytical Fragility Curves for Horizontally Curved Steel Girder Highway Bridges," Center for Civil Engineering Earthquake Research, Department of Civil and Environmental Engineering, University of Nevada, Reno, Nevada, Report No. CCEER-13-03, February 2013.

CCEER 13-04 Almer, K. and Sanders, D., "Longitudinal Seismic Performance of Precast Bridge Girders Integrally Connected to a Cast-in-Place Bentcap," Center for Civil Engineering Earthquake Research, Department of Civil and Environmental Engineering, University of Nevada, Reno, Nevada, Report No. CCEER-13-04, April 2013.

CCEER 13-05 Monzon, E.V., Itani, A.I., and Buckle, I.G., "Seismic Modeling and Analysis of Curved Steel Plate Girder Bridges," Center for Civil Engineering Earthquake Research, Department of Civil and Environmental Engineering, University of Nevada, Reno, Nevada, Report No. CCEER-13-05, April 2013.

CCEER 13-06 Monzon, E.V., Buckle, I.G., and Itani, A.I., "Seismic Performance of Curved Steel Plate Girder Bridges with Seismic Isolation," Center for Civil Engineering Earthquake Research, Department of Civil and Environmental Engineering, University of Nevada, Reno, Nevada, Report No. CCEER-13-06, April 2013.

CCEER 13-07 Monzon, E.V., Buckle, I.G., and Itani, A.I., "Seismic Response of Isolated Bridge Superstructure to Incoherent Ground Motions," Center for Civil Engineering Earthquake Research, Department of Civil and Environmental Engineering, University of Nevada, Reno, Nevada, Report No. CCEER-13-07, April 2013.

CCEER 13-08 Haber, Z.B., Saiidi, M.S., and Sanders, D.H., "Precast Column-Footing Connections for Accelerated Bridge Construction in Seismic Zones," Center for Civil Engineering Earthquake Research, Department of Civil and Environmental Engineering, University of Nevada, Reno, Nevada, Report No. CCEER-13-08, April 2013.

CCEER 13-09 Ryan, K.L., Coria, C.B., and Dao, N.D., "Large Scale Earthquake Simulation of a Hybrid Lead Rubber Isolation System Designed under Nuclear Seismicity Considerations," Center for Civil Engineering Earthquake Research, Department of Civil and Environmental Engineering, University of Nevada, Reno, Nevada, Report No. CCEER-13-09, April 2013.

CCEER 13-10 Wibowo, H., Sanford, D.M., Buckle, I.G., and Sanders, D.H., "The Effect of Live Load on the Seismic Response of Bridges," Center for Civil Engineering Earthquake Research, Department of Civil and Environmental Engineering, University of Nevada, Reno, Nevada, Report No. CCEER-13-10, May 2013.

CCEER 13-11 Sanford, D.M., Wibowo, H., Buckle, I.G., and Sanders, D.H., "Preliminary Experimental Study on the Effect of Live Load on the Seismic Response of Highway Bridges," Center for Civil Engineering Earthquake Research, Department of Civil and Environmental Engineering, University of Nevada, Reno, Nevada, Report No. CCEER-13-11, May 2013.

CCEER 13-12 Saad, A.S., Sanders, D.H., and Buckle, I.G., "Assessment of Foundation Rocking Behavior in Reducing the Seismic Demand on Horizontally Curved Bridges," Center for Civil Engineering Earthquake Research, Department of Civil and Environmental Engineering, University of Nevada, Reno, Nevada, Report No. CCEER-13-12, June 2013.

CCEER 13-13 Ardakani, S.M.S. and Saiidi, M.S., "Design of Reinforced Concrete Bridge Columns for Near-Fault Earthquakes," Center for Civil Engineering Earthquake Research, Department of Civil and Environmental Engineering, University of Nevada, Reno, Nevada, Report No. CCEER-13-13, July 2013.

CCEER 13-14 Wei, C. and Buckle, I., "Seismic Analysis and Response of Highway Bridges with Hybrid Isolation," Center for Civil Engineering Earthquake Research, Department of Civil and Environmental Engineering, University of Nevada, Reno, Nevada, Report No. CCEER-13-14, August 2013.

CCEER 13-15 Wibowo, H., Buckle, I.G., and Sanders, D.H., "Experimental and Analytical Investigations on the Effects of Live Load on the Seismic Performance of a Highway Bridge," Center for Civil Engineering Earthquake Research, Department of Civil and Environmental Engineering, University of Nevada, Reno, Nevada, Report No. CCEER-13-15, August 2013.

CCEER 13-16 Itani, A.M., Monzon, E.V., Grubb, M., and Amirihormozaki, E. "Seismic Design and Nonlinear Evaluation of Steel I-Girder Bridges with Ductile End Cross-Frames," Center for Civil Engineering Earthquake Research, Department of Civil and Environmental Engineering, University of Nevada, Reno, Nevada, Report No. CCEER-13-16, September 2013.

CCEER 13-17 Kavianipour, F. and Saiidi, M.S., "Experimental and Analytical Seismic Studies of a Four-span Bridge System with Composite Piers," Center for Civil Engineering Earthquake Research, Department of Civil and Environmental Engineering, University of Nevada, Reno, Nevada, Report No. CCEER-13-17, September 2013.

CCEER 13-18 Mohebbi, A., Ryan, K., and Sanders, D., "Seismic Response of a Highway Bridge with Structural Fuses for Seismic Protection of Piers," Center for Civil Engineering Earthquake Research, Department of Civil and Environmental Engineering, University of Nevada, Reno, Nevada, Report No. CCEER-13-18, December 2013.

CCEER 13-19 Guzman Pujols, Jean C., Ryan, K.L., "Development of Generalized Fragility Functions for Seismic Induced Content Disruption," Center for Civil Engineering Earthquake Research, Department of Civil and Environmental Engineering, University of Nevada, Reno, Nevada, Report No. CCEER-13-19, December 2013.

CCEER 14-01 Salem, M. M. A., Pekcan, G., and Itani, A., "Seismic Response Control Of Structures Using Semi-Active and Passive Variable Stiffness Devices," Center for Civil Engineering Earthquake Research, Department of Civil and Environmental Engineering, University of Nevada, Reno, Nevada, Report No. CCEER-14-01, May 2014.

CCEER 14-02 Saini, A. and Saiidi, M., "Performance-Based Probabilistic Damage Control Approach for Seismic Design of Bridge Columns," Center For Civil Engineering Earthquake Research, Department Of Civil and Environmental Engineering, University of Nevada, Reno, Nevada, Report No. CCEER-14-02, May 2014.

CCEER 14-03 Saini, A. and Saiidi, M., "Post Earthquake Damage Repair of Various Reinforced Concrete Bridge Components," Center For Civil Engineering Earthquake Research, Department Of Civil and Environmental Engineering, University of Nevada, Reno, Nevada, Report No. CCEER-14-03, May 2014.

CCEER 14-04 Monzon, E.V., Itani, A.M., and Grubb, M.A., "Nonlinear Evaluation of the Proposed Seismic Design Procedure for Steel Bridges with Ductile End Cross Frames," Center For Civil Engineering Earthquake Research, Department Of Civil and Environmental Engineering, University of Nevada, Reno, Nevada, Report No. CCEER-14-04, July 2014.

CCEER 14-05 Nakashoji, B. and Saiidi, M.S., "Seismic Performance of Square Nickel-Titanium Reinforced ECC Columns with Headed Couplers," Center For Civil Engineering Earthquake Research, Department Of Civil and Environmental Engineering, University of Nevada, Reno, Nevada, Report No. CCEER-14-05, July 2014.

CCEER 14-06 Tazarv, M. and Saiidi, M.S., "Next Generation of Bridge Columns for Accelerated Bridge Construction in High Seismic Zones," Center For Civil Engineering Earthquake Research, Department Of Civil and Environmental Engineering, University of Nevada, Reno, Nevada, Report No. CCEER-14-06, August 2014.

CCEER 14-07 Mehrsoroush, A. and Saiidi, M.S., "Experimental and Analytical Seismic Studies of Bridge Piers with Innovative Pipe Pin Column-Footing Connections and Precast Cap Beams," Center For Civil Engineering Earthquake Research, Department Of Civil and Environmental Engineering, University of Nevada, Reno, Nevada, Report No. CCEER-14-07, December 2014.

CCEER 15-01 Dao, N.D. and Ryan, K.L., "Seismic Response of a Full-scale 5-story Steel Frame Building Isolated by Triple Pendulum Bearings under 3D Excitations," Center For Civil Engineering Earthquake Research, Department Of Civil and Environmental Engineering, University of Nevada, Reno, Nevada, Report No. CCEER-15-01, January 2015.

CCEER 15-02 Allen, B.M. and Sanders, D.H., "Post-Tensioning Duct Air Pressure Testing Effects on Web Cracking," Center For Civil Engineering Earthquake Research, Department Of Civil and Environmental Engineering, University of Nevada, Reno, Nevada, Report No. CCEER-15-02, January 2015.

CCEER 15-03 Akl, A. and Saiidi, M.S., "Time-Dependent Deflection of In-Span Hinges in Prestressed Concrete Box Girder Bridges," Center For Civil Engineering Earthquake Research, Department Of Civil and Environmental Engineering, University of Nevada, Reno, Nevada, Report No. CCEER-15-03, May 2015.

CCEER 15-04 Zargar Shotorbani, H. and Ryan, K., "Analytical and Experimental Study of Gap Damper System to Limit Seismic Isolator Displacements in Extreme Earthquakes," Center For Civil Engineering Earthquake Research, Department Of Civil and Environmental Engineering, University of Nevada, Reno, Nevada, Report No. CCEER-15-04, June 2015.

CCEER 15-05 Wieser, J., Maragakis, E.M., and Buckle, I., "Experimental and Analytical Investigation of Seismic Bridge-Abutment Interaction in a Curved Highway Bridge," Center For Civil Engineering Earthquake Research, Department Of Civil and Environmental Engineering, University of Nevada, Reno, Nevada, Report No. CCEER-15-05, July 2015.

CCEER 15-06 Tazarv, M. and Saiidi, M.S., "Design and Construction of Precast Bent Caps with Pocket Connections for High Seismic Regions," Center For Civil Engineering Earthquake Research, Department Of Civil and Environmental Engineering, University of Nevada, Reno, Nevada, Report No. CCEER-15-06, August 2015.

CCEER 15-07 Tazarv, M. and Saiidi, M.S., "Design and Construction of Bridge Columns Incorporating Mechanical Bar Splices in Plastic Hinge Zones," Center For Civil Engineering Earthquake Research, Department Of Civil and Environmental Engineering, University of Nevada, Reno, Nevada, Report No. CCEER-15-07, August 2015.